ASTROGEOLOGIC STUDIES

ANNUAL PROGRESS REPORT

July 1, 1964 to

July 1, 1965

PART C: COSMIC CHEMISTRY AND PETROLOGY

November 1965

This preliminary report is distributed
without editorial and technical review
for conformity with official standards
and nomenclature. It should not be
quoted without permission.

This report concerns work done on behalf of the
National Aeronautics and Space Administration.

DEPARTMENT OF THE INTERIOR
UNITED STATES GEOLOGICAL SURVEY

CONTENTS

PART C--COSMIC CHEMISTRY AND PETROLOGY

CONTENTS--Continued

INTRODUCTION

This Annual Report is the sixth of a series describing the results of research conducted by the U.S. Geological Survey on behalf of the National Aeronautics and Space Administration. The report is in three volumes corresponding to three main areas of research: Part A, Lunar and Planetary Investigations: Part B, Crater Investigations; and Part C, Cosmic Chemistry and Petrology; and a map supplement. An additional volume presents abstracts of the papers in Parts A, B, and C.

The major long-range objectives of the astrogeologic studies program are to determine and map the stratigraphy and structure of the Moon's crust, to work out from these the sequence of events that led to the present condition of the Moon's surface, and to determine the processes by which these events took place. Work that leads toward these objectives includes a program of lunar geologic mapping; studies on the discrimination of geologic materials on the lunar surface by their photometric, polarimetric, and infrared properties; field studies of structures of impact, explosive, and volcanic origin; laboratory studies on the behavior of rocks and minerals subjected to shock; and study of the chemical, petrographic and physical properties of materials of possible lunar origin and the development of special techniques for their analysis.

Part C, Cosmic Chemistry and Petrology, includes reports on techniques of study, analysis, and interpretation of data on materials of known or suspected extraterrestrial origin. A study jointly supported by the Branch of Geochemical Census of the Geological Survey describes the statistical treatment of superior analyses of tektites and the petrologic interpretation of the results. A study jointly supported by the Southwest States Branch of the Geological Survey deals with the petrologic significance of tektite analyses. Minor-element data for basaltic meteorites are reported. A theoretical and experimental study of the stability of meteoritic cohenite as a function of temperature and pressure is presented. The cosmic dust investigations, supported by the National Aeronautics and Space Administration and other government agencies, contributes a report on the application of the scanning electron microscope and a progress report on the construction of laboratory facilities.

USE OF THE SCANNING ELECTRON MICROSCOPE IN GEOLOGIC STUDIES

by Edward J. Dwornik

To evaluate the applicability of scanning electron microscopy to various types of sample materials to be studied in the cosmic dust program, a visit to the laboratory of the Pulp and Paper Research Institute of Canada was arranged. Here, the instrument designed and built in the research laboratories of Cambridge University, England (Oatley and Smith, 1955) has been used as an adjunct to the conventional high resolution electron microscope in research on paper and pulp fibers and related problems.

In the scanning electron microscope, a finely focused beam of electrons approximately 500 A in diameter is accelerated by a voltage of 15 kv and focused onto a sample at a 45° angle by magnetic lenses. Deflection coils sweep the beam over the area of interest in a scanning sequence, "kicking out" secondary low energy electrons from the sample surface. These electrons are collected by a scintillation counter whose light output is detected by a photomultiplier tube. The output from the photomultiplier is converted to a voltage, amplified and used to control the brightness of a cathode ray tube in synchronization with the primary beam scan. An image of the surface topography of the sample is presented on the screen, and is photographed with a 35-mm camera. The area scanned governs the magnification and is varied by controlling the deflection coils. The area can be varied from several microns to several millimeters, allowing useful magnifications from 40,000X to 100X. A mechanical stage allows for traversing up to a square centimeter of sample surface.

The resolution of the scanning electron microscope is limited to 500 A by the size of the focused electron beam. Theoretically, it is possible to focus the beam to about 30 A, closer to the resolution of a transmission electron microscope (< 10 A). For many electron-microscopic studies in which replicas are made, the scanning electron microscope approaches the same capabilities with less sample preparation difficulty. It is not possible to obtain electron diffraction information with the instrument.
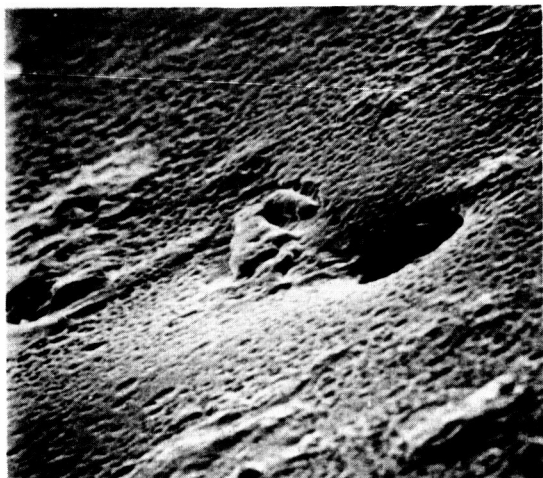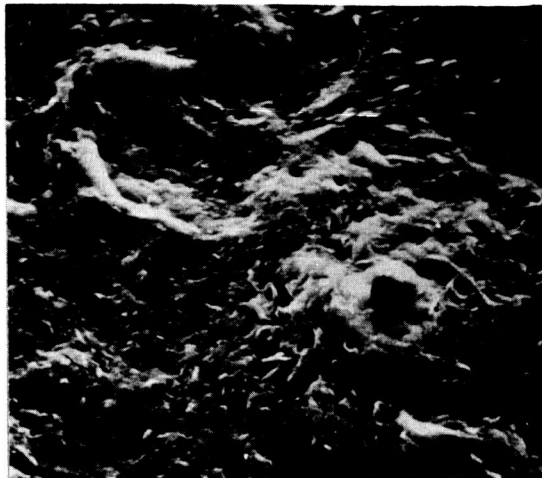
Fig. 1. Tektite; 860X

Fig. 2. Obsidian; 1170X

Fig. 3. Coccolith; 2730X
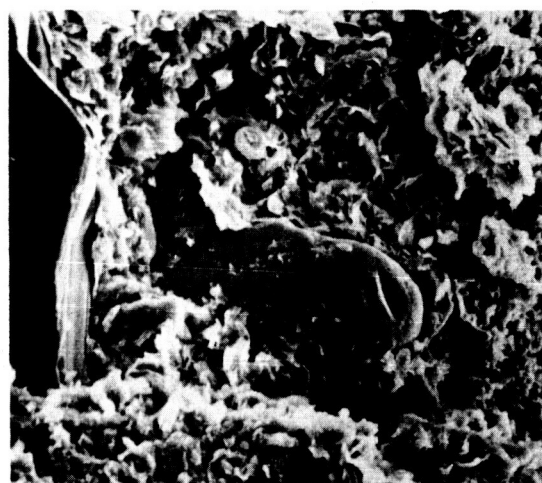
Fig. 4. Glauconitic clay; 690X
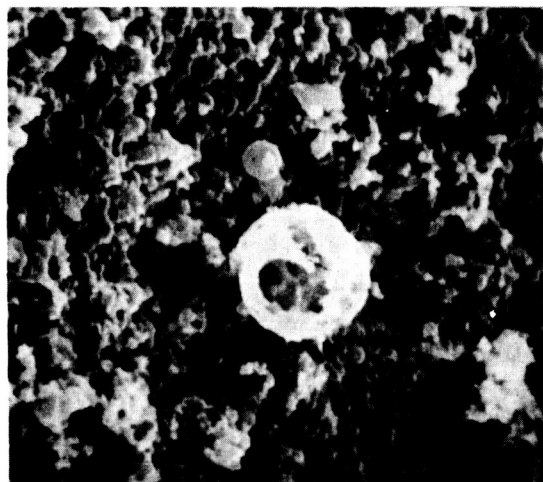
Fig. 5. Airborne dust; 4300X
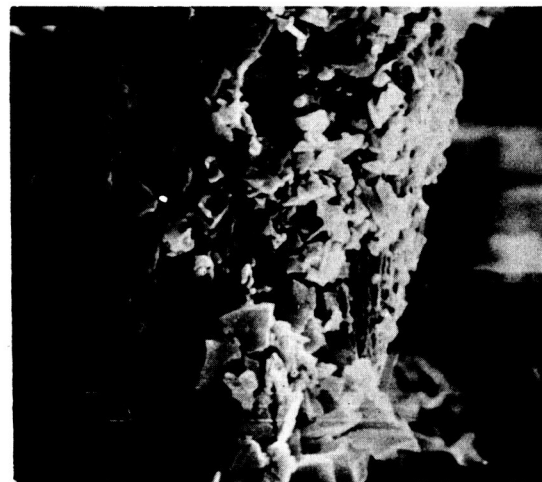
Fig. 6. Airborne dust; 2400X

Fig. 1.--Surface of a freshly fractured tektite showing pock-marked character. (Specimen from E. C. T. Chao, U.S. Geological Survey.)

Fig. 2.--Surface of obsidian (volcanic glass) showing a void that is almost square in cross section.

Fig. 3.--Coccolith from glauconitic clay, New Jersey. These micro-fossils represent ideal subjects for scanning electron microscopy. The intricate architecture is readily depicted and study of many species would be simplified by this technique. This specimen was located on a mount prepared for conventional electron microscopy.

Fig. 4.--Part of a bulk sample of glauconitic clay from which the specimen in figure 3 was recovered. A glauconite pebble, a book of mica, and several coccoliths are evident. This direct observation of the bulk dry sample makes separation and suspension of constituents unnecessary and reduces the possibility of introducing artifacts that could cause difficulty in interpretation of standard electron micrographs. Microtextural study of loosely compacted sediments is greatly facilitated. (Specimens from H. Gill, Water Resources Division, U.S. Geological Survey.)

Fig. 5.--Particles trapped on a millipore membrane filter. The hollowed-out spherules would appear solid in a transmission electron micrograph, due to absorption of the electron beam, and the true shape would be lost. The particles adhering to the surface of the spherules are readily observable by this technique, but might be missed in conventional transmission micros-copy. Filter pores of 1 μ can be seen in background.

Fig. 6.--Angular dust particles trapped on a cotton filter fiber. Hygroscopic particles and those soluble in water or organic liquids can be prepared for the scanning electron microscope directly, without suspension in distilled water.

Fig. 7. Hewettite; 130X
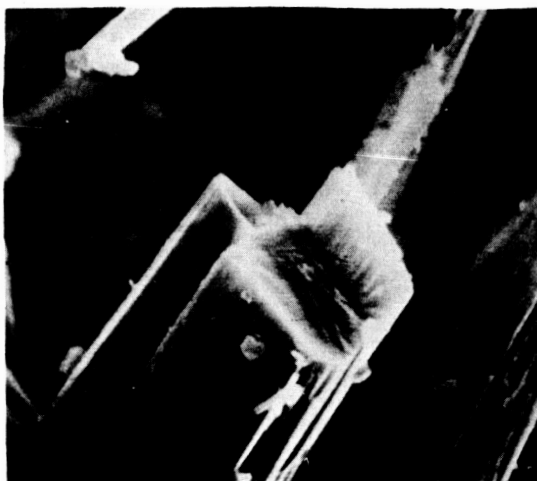
Fig. 8. Serpentine; 4500X
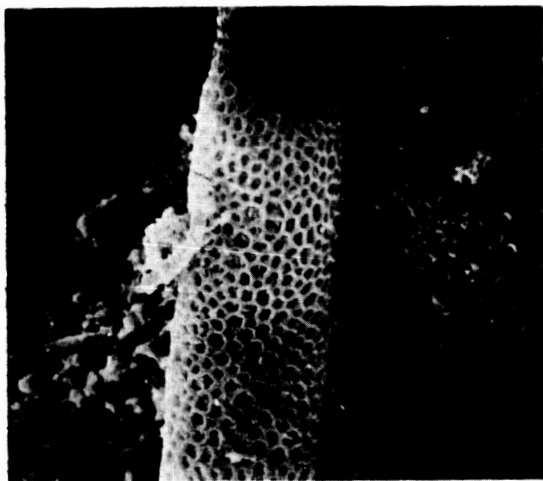
Fig. 9. Alga; 2530X

Fig. 10. Calcitic tubes; 390X

Fig. 11. Metallic spherule; 680X
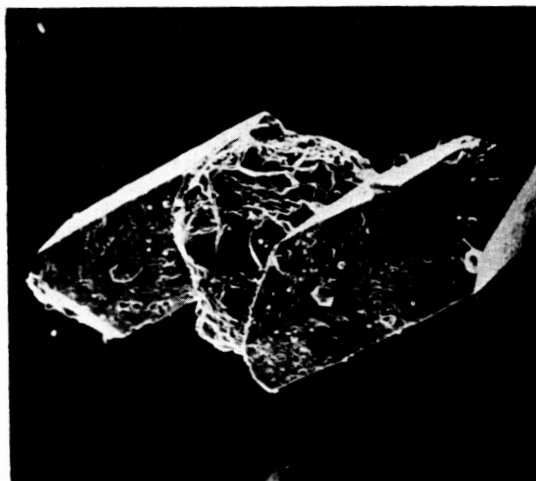
Fig. 12. Quartz crystals; 210X

Fig. 7.--Fibrous crystals of hewettite, a calcium vanadate. The large depth of focus of the scanning electron microscope is emphasized in this relatively low magnification photograph.

Fig. 8.--Termination of serpentine fiber. This 3/4 end view shows that the fiber is solid rather than tubular. Cleavage would produce lathlike particles.

Fig. 9.--Part of a blue-green alga (fig. 10), devoid of the calcareous overgrowth, showing pores which may have served as loci for secreting calcite. The skeletal character of the "wooly" calcite is resolved in the background.

Fig. 10.--Calcite-secreting algae from Russell Cave, Alabama. Each of the "wooly" calcite tubules surrounds an alga responsible for its secretion. (Specimen from J. Hack, U.S. Geological Survey.)

Fig. 11.--A metallic spherule exposed on a fracture surface of a philippinite (tektite). This technique offers an excellent means for study of surface irregularities and features of metallic and other inclusions in tektites. (Specimen from E. C. T. Chao, U.S. Geological Survey.)

Fig. 12.--Two well-developed quartz crystals growing from a common seed. The crystals in various stages of growth were recovered by digestion of an oolitic limestone in boiling HCl and an oxidizing bleach. Information on morphologic development, etch patterns, and surface features of crystals and seeds can be obtained. Replication of these features is virtually impossible by conventional electron microscope techniques. (Specimens from L. G. Henbest, U.S. Geological Survey.)

For highly irregular surfaces, the inherently great depth of field of the scanning electron microscope allows the complete depiction of the object's surface. If necessary, stereomicrographs may be prepared by changing the specimen angle slightly between exposures. The increased resolution (about 10 times better) of the instrument over the optical microscope, together with the depth of field, gives the scanning electron microscope unique capabilities for studying etched mineral grain surfaces, microfossils, filters, etc. Examples of scanning electron micrographs are shown in figures 1-12.

The samples are prepared for examination simply by cementing them to the surface of an aluminum disc. The disc and sample are placed in a special holder and rotated at 200 rpm in a vacuum while a weighed amount of Au-Pd wire is evaporated onto the whirling disc from an angle of 60°. This insures that all surfaces of the sample are electrically conducting.

The placement of the specimen in a high vacuum and resultant desiccation may preclude the study of some materials. Also, bombardment by the electron beam can cause some difficulty in samples that are nonconducting and hollow or skeletal. This limitation can be overcome to a great extent by evaporating the conductive metal coating onto the specimen and working with a lower accelerating potential of the electron beam. Direct observation of nonconducting materials is an objective of the scientists engaged in developing this instrument.

Acknowledgments

Reference

Oatley, C. W., and Smith, K. C. A., 1955, The scanning electron microscope and its field of application: Brit. Jour. Appl. Physics, v. 6, p. 391.

MULTIVARIATE ANALYSIS OF GEOCHEMICAL DATA
ON TEXAS TEKTITES (BEDIASITES)

by A. T. Miesch[1] , E. C. T. Chao, and Frank Cuttitta

Introduction

Tektites are small, variably shaped masses of silicate glass which occur at a number of widely separated localities on the earth. Some of the better known localities are Czechoslovakia, southeast Asia, Australia, the Ivory Coast of Africa, and east-central Texas and Georgia in the United States. Most tektites are less than an inch or two across; complete specimens have definite shapes characteristic of the localities in which they were found, and most are completely lacking in crystalline mineral matter. Crystalline metallic nickel-iron, in small spherules, has been observed in some specimens from the Philippine Islands and Indochina.

Tektites have been found in a wide variety of geologic environments and it is generally agreed that they have been transported some distance from their sites of origin. The shapes of tektites, considered in view of aerodynamic principles, indicate that they were transported through the atmosphere, and it is commonly, though by no means universally, held that they are of extraterrestrial origin, derived, perhaps, as a result of meteoritic impact on the surface of the moon (Chapman, 1964; Chao and others, 1964). If this is true, the compositions of tektites have broader implications than those pertaining to their own character and origin; they may have especially important bearing on problems of lunar geology.

There are, of course, many aspects of compositional data on tektites that are of interest in searching for clues to the nature of their parent material or the processes that have affected their compositions. Of fundamental interest are the absolute amounts of each constituent, as

---

well as ratios and other functions of the constituent abundances. These properties of tektite compositional data have already received a great deal of attention in the literature. So far, however, no rigorous analysis has been made of correlation relations among various constituents or constituent ratios in tektites; most published work is based on graphical analysis only, and other work has failed to take some complexities of compositional data into account or to extract much of the information that is present.

Techniques of multivariate statistical analysis now available make it possible to evaluate the complexities and to gain some insight regarding causes that have operated in fixing the tektite compositions. As theory pertinent to the problems treated has not been completely developed, our approach has been largely empirical. Nonetheless, the applied techniques have been found to lead to results that are both intuitively valid and geologically meaningful. Moreover, the techniques are probably useful in a broad range of petrologic problems.

The complexities in compositional data referred to stem partly from the effects of closed arrays, a subject studied and discussed extensively by Chayes (1960, 1962, 1964). Closed arrays of data are those in which rows, each representing a specimen or sample, have a constant sum; constituents in each specimen add up to 100 percent, 10^6 parts per million, etc., depending on how the data are expressed. The problem with data of this sort has been vaguely considered by geologists for some time, but the work of Chayes has shown that it is far more serious, and of broader importance, than previously realized. In addition, his analysis of the problem has led to a foundation upon which further studies may be based.

The problem created by the closed array is most easily explained, in a qualitative way, in terms of a set of rock samples containing only two major components (say, quartz and feldspar). The two components necessarily have a perfect negative correlation with each other among the specimens. This is a correlation caused not necessarily by geologic processes, but by the fact that the compositional data, to be meaningful, must be expressed on an equal weight (or volume) basis. If the rock samples contained three major components (say, biotite, in addition to quartz and feldspar) the

effect of the closed array would still be present, but less pronounced. Commonly five or six major components are present, but the effect of the closed array is still highly significant.

All of our work verifies Chayes' analysis of the problem, and clearly substantiates his alarm about the seriousness and widespread consequences of the matter. We find, in fact, that the situation is perhaps even more alarming than he tells us, for not only the major components, but some minor components as well, are affected by the closed array to an important degree.

One important consequence of the closed array, as shown by Chayes, is that correlation coefficients derived from compositional data cannot be meaningfully compared with or tested against zero, as is normally the custom with data from open arrays. Chayes gives methods for determining average test values, but they are not useful for testing individual correlation coefficients (Chayes, 1960, p. 4190-4191). The difficulty does not stem from use of correlation coefficients, as equally troublesome difficulties arise in interpretation by just scanning the data or by plotting it on any type of variation diagram. Strong observed relationships may actually be no greater than one should expect from values drawn from a random-number table, if the random numbers are forced into a closed array.

Aside from examination and testing of correlations among individual constituents of the tektites, ratios of constituents and sums of various constituents are of fundamental importance in tektite studies. Such multivariate functions treated by Chao (1963) are:

$FeO + MgO$

$Na_2O + K_2O$

$(FeO + MgO + CaO)/(Na_2O + K_2O)$

Fe_2O_3/FeO

$Cr + Co + Ni$
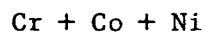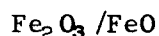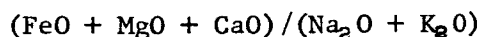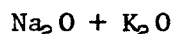
A few of the other multivariate variate functions regarded as having possible significance are:

$Rb + Li$

MgO/Li

K_2O/Na_2O

Rb/Li
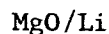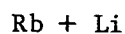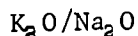
Some of these, and a number of others, have been of interest to other investigators of tektite compositions. Their importance and meaning in tektite petrology are discussed in other papers (cf. Chao, 1963; Schnetzler and Pinson, 1963; Cuttitta and others, 1964; Schüller and Ottemann, 1963).

Although these multivariate functions (and, especially, relations among them) are of basic importance, they introduce some difficulty in statistical analysis. For example, the ratio $(FeO + MgO + CaO)/(Na_2O + K_2O)$ has been used to discriminate between tektites from different strewn fields (Chao, 1963, p. 74, 79), and may be a useful index of magmatic differentiation in tektite petrology. Therefore, correlations between this ratio and other variables (some of which are contained in the ratio) are of interest. However, there is no a priori certainty that it is proper to test these correlations against zero, or to accept an orderly trend on a variation diagram as having any petrographic significance.

In the absence of theory on which tests of correlations derived from closed arrays or from ratio data may be based, we have tested observed correlations against those derived from simulation studies, wherein closed arrays of random normal deviates are constructed to simulate the real data on hand. The basis for the method of construction was given by Chayes (1960, p. 4191-4192), but has been extended here to make its use practical. Correlation values derived from the real data which we studied were tested against those derived from the closed random deviates. The original correlations were then corrected and used to interpret petrographic relations among the variables by means of factor analysis techniques.

The data employed are chemical, spectrographic, and physical property determinations on 21 bediasite specimens from east-central Texas.

Geology and character of the bediasites

The bediasites of east-central Texas occur in a lag gravel, several inches thick, of post-Eocene and pre-Recent age, and overlying sandstone and shale of the Eocene Jackson Group. Specimens have been found in a belt, about 140 miles long, extending from Gonzales County in the

southwest to Grimes County in the northeast. The lag gravel consists of predominantly red, gray, white, yellow, and black chert; rounded milky to buff-colored quartz pebbles; and fragments of black to grayish-white silicified fossil wood.

The bediasite specimens are jet black in reflected light and are rounded owing to sedimentary transport. They range in diameter from less than a quarter of an inch to 2 or 3 inches and show no apparent effects of chemical weathering. Additional characteristics of bediasite specimens are given by Barnes (1939, p. 493-511) and Chao (1963, p. 68).

Analytical data

The analytical data used in this study have been given in a previous paper by Chao (1963, tables 5, 8). They consist of chemical and spectrographic determinations of 22 major and minor elements, and measurements of refractive index, specific gravity, and magnetic susceptibility, on 21 specimens. Means, $\overline{X}_j$, and standard deviations, s_j, for each variable, as well as relative deviations ($C_j = s_j / \overline{X}_j$), are given in table 1 (columns 2-4). Other general characteristics of the analytical data, and of the analytical techniques are given by Chao (1963, p. 66-85). It will be sufficient to note here only a few points that will be pertinent to the following discussion.

The bediasites are remarkably uniform in composition, as are most tektites from a single strewn field. The relative deviations (table 1, column 4) are all less than 0.6. The variation for most elements, however, is considerably greater than the standard error of the corresponding analytical method. (Compare columns 3 and 9 in table 1.)

The low relative deviations, especially of the minor elements, are uncommon in geochemical data. In most minor-element data for terrestrial rocks, the relative deviations approach or greatly exceed 1, making it necessary to transform the data in order to achieve frequency distributions that more closely approximate the normal form. Such transformations were not necessary in the present work.

Chao (1963, p. 87-88) has shown that the bediasites and other tektites resemble, in gross compositional character, a number of terrestrial

11

Table 1. Statistical data

j	Variable (1) X_j	Bediasite data			Average values for 30 closed arrays of random deviates			Average "low-calcium granite"[1] (8) $\bar{X}_j$	Standard error of analytical technique (9) s_e	Communalities (10) h^2	Unexplained deviation (11) $\sqrt{(1-h^2)}\,s_j$
		(2) $\bar{X}_j$	(3) s_j	(4) c_j	(5) $\bar{X}_m$	(6) s_m	(7) c_m				
	Major elements (percent)										
1	SiO$_2$ ------	76.37	2.26	0.03	76.31	2.38	0.03	74.3	0.38	0.77	1.08
2	Al$_2$O$_3$ -----	13.78	1.55	.11	13.78	1.60	.12	13.6	.14	.85	.60
3	Fe$_2$O$_3$ -----	.19	.11	.58	.20	.11	.55	} [2]1.8	.01	1.00	.00
4	FeO -------	3.81	.74	.19	3.84	.74	.19		.08	.70	.34
5	MgO -------	.63	.16	.25	.64	.16	.25	.27	.02	.54	.11
6	CaO -------	.65	.14	.22	.65	.15	.23	.71	.02	.72	.07
7	Na$_2$O ------	1.54	.19	.13	1.56	.20	.13	3.5	.05	.82	.08
8	K$_2$O -------	2.08	.26	.13	2.08	.28	.13	5.1	.06	.82	.11
9	TiO$_2$ ------	.77	.12	.16	.76	.13	.17	.20	.04	.96	.02
10	P$_2$O$_5$ ------	.039	.018	.46	.041	.018	.44	.14	.004	.77	.000
11	MnO -------	.041	.016	.39	.040	.017	.43	.05	.002	.66	.000
	Physical properties										
12	R.I.[3] ------	1.459	0.006	0.0041	1.496	0.006	------	-------	0.0004	0.98	0.0008
13	Sp.G.[4] -----	2.380	.023	.0097	2.381	.024	------	-------	.005	.87	.008
14	M.Su.[5] -----	5.62x10^{-6}	1.24x10^{-6}	.22	5.62x10^{-6}	1.26x10^{-6}	------	-------	-------	.96	.25x10^{-6}
	Minor elements (parts per million)										
15	Cu --------	12	4	0.33	12	4	0.33	10	1.1	0.67	2.x
16	Ga --------	10	4	.40	10	4	.40	17	.9	.96	8
17	Rb --------	62	10	.16	63	11	.17	170	3.7	.43	7.5
18	Li --------	18	6	.33	18	6	.33	40	1.1	.86	2.2
19	Cr --------	36	12	.33	37	12	.32	4	4.3	.84	4.8
20	Co --------	10	2	.20	10	2	.20	1	.7	.63	1.2
21	Ni --------	13	4	.31	13	4	.31	4.5	1.0	.92	1.1
22	Ba --------	609	205	.34	610	221	.36	840	67	.63	125
23	Sr --------	100	28	.28	101	30	.30	100	12	.28	24
24	V ---------	87	28	.32	85	29	.34	44	9	.68	16
25	B --------	2.2	1.0	.45	2.2	1.1	.50	3	.2	.73	.5

[1] From Turekian and Wedepohl, 1961, table 2.

[2] Total iron as FeO.

[3] Refractive index.

[4] Specific gravity.

[5] Magnetic susceptibility (emu/gm)

materials, including alkali rhyolites, granophyres, loesses, and soils.
A comparison of the average bediasite composition with that of the average
"low-calcium granite" (Turekian and Wedepohl, 1961), nearly identical in
composition with the average granophyre used by Chao, is given in table 1
(columns 2, 8). The bediasites are apparently higher in total iron, MgO,
TiO_2, Cr, Co, Ni, and V, and lower in the alkalies, Na_2O, K_2O, Rb, and Li,
as well as P_2O_5. The average concentrations of SiO_2, Al_2O_3, and a few
other constituents, however, are remarkably similar.

Testing correlation coefficients

Prior to Chayes' work (1960, 1962) on closed arrays of compositional
data, most geologists gave careful thought to only two factors as con-
trolling the magnitudes of correlation coefficients or the nature of pat-
terns on variation diagrams. One factor, of course, was petrogenetic
association caused by chemical and physical properties of the constituents
and their response to processes acting during rock genesis. The other
factor was chance; it was always realized that some high correlation co-
efficients or well-defined trends on variation diagrams could be fortui-
tous, especially where the data were meager.

The work of Chayes has created an awareness that correlations and
variation trends can also be affected by the particular numerical struc-
ture of the data. This structure, or system into which the data are
forced, may affect correlations in either a positive or negative direc-
tion, and may either create or reduce scatter about a variation diagram
trend; it may also affect the direction of the trend slope. The part
of the numerical structure of compositional data of principal concern
to Chayes has been the constant row sum, when the data are arranged in
a rectangular array with rows representing individual rock samples and
columns representing rock constituents.

Many arrays of compositional data in geology are augmented with ad-
ditional columns representing functions of the original data, such as
ratios and sums. The ratios and other functions are only rearrangements
of the original data, and although they do not represent any basically
new information, they are more easily interpreted in terms of response

13

to geologic processes. However, correlation among the functions or between the functions and original variables can result from their numerical structure, or from the structure of the closed data from which they are derived, in the absence of petrogenetic associations among the variables. Chayes' (1949) work, based on a mathematical analysis by Reed (1921), has shown that the correlation of X_1/X_2 with X_1, for example, where the correlation between X_1 and X_2 is zero, is determined entirely by the means and variances of X_1 and X_2 and cannot be zero if any variance whatsoever is present in X_2. It showed, further, that a correlation between such variables as X_1/X_2 and X_3 is dependent largely on the correlations of X_1 and X_2 with X_3; such correlation, of course, may be introduced solely by the numerical structure of the closed array.

In statistical analysis of the bediasite data, because of the absence of completely developed theory useful for correcting the effect of the numerical structure, we approached the problem through data simulation studies, by an extension of the technique given by Chayes (1960, p. 4191-4192). The general procedure, executed entirely within a B5500 computer, is as follows:

1. Construct P <u>open</u> arrays of normal random deviates, d_{ij}, each having 21 rows (designated by i), representing the 21 bediasite specimens, and 25 columns (designated by j), representing the 22 elements and 3 physical properties listed on table 1. Each column has a population mean of zero and variance of one. The row sums in each array will be variable, and correlations among columns will be close to zero if the derivation of d_{ij} is unbiased.

2. The means and variances of each column in each <u>open</u> array are adjusted to new values μ_j and σ_j, respectively, using the equation:

$$D_{ij} = \sigma_j d_{ij} + \mu_j \qquad (1)$$

Row sums in each array of D_{ij} will still be variable, and correlations among columns will still be close to zero.

The squares of the constant σ_j are the variances of columns in the open arrays. On closing the arrays (adjusting each row sum to 100), the variances of columns having large variance will change. The objective

14

in selecting the σ_j values is to set column variances in the open arrays so that on closure the new column variances will closely approximate the column variances in the real data array. For columns representing variables with small variance ($s_j < 0.1$ percent, table 1, column 3), σ_j is set equal to s_j. For columns representing the other variables, $j = 1$ to $j = 9$ (table 1), σ_j is derived by extension of a technique given by Chayes (1960, p. 4192). His fundamental equation is:

$$\text{Var}\left(\frac{X_j}{T}\right) = \left(\frac{\mu_j}{\tau}\right)^2 \left[\frac{\sigma_j^2}{\mu_j^2} + \frac{\sigma_t^2}{\tau^2} - 2\frac{\sigma_j^2}{\mu_j \tau} \right] \tag{2}$$

where the quantity on the left side of the equation is the variance of the jth variable in the closed array (when the variable is expressed as a decimal fraction of the row sum), μ_j and σ_j^2 are the population mean and variance of the jth column in the open (D_{ij}) arrays to be generated, τ is the sum of μ_j values across j, and σ_t^2 is the sum of the σ_j^2 values across j.

Setting τ equal to 100, and multiplying both sides of (2) by 10^4 gives the equation for the variance of the jth variable in the closed array in units of percent:

$$\text{Var}(X_j) = \mu_j^2 \left[\frac{\sigma_j^2}{\mu_j^2} + \frac{\sigma_t^2}{10^4} - 2\frac{\sigma_j^2}{100\mu_j} \right] \tag{3}$$

Writing the quantity σ_t^2 as ($\sigma_1^2 + \sigma_2^2 + \sigma_3^2 + \sigma_4^2 \ldots$), equation (3) may be rearranged, for $j = 1$, to:

$$\text{Var } X_1 = \left(\frac{10^4 + \mu_1^2 - 200\mu_1}{10^4}\right) \sigma_1^2 + \frac{\mu_1^2}{10^4} (\sigma_2^2 + \sigma_3^2 + \sigma_4^2 \ldots). \tag{4}$$

If we let

$$a_j = \frac{10^4 + \mu_j^2 - 200\mu_j}{10^4} , \tag{5}$$

and

$$b_j = \frac{\mu_j^2}{10^4} , \tag{6}$$

a set of linear equations, each equation representing a variable, is obtained as follows:

$$\text{Var } X_1 = a_1 \sigma_1^2 + b_1 \sigma_2^2 + b_1 \sigma_3^2 + \ldots b_1 \sigma_j^2 \ldots$$

$$\text{Var } X_2 = b_2 \sigma_1^2 + a_2 \sigma_2^2 + b_2 \sigma_3^2 + \ldots b_2 \sigma_j^2 \ldots$$

$$\text{Var } X_3 = b_3 \sigma_1^2 + b_3 \sigma_2^2 + a_3 \sigma_3^2 + \ldots b_3 \sigma_j^2 \ldots \quad (7)$$

$$\vdots$$

$$\text{Var } X_j = b_j \sigma_1^2 + b_j \sigma_2^2 + b_j \sigma_3^2 + \ldots a_j \sigma_j^2 \ldots$$

$$\vdots$$

Using the variances from the original data on the left sides of the equations, and the means from the original data in (5) and (6), the equations are solved for values of σ_j^2.

Using means and variances of the first 9 variables (table 1, column 1) in the bediasite data, and grouping the remaining chemical elements into a tenth variable, all 10 values of σ_j^2 derived from (7) were positive. The mean for the tenth variable was taken as the sum of the means within the group, and the variance was taken as the sum of their variances. Then the first 9 derived values of σ_j were used in (1).

In application of the method to other data sets pertaining to terrestrial igneous rocks, some of the σ_j^2 solutions were negative, making it impossible, of course, to obtain σ_j for use in (1). We have found that zero values used in place of the undefined square roots are satisfactory for at least some problems, but further investigation is needed.

3. Within each of the P arrays of D_{ij}, each row is summed across the 22 columns representing chemical constituents, and each of these 22 values in the row is multiplied by the quantity 100 over this sum. After this closure procedure, the means of columns are essentially unchanged. If the initial values of σ_j in (1) are completely satisfactory, the variances of all 25 columns are very similar to the corresponding columns in the real data. In addition, correlation among the 22 columns involved in the closure may now be present--correlations in excess of those that can reasonably be ascribed to chance. These correlations result primarily from the numerical structure of the closed arrays. None of the correlation, of course, is due to petrogenetic association.

4. In this experiment the number of closed arrays of random deviates generated, P, was 30. The grand mean and square root of the mean variance

16

for each column across the 30 arrays was then derived. These are given in table 1, along with relative deviations (table 1, columns 5-7). The generally close correspondence of the overall statistics on the closed arrays of random deviates to those derived from the real data attests to the success of the simulation procedure, and particularly to the usefulness of Chayes' equation for the estimation of σ_j values in this problem.

5. Each of the P matrices is next augmented by the addition of 9 columns, each representing one of the ratios or other functions listed previously. The functions were computed from values in the closed arrays. The first augmented column in each array represents the variable FeO + MgO, and was derived, row by row, by summing the values in the columns representing these two constituents. A similar procedure was used for the other 8 columns.

6. The 30 arrays of closed random deviates simulating the original data set then each consisted of 21 rows and 34 columns (22 representing chemical constituents, 3 representing physical property measurements, and 9 representing ratios or other functions). Correlation coefficients were then derived for each pair of columns in each array. Each coefficient was then transformed to Fisher's Z (Snedecor, 1956, p. 175) and the mean, Z_m, and variance of Z were computed. The variance of Z for each coefficient among the 30 arrays agreed reasonably well with the theoretical value given by $1/(N_1 - 3)$, where $N_1 = 21$, the number of pairs on which each coefficient is based. The mean Z (Z_m) was transformed back to a value we have called r_m, the average correlation coefficient for the P matrices of closed random deviates. The quantity, r_m, is also an estimate of the expected correlation from the bediasite data in the absence of petrogenetic association. Departures of r_m from zero are due entirely to the numerical structure of the closed arrays and the functional variables, and to correlation arising by chance.

Significance of differences between a correlation coefficient, r, derived from the real data and the equivalent value of r_m, derived from the closed arrays of random deviates was tested, finally, using a method based on Snedecor (1956, p. 178):

17
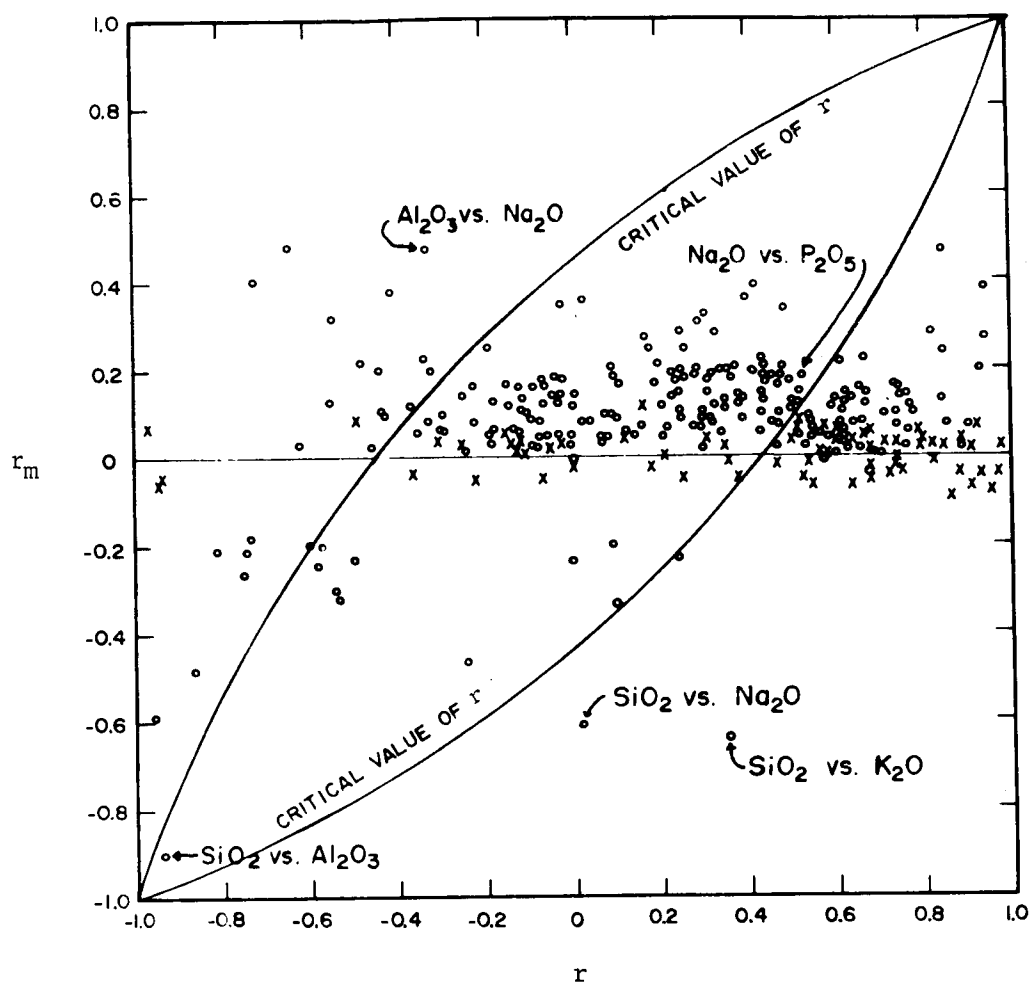
Fig. 1.--Comparison of correlations in the bediasite data, r, with those from closed arrays of random deviates, r_m. Circles represent correlations involving chemical constituents only. Crosses represent correlations involving physical property measurements. Correlations involving functional variables are not represented. Arcs show critical values of r for corresponding values of r_m, at the 95 percent confidence level. Some points falling within clusters of others are not shown.

Table 2. Adjusted correlation coefficients, r_a, derived from correlation coefficients, r, computed from data on 21 bediasites, and correlation coefficients, r_m, computed from closed arrays of random deviates

[Variables designated by R.I., Sp.G., and M.Su. are, respectively, refractive index, specific gravity, and magnetic susceptibility. Variables designated by letters (a) through (i) are functions of the analytical data: (a) = $FeO + MgO$; (b) = $Na_2O + K_2O$; (c) = $(FeO + MgO + CaO)/(Na_2O + K_2O)$; (d) = Fe_2O_3/FeO; (e) = $Cr + Co + Ni$; (f) = $Rb + Co + Ni$; (g) = MgO/Li; (h) = K_2O/Na_2O; (i) = Rb/Li]

SiO2

	Al2O3	Fe2O3	FeO	MgO	CaO	Na2O	K2O	TiO2	P2O5	MnO	R.I.	Sp.G.	M.Su.	Cu	Ga	Rb	Li	Cr	Co	Ni	Ba
r	-0.94	-0.60	-0.96	-0.54	0.07	0.02	0.36	-0.87	-0.59	0.10	-0.97	-0.94	-0.95	-0.75	-0.74	-0.22	-0.81	-0.74	-0.54	-0.50	0.00
r_m	-.91	-.20	-.59	-.30	-.33	-.61	-.64	-.48	-.24	-.20	.08	-.04	-.06	-.26	-.18	-.46	-.21	-.21	-.32	-.23	-.23
r_o	-.17	-.46	-.86	-.28	.40	.62	.81	-.66	-.41	.29	-.98	-.93	-.94	-.60	-.64	.27	-.73	-.63	-.26	-.31	.23

	Sr	v	Be	(a)	(b)	(c)	(d)	(e)	(f)	(g)	(h)	(i)
r	0.24	-0.57	-0.44	-0.98	0.23	-0.87	-0.34	-0.76	-0.50	0.03	0.21	0.00
r_m	-.23	-.20	-.09	-.63	-.73	-.16	.01	-.31	-.49	.40	.12	.12
r_o	.45	-.41	-.37	-.91	.82	-.82	-.35	-.58	-.02	-.37	.09	-.12

Al2O3

	Fe2O3	FeO	MgO	CaO	Na2O	K2O	TiO2	P2O5	MnO	R.I.	Sp.G.	M.Su.	Cu	Ga	Rb	Li	Cr	Co	Ni	Ba
r	0.91	0.82	0.91	0.61	0.50	0.03	0.67	0.75	0.26	0.24	-0.12	-0.32	0.48	0.43	0.94	-0.53	0.97	0.14	0.67	0.31
r_m	-.06	.04	.02	.22	.18	.40	.17	.16	.25	.17	.16	.20	.19	.06	.30	.56	-.07	.02	.24	.42
r_o	.92	.81	.90	.45	.35	-.37	.56	.67	.02	.07	-.28	-.49	.32	.38	.89	-.84	.97	.11	.51	-.12

Fe2O3

	FeO	MgO	CaO	Na2O	K2O	TiO2	P2O5	MnO	R.I.	Sp.G.	M.Su.	Cu	Ga	Rb	Li	Cr	Co	Ni	Ba
r	-0.69	-0.62	0.59	0.51	-0.06	0.47	0.69	0.47	0.69	-0.07	0.68	0.55	0.68	0.66	0.68	0.62	0.85	0.98	0.65
r_m	.03	.02	.12	.05	.06	.07	.00	.07	.00	.05	-.05	-.07	.06	.07	-.04	.10	.13	.06	.07
r_o	-.71	-.63	.51	.48	-.12	.41	.69	.41	.69	-.11	.71	.59	.64	.62	.70	.55	.81	.54	.61

FeO

	MgO	CaO	Na2O	K2O	TiO2	P2O5	MnO	R.I.	Sp.G.	M.Su.	Cu	Ga	Rb	Li	Cr	Co	Ni	Ba
r	0.98	0.67	0.65	0.09	0.75	0.74	0.46	0.54	0.60	0.48	0.58	0.47	0.46	0.62	0.60	0.50	0.61	-0.18
r_m	.03	.15	.04	.21	.14	.10	.14	-.05	.05	.07	.04	.02	.15	.07	.13	.13	.08	.04
r_o	.98	.58	.62	-.13	.68	.69	.34	.58	.56	.42	.55	.45	.33	.58	.52	.39	.56	-.21

	Sr	v	Be	(a)	(b)	(c)	(d)	(e)	(f)	(g)	(h)	(i)
r	-0.58	-0.70	-0.82	0.98	0.95	0.94	-0.82	0.94	0.75	0.17	0.31	0.09
r_m	.00	.08	.01	.98	.93	.76	.01	.76	.14	.27	.18	.21
r_o	-.58	-.74	-.82	.13	.16	.61	-.82	.61	.68	-.10	.13	-.13

Table 2--Continued

Note: this is a rotated, densely packed correlation matrix. Values are given in three rows per oxide: r, r_m, r_o. Column headers combine letter footnotes (a)–(1) with element/oxide names.

	Sr	v	Be	(a)	(b)	(c)	(d)	(e)	(f)	(g)	(h)	(1)	CaO	Na₂O	K₂O	TiO₂	P₂O₅	MnO	R.I.	Sp.G.	M.Su.
MgO r	0.16	0.55	-0.05	0.55	0.29	0.30	0.42	0.67	0.58	0.01	-0.47	-0.52	0.87	0.82	0.85	-0.48	0.30	0.32	-0.13	0.18	-0.25
MgO r_m	.09	.09	.05	.05	.29	.10	.01	.16	.16	.40	.03	.01	.30	.28	.24	.22	.09	.09	.02	-.02	.04
MgO r_o	.06	.48	-.08	.30	.00	.20	.41	.58	.46	-.39	-.49	-.53	.77	.70	.76	-.63	.22	.24	-.16	.20	-.29

	Cu	Ga	Rb	(a)	(b)	(c)	(d)	(e)	(f)	(g)	(h)	(1)	Co	Ni	Cr	Sr	V	Cr	R.I.	Sp.G.	M.Su.
CaO r	0.10	0.32	0.29	0.04	-0.33	0.34	0.38	0.30	0.31	-0.10	-0.03	-0.18	0.49	0.67	-0.09	0.31	0.11	-0.44	-0.09	0.95	-0.47
CaO r_m	.10	.09	.31	.09	.09	.20	.14	.11	.16	.11	.13	.16	.34	.23	.16	.18	.17	.20	.29	.81	.27
CaO r_o	.00	.25	-.02	-.04	-.41	.16	.25	.19	.16	-.21	-.16	-.33	.18	.51	-.25	.14	-.06	-.58	-.37	.61	-.23

	K₂O	v	Be	(a)	(b)	(c)	(d)	(e)	(f)	(g)	(h)	(1)	MnO	Be	Cr	Sr	V	Ga	R.I.	Sp.G.	M.Su.
Na₂O r	0.85	-0.41	0.53	0.44	0.00	0.21	-0.13	-0.72	0.51	0.42	0.23	-0.09	0.33	-0.15	0.29	0.40	-0.06	-0.24	-0.36	0.29	0.29
Na₂O r_m	.47	.38	.19	.17	-.02	.00	.04	.41	.12	.39	.14	.16	.18	.07	.54	.37	.13	.50	.04	.06	.21
Na₂O r_o	.64	-.68	.38	.29	.02	.21	-.17	-.87	.42	.04	.09	-.25	.15	-.22	-.29	.05	-.20	-.70	-.33	.29	.09

	Na₂O	v	Be	(a)	(b)	(c)	(d)	(e)	(f)	(g)	(h)	(1)	P₂O₅	MnO	TiO₂	Cr	V	Be	R.I.	Sp.G.	M.Su.
Na₂O r	0.44	-0.22	0.38	-0.46	0.97	-0.33	0.50	0.45	0.90	-0.62	0.97	0.20	0.35	-0.38	0.23	-0.33	0.36	0.29	0.47	0.44	0.38
Na₂O r_m	.21	.16	.40	.36	.90	.14	.12	.12	.24	.46	.06	.06	.13	.04	.38	.14	.12	.54	.16	.13	.21
Na₂O r_o	.25	-.37	-.02	-.70	.58	-.45	.41	.35	.85	-.84	.97	.02	.23	-.35	.23	-.17	-.14	-.29	.33	.33	.18

	Sr	v	Be	(a)	(b)	(c)	(d)	(e)	(f)	(g)	(h)	(1)	Co	Ni	Cr	MnO	Be	V	R.I.	Sp.G.	M.Su.
K₂O r	0.44	-0.22	-0.24	-0.46	0.97	-0.77	0.21	-0.20	0.24	0.04	0.29	0.08	0.23	-0.38	0.19	0.40	0.07	0.66	0.47	0.44	-0.02
K₂O r_m	.21	.16	.10	.36	.90	-.28	.02	.29	.36	.06	.54	.06	.38	-.04	-.01	.37	.04	.08	.16	.13	.35
K₂O r_o	.25	-.37	-.33	-.70	.58	-.62	.20	-.47	-.14	-.01	-.29	.02	-.16	-.35	.21	.05	.03	.61	.33	.33	-.37

	Li	Cu	Ga	(a)	(b)	(c)	(d)	(e)	(f)	(g)	(h)	(1)	Be	Sr	Ba	Rb	Sr	V	R.I.	Sp.G.	M.Su.
TiO₂ r	0.56	0.58	0.85	0.18	-0.14	-0.33	0.67	0.45	0.90	-0.62	0.97	0.20	0.07	0.31	0.10	0.40	0.29	0.63	0.30	0.64	0.68
TiO₂ r_m	.17	.02	.05	.25	.12	.14	.12	.12	.24	.46	.06	.01	.04	.18	.19	.37	.54	.04	.32	.07	.01
TiO₂ r_o	.44	.57	.84	-.07	-.26	-.45	.60	.35	.85	-.84	.97	.21	.03	.14	-.09	.05	-.29	.65	-.03	.68	.69

	M.Su.	Cu	Ga	(a)	(b)	(c)	(d)	(e)	(f)	(g)	(h)	(1)	Be	Ba	MnO	Sr	Cr	Co	R.I.	Sp.G.	M.Su.
P₂O₅ r	0.59	0.58	0.85	0.48	0.70	0.51	0.67	0.88	-0.11	-0.09	0.66	0.07	0.56	0.28	0.63	0.69	0.69	0.63	-0.62	-0.63	-0.69
P₂O₅ r_m	.07	.02	.05	.20	.00	.05	.12	.07	.06	.09	.08	.04	.11	-.05	-.01	.08	.08	.17	.06	.03	.06
P₂O₅ r_o	.54	.57	.84	.32	.70	.47	.60	.86	-.17	-.18	.61	.03	.49	.32	.64	.65	.65	.52	-.65	-.64	-.72

	Sp.G.	Cu	Ga	(a)	(b)	(c)	(d)	(e)	(f)	(g)	(h)	(1)	V	Ba	Sr	Li	Ba	Sr	R.I.	Sp.G.	M.Su.
MnO r	-0.02	0.12	-0.10	0.08	0.03	0.28	0.00	0.07	-0.07	0.28	-0.42	0.57	0.22	-0.12	0.39	-0.26	0.01	0.11	0.30	0.38	0.29
MnO r_m	.04	.04	.14	.10	.08	.19	.02	.04	.09	.07	.10	.08	.06	.09	.20	-.04	.02	.07	.32	.21	.21
MnO r_o	-.07	.08	-.24	-.02	-.05	.09	-.03	.02	-.16	.21	-.51	.52	.17	-.21	.20	-.23	-.01	.04	-.03	.18	.09

Table 2--Continued

		(h)	(i)		Sp.G.	M.Su.	Cu	Ga	Rb	Li	Cr	Co	Ni	Ba	Sr	V	Be	(a)	(b)	(c)	(d)	(e)
r	MnO	−0.16	0.09	R.I.	0.93	0.97	0.72	0.74	0.26	0.82	0.75	0.51	0.54	−0.08	−0.22	0.58	0.38	0.97	−0.22	0.85	0.45	0.77
r_m	MnO	.01	.05	R.I.	−.05	−.04	−.03	.01	−.05	−.01	−.03	.05	−.02	−.06	−.05	.02	−.05	−.09	−.03	−.06	−.02	−.03
r_o	MnO	−.17	.03	R.I.	.93	.97	.74	.73	.31	.82	.77	.48	.55	−.01	−.17	.57	.41	.97	−.19	.87	.46	.79
		(f)	(g)	(h)	(i)		M.Su.	Cu	Ga	Rb	Li	Cr	Co	Ni	Ba	Sr	V	Be	(a)	(b)	(c)	(d)
r	R.I.	0.53	−0.57	−0.73	−0.84	Sp.G.	0.86	0.71	0.80	0.32	0.77	0.65	0.52	0.59	−0.06	−0.13	0.57	0.35	0.89	0.00	0.72	0.32
r_m	R.I.	−.05	−.02	−.01	−.01	Sp.G.	.10	.03	.04	.05	−.01	.05	.06	.00	.02	.06	.01	.03	.04	.04	.00	−.06
r_o	R.I.	.57	−.56	−.73	−.84	Sp.G.	.84	.70	.79	.27	.78	.62	.48	.59	−.07	−.18	.57	.33	.88	−.04	.71	.38
		(e)	(f)	(g)	(h)	(i)		Cu	Ga	Rb	Li	Cr	Co	Ni	Ba	Sr	V	Be	(a)	(b)	(c)	(d)
r	Sp.G.	0.71	0.55	−0.52	−0.70	−0.80	M.Su.	0.70	0.68	0.17	0.78	0.79	0.52	0.47	−0.12	−0.30	0.66	0.36	0.98	−0.35	0.90	0.43
r_m	Sp.G.	.06	.04	.06	.07	.03	M.Su.	.04	.02	.13	.02	.07	.09	−.02	.01	.04	.06	−.01	.05	.08	−.01	.04
r_o	Sp.G.	.68	.52	−.56	−.73	−.82	M.Su.	.68	.67	.04	.77	.76	.45	.48	−.13	−.34	.63	.37	.98	−.42	.90	.40
		(e)	(f)	(g)	(h)	(i)		Ga	Rb	Li	Cr	Co	Ni	Ba	Sr	V	Be	(a)	(b)	(c)	(d)	(e)
r	M.Su.	0.79	0.45	−0.57	−0.71	−0.83	Cu	0.73	0.46	0.86	0.60	0.55	0.63	−0.07	0.01	0.54	0.11	0.73	0.10	0.50	0.49	0.68
r_m	M.Su.	.07	.11	.06	.05	.06	Cu	.07	.18	.01	.07	.07	.11	.16	.14	−.01	.09	.15	.21	.01	.01	.11
r_o	M.Su.	.76	.36	−.61	−.73	−.85	Cu	.70	.31	.86	.55	.50	.56	−.23	−.13	.55	.02	.65	−.11	.49	.48	.62
		(f)	(g)	(h)	(i)		Rb	Li	Cr	Co	Ni	Ba	Sr	V	Be	(a)	(b)	(c)	(d)	(e)	(f)	(g)
r	Cu	0.68	−0.60	−0.52	−0.76	Ga	0.45	0.80	0.62	0.78	0.89	−0.09	−0.18	0.61	0.34	0.69	0.34	0.42	0.56	0.80	0.66	−0.68
r_m	Cu	.15	−.02	.01	.02	Ga	.18	.08	.07	.10	.03	.03	.13	.05	.06	.05	.17	−.06	−.07	.08	.19	−.03
r_o	Cu	.60	−.58	−.53	−.77	Ga	.30	.77	.58	.74	.89	−.12	−.31	.58	.28	.66	.18	.46	.61	.76	.53	−.66
		(h)	(i)		Li	Cr	Co	Ni	Ba	Sr	V	Be	(a)	(b)	(c)	(d)	(e)	(f)	(g)	(h)	(i)	
r	Ga	−0.64	−0.83	Rb	0.62	0.24	0.33	0.62	−0.04	0.25	0.34	−0.29	0.17	0.42	−0.07	0.65	0.38	0.94	−0.39	−0.05	−0.26	Li
r_m	Ga	.06	−.02	Rb	.12	.15	.29	.14	.18	.20	.10	.10	.24	.43	−.02	.02	.22	.89	.02	.01	.27	Li
r_o	Ga	−.67	−.83	Rb	.54	.09	.04	.53	−.22	.05	.25	−.38	−.07	−.01	−.05	.64	.17	.28	−.40	−.06	−.49	Li
		Cr	Co	Ni	Ba	Sr	V	Be	(a)	(b)	(c)	(d)	(e)	(f)	(g)	(h)	(i)		Co	Ni	Ba	Sr
r	Li	0.72	0.62	0.73	−0.06	−0.14	0.66	0.14	0.80	0.06	0.58	0.69	0.81	0.85	−0.74	−0.56	−0.87	Cr	0.39	0.57	−0.55	−0.42
r_m	Li	.05	.13	.02	.02	.06	.01	.06	.15	.16	.04	.07	.07	.57	−.73	.00	−.77	Cr	.14	.06	.13	.10
r_o	Li	.69	.53	.72	−.07	−.20	.65	.08	.74	−.10	.55	.65	.78	.54	−.02	−.57	−.30	Cr	.27	.53	−.63	−.50
		V	Be	(a)	(b)	(c)	(d)	(e)	(f)	(g)	(h)	(i)		Ni	Ba	Sr	V	Be	(a)	(b)	(c)	(d)
r	Cr	0.77	0.12	0.79	−0.30	0.75	0.38	0.95	0.48	−0.34	−0.67	−0.66	Co	0.77	0.24	−0.06	0.44	0.29	0.52	0.40	0.22	0.61
r_m	Cr	.06	.05	.12	.21	−.01	.03	.94	.14	.00	.04	−.03	Co	.12	.19	.17	.10	.07	.17	.38	−.08	.01
r_o	Cr	.75	.08	.73	−.48	.75	.35	.13	.36	−.34	−.69	−.64	Co	.71	.06	−.22	.35	.22	.38	.02	.29	.60

Table 2--Continued

Note: This page contains a large trace-element correlation table printed sideways. Each cell contains three coefficients read as r, r_m, r_o (given here as the three stacked values), with a footnote letter in parentheses. The transcription below reproduces the cell values as read, grouped by variable.

Variable	$r,\;r_m,\;r_o$ (by column, with footnote)
Co (r / r_m / r_o)	(e) 0.62/.33/.36 · (f) 0.49/.30/.22 · (g) -0.51/-.01/-.50 · (h) -0.38/-.02/-.36 · (i) -0.77/.05/-.79 · Ba -0.18/.06/-.24 · Sr -0.04/.14/-.18 · V 0.64/.03/.63 · Be 0.00/-.01/.01 · (a) 0.47/.13/.36 · (b) 0.52/.26/.30 · (c) 0.15/-.04/.19 · (d) 0.64/.11/.57 · (e) 0.78/.36/.58 · (f) 0.74/.12/.68 · (g) -0.53/-.02/-.52 · (h) -0.54/.00/-.54 · (i) -0.69/-.03/-.68 · Ba (Ba) · Sr 0.25/.09/.16
Ba (r / r_m / r_o)	(v) -0.46/.02/-.48 · Be 0.30/.06/.24 · (a) -0.07/.16/-.23 · (b) 0.22/.23/-.01 · (Be) · (i) -0.17/.01/-.18 · Ni 0.03/-.01/-.04 · Ba -0.43/.17/-.56 · Sr -0.05/.16/-.21 · V -0.11/.03/-.15 · Be 0.33/.02/.31 · (a) -0.07/.07/-.14 · (Sr) · (c) -0.30/.05/-.35 · (d) -0.35/.06/-.41 · (e) -0.30/.13/-.42 · (f) 0.40/.23/.19 · (g) -0.43/-.01/-.42 · (h) 0.04/-.01/-.05 · (i) -0.33/.15/-.46 · Ba 0.10/.19/-.09 · Sr 0.22/.07/.15
Sr (r / r_m / r_o)	(e) 0.26/.05/.21 · (f) 0.25/.09/.16 · (V) · (h) -0.07/.01/-.08 · (i) 0.63/.05/.60 · Ni -0.09/.19/-.27 · Ba 0.51/-.06/.55 · Sr 0.41/.02/.40 · V 0.80/.08/.78 · Be 0.52/.08/.46 · (a) -0.38/-.01/-.39 · (b) -0.60/.01/-.61 · (c) -0.59/-.01/-.59 · (Be) · (e) 0.42/.03/.39 · (f) -0.19/.12/-.30 · (g) 0.45/-.03/.47 · (h) -0.07/.05/-.12 · (i) 0.14/.05/.08 · Ba -0.14/.12/-.25 · Sr -0.24/-.02/-.23
Be (r / r_m / r_o)	(e) -0.28/-.01/-.27 · (f) -0.33/-.02/-.31 · (a)(a)(a) · (b) -0.31/.38/-.62 · (c) 0.91/.75/.49 · (d) 0.37/-.22/.55 · Ba 0.78/.18/.70 · Sr 0.46/.27/.22 · V -0.53/.07/-.58 · Be -0.72/.08/-.76 · (a) -0.85/-.01/-.85 · (b)(b)(b) · (c) -0.66/-.32/-.44 · (d) 0.27/.03/.25 · (e) -0.05/.33/-.38 · (f) 0.31/.43/-.14 · (g) -0.02/.04/-.07 · (h) 0.07/.12/-.05 · (i) -0.06/.06/-.12 · (c)(c)(c) · Sr 0.11/-.25/.34
(c) (r / r_m / r_o)	(e) 0.64/-.03/.66 · (f) 0.20/.00/.21 · (g) -0.39/-.06/-.44 · (h) -0.60/-.03/-.58 · (i) -0.63/-.01/-.62 · (d)(d)(d) · Ba 0.52/.06/.48 · Sr 0.74/.05/.71 · V -0.57/-.11/-.50 · Be -0.24/-.03/-.21 · (a) -0.52/-.09/-.45 · (e)(e)(e) · (c) 0.61/.21/.46 · (d) -0.46/-.01/-.45 · (e) -0.70/-.03/-.71 · (f) -0.77/-.03/-.76 · (f)(f)(f) · (h) -0.58/-.32/-.32 · (i) -0.28/.00/-.28 · (c)(c)(c) · (g)(g)(g)
(g) (r / r_m / r_o)	(h) 0.32/.05/.30 · (f) 0.73/.92/-.56 · (h)(h)(h) · (i) 0.66/.02/.65

22

$$t = \frac{Z \pm Z_m}{\sigma_d}, \tag{8}$$

where σ_d is the standard error of the difference between Z and Z_m, and Z and Z_m are the corresponding Z values for r and r_m. The standard error is derived from:

$$\sigma_d = \left(\frac{1}{P(N_1 - 3)} + \frac{1}{N_2 - 3} \right)^{\frac{1}{2}} = 0.24, \tag{9}$$

where $p = 30$ and N_1 and N_2, the number of rows in the arrays of random deviates and the original data, respectively, are both equal to 21. The significance of t at the 95 percent confidence level is determined from a table of t for ∞ degrees of freedom (Snedecor, 1956, p. 46).

Where a value of r is significantly different from the corresponding value of r_m, at the 95 percent confidence level, it is concluded that the value of r, regardless of its absolute magnitude (i.e., whether it is very high or near zero), could result less than 5 times in 100 by chance alone. The presence of a petrogenetic association is then indicated.

It is apparent from (9) that relatively little would be accomplished by extending the simulation (increasing P). The power of the test for significance is severely limited by the small size of N_2--the number of bediasite specimens studied. The critical value of r where r_m equals zero is $|0.44|$. If P were ∞ the critical value would be $|0.43|$. Where r_m is equal to -0.5, values of r are significant when $r < -0.75$ or $r > -0.03$. If P were ∞ these critical values would be essentially unchanged.

Comparison of correlations in the bediasite data, r, with those from closed arrays of random deviates, r_m

Values of both r and r_m for each pair of variables are given in table 2, and those not involving the 9 functional variables are compared graphically in figure 1. Two properties of the r_m values are especially noteworthy. First, all r_m values involving an open variable (i.e., a column representing a physical property measurement and, therefore, not involved in the closure) are close to zero, the spread about $r_m = 0$

corresponds well to the theoretical standard error of Z[1] :

$$\sigma_Z = \left(\frac{1}{P(N_1 - 3)} \right)^{\frac{1}{2}} = 0.043 \qquad (10)$$

The second property of the r_m values is interesting in view of the fact that the variance of SiO_2 in the bediasite data exceeds the sum of the variances of all other constituents (table 1). All values of r_m involving the column representing SiO_2 are negative, whereas nearly all correlations involving columns representing chemical constituents other than SiO_2 are positive. There are 3 exceptions out of 210 values, and none of these exceeds the absolute quantity of 0.04. This is strong verification of Chayes' conclusion regarding the effects of closure in arrays of this type--namely, that all the correlations of the highly variable column are negative, and that one or more of the other correlations must be positive (Chayes, 1960, p. 4186).

From figure 1 it is apparent that the high correlation, r, between SiO_2 and Al_2O_3 in the bediasite data is not significantly different from that which may be expected solely from the effects of closure. On the other hand, low correlations of SiO_2 with Na_2O and K_2O, while not significant when tested against zero, do depart significantly from the high negative correlations expected in the absence of petrogenetic association. Similarly, the relatively low negative correlation between Al_2O_3 and Na_2O (-0.33) is notably different from the high positive value (0.48) derived from the closed arrays of random deviates, whereas the apparently high correlation between Na_2O and P_2O_5 (0.53) cannot actually be regarded as significant.

An unexpected result of the testing procedure was the discovery that some of the correlations among the minor elements are greatly affected by closure. For example, some values of r_m involving.the column representing Rb are notably high (table 2: Rb vs. SiO_2, Al_2O_3, Co, Na_2O, and K_2O). Rb, however, contributes less than 0.15 percent of the total variance in the original data array, or in the closed arrays of random

---

[1] Values of r less than 0.25 are equal to corresponding values of Z to 2 significant figures.

deviates. Examination of table 1 discloses that the relative deviation
of Rb is notably low, as are the relative deviations of the major constit-
uents, SiO_2 and Al_2O_3. We find, in fact, that the magnitudes of r_m values
correspond rather well, although not perfectly, to the relative deviations
of the constituents involved (table 3). A prevalent feeling among petrolo-
gists seems to be that correlation coefficients involving minor elements
are independent of closure effects and may be interpreted without regard
to such effects. Our experiments suggest, however, that this is not al-
ways true, and that correlations involving any element having a low stand-
ard deviation in proportion to its mean may be affected to an important
degree. On the other hand, the relative deviations of minor elements in
most geochemical data, unlike the bediasite data, are large, and Chayes'
assertion that the closure effects can nearly always be ignored when the
absolute variances are small is undoubtedly true (Chayes, 1960, p. 4185).

Many of the correlations among the nine functional variables, and
between the functional variables and the individual chemical constituents,
that would have attracted interest if we were entirely blind to their
underlying numerical structure, are revealed as completely nonsignificant
(table 2). The correlation between Fe_2O_3 and the Fe_2O_3/FeO ratio, for
example, is almost exactly that obtained from the closed arrays of random
deviates (0.95 vs. 0.93, table 2). On the other hand, the rather weak
correlation between FeO and the Fe_2O_3/FeO ratio in the bediasite data
(0.32) is revealed as a significant indication of an actual positive
relationship; the correlation is significantly more positive than one
should expect from variables with this underlying numerical structure.
The correlation between SiO_2 and the function $Na_2O + K_2O$ (0.23) would be
regarded as nonsignificant without consideration of the effects of the
closure; as shown in table 2, however, the closure imposes strong negative
correlations of SiO_2 on Na_2O and K_2O, thereby causing an even stronger
negative correlation with their sum. As a result, the expected correla-
tion between SiO_2 and $Na_2O + K_2O$ is in the order of -0.73, and the value
of 0.23 is determined to be highly significant.

The preceding discussion has emphasized reversals in judgments ne-
cessitated by observations on the effects of closure. A great many

25

Table 3. Values of r_m arranged in order of increasing relative deviation, C_j, in the constituents represented

Increasing C_j →	SiO_2	Al_2O_3	Na_2O	K_2O	TiO_2	Rb	FeO	Co	CaO	MgO	Ni	Sr	Cr	V	Cu	Ba	Li	MnO	Ga	P_2O_5	Be	Fe_2O_3
Fe_2O_3	-0.20	.11	.12	.12	.07	.10	.12	.07	.06	.05	.15	.03	.06	.04	.07	.05	.13	.05	-.04	.00	.04	Fe_2O_3
Be	-.09	.06	.11	.10	.12	.10	.02	.07	.13	.05	-.01	.06	.05	.01	.09	.06	.06	.03	.06	.04	Be	
P_2O_5	-.24	.20	.19	.21	.13	.20	.08	.12	.09	.15	.07	.09	.05	.08	.02	.06	.00	.05	.05	P_2O_5		
Ga	-.18	.18	.12	.17	.13	.18	.04	.10	.09	.06	.03	.13	.07	.05	.07	.03	.08	.08	Ga			
MnO	-.20	.17	.17	.18	.07	.19	.08	.09	.09	.08	.07	.08	.04	.06	.10	.10	.02	MnO				
Li	-.21	.17	.14	.13	.17	.12	.14	.13	.09	.07	.02	.06	.05	.01	.01	.02	Li					
Ba	-.23	.16	.19	.21	.12	.18	.15	.19	.11	.04	.06	.09	.13	.02	.16	Ba						
Cu	-.26	.22	.18	.18	.16	.18	.15	.07	.10	.01	.11	.14	.07	-.01	Cu							
V	-.20	.19	.17	.16	.12	.10	.04	.10	.11	.09	.03	.05	.06	V								
Cr	-.21	.16	.16	.20	.10	.15	.10	.14	.09	.13	.06	.10	Cr									
Sr	-.23	.20	.18	.21	.14	.20	.12	.17	.16	.09	.14	Sr										
Ni	-.23	.17	.23	.21	.25	.14	.12	.12	.14	.08	Ni											
MgO	-.30	.20	.23	.27	.18	.15	.09	.13	.11	MgO												
CaO	-.33	.23	.28	.24	.22	.31	.14	.20	CaO													
Co	-.32	.25	.34	.32	.29	.29	.14	Co														
FeO	-.59	.27	.25	.32	.20	.21	FeO															
Rb	-.46	.40	.39	.37	.35	Rb																
TiO_2	-.48	.38	.38	.41	TiO_2																	
K_2O	-.64	.49	.47	K_2O																		
Na_2O	-.61	.48	Na_2O																			
Al_2O_3	-.91	Al_2O_3																				
SiO_2	SiO_2																					

Increasing C_j ⟶

← Increasing C_j ⟶

correlations are not affected by closure, and the correlations in the original bediasite data may be properly compared and tested against zero. However, knowing that this procedure is proper would have been difficult without the information gained through the simulation and testing process.

Correlations of the ratio $(FeO + MgO + CaO)/(Na_2O + K_2O)$ with chemical constituents in the bediasites appear to be almost free of closure effects; few r_m values differ very greatly from zero (table 2). (The r_m value representing FeO vs. this ratio is a notable exception.) This ratio, therefore, may be a useful variable in variation diagrams, at least for the bediasites and possibly for other tektite groups. We can be reasonably certain, for example, that the high correlation of SiO_2 with this ratio, as indicated in table 2 or in a variation diagram given by Chao (1963, p. 78), is beyond that which could be caused by the numerical structure of the variables.

Methods of factor analysis

Without attempting an elaborate account of the aims of factor analysis methods, we can nevertheless present a brief qualitative explanation. The primary aim of the procedures is to resolve an array of measures such as the correlations in table 2 into a framework that can be interpreted in terms of geologic processes thought to have been responsible for the variation and covariation in the data. It is rather easy to demonstrate that only a few very simple underlying geologic processes can be fundamentally responsible for matrices of correlation coefficients that are nearly beyond any meaningful overall appraisal by inspection alone. This has already been done by Imbrie (1963, p. 7-12).

An excellent introduction to factor analysis techniques, and their geologic applications, is given by Imbrie (1963). He also provided a FORTRAN computer program for the basic operations (see also Manson and Imbrie, 1964). The methods have already been applied in a number of geologic problems (cf. Imbrie and Purdy, 1962; Griffiths, 1964; Harbaugh and Demirmen, 1964). We used the program given by Imbrie (1963) translated into ALGOL for the B220 computer; this necessitated reducing the maximum number of columns in the data array from 70 to 25. The factor

27

analysis methods, then, included the principal component method of factoring and the varimax method of factor rotation (cf. Harman, 1960, p. 154, 301). Unities were inserted in the diagonals of correlation matrices used as input, thus providing a closed model in the terminology of Cattell (1965, p. 198).

The methods consist, in essence, of plotting n vectors of unit length in n dimensional space by techniques of matrix algebra (or, more correctly, of finding the coordinates of n unit vectors in n dimensional space), where each vector represents a variable and n is the number of variables. The cosine of the angle between any two vectors plotted is equal to the correlation coefficient (or some other measure of association used as input to the procedure) between the variables the vectors represent. Although the n vectors are free to occupy the n dimensional space they commonly occupy somewhat fewer dimensions or occur mostly within fewer dimensions (three vectors would occur mostly in 2 dimensions, for example, when they lie almost in the same plane, or in one dimension when they almost coincide).

Orthogonal axes are placed within the n dimensional cluster of vectors and used as a reference system for describing the vector orientations. The coordinates of the vectors, referred to the axes, comprise the factor matrix. By use of the principal components method of deriving the factor matrix, the reference axes are placed so that the sum of the squares of the vector projections on axis I is a maximum. Axis II is then perpendicular to axis I, but oriented so that the vector projections on it are a maximum. Successive axes are orthogonal to all preceding axes, each placed within the n dimensional space so that vector projections on it are as high as possible in view of the orthogonality restriction (Harman, 1960, p. 155).

Each row in the factor matrix represents one of the n variables and each column refers to one of the n reference axes. The sums of the squares for each of the columns are equal to the eigenvalues of the correlation matrix, whereas the sums of squares for each of the rows are unity. The eigenvalues indicate the degree of clustering of the vectors about the successive axes. If the input to the factor analysis procedure
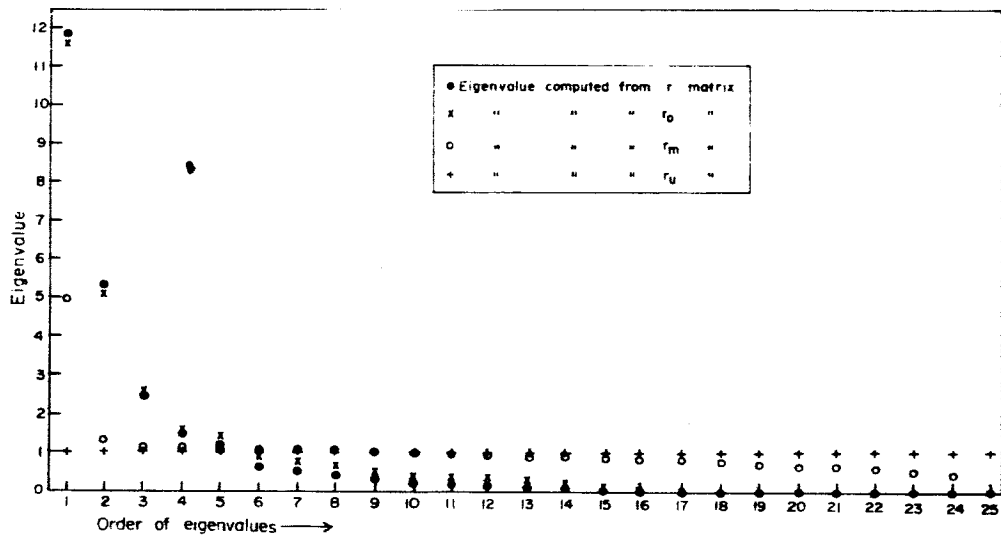
Fig. 2.--Eigenvalues of correlation matrices.

is a matrix of correlation coefficients where all values of $r_{jk} = 0$ ($j \neq k$) and values of $r_{jj} = 1$ (i.e., a unit matrix) all eigenvalues are unity (see eigenvalues of r_u on figure 2), indicating no clustering about any reference axis.

Where some of the correlation values are nonzero, the vectors representing the variables _may_ cluster about the reference axes and, therefore, lie mostly in space of less than n, say m, dimensions. If this is true, it is appropriate to rotate m reference axes so that the vectors will be as closely associated with the new reference system as possible. This is accomplished by applying a mathematical criterion included in the varimax method (Harman, 1960, p. 301). The vectors are then projected into the m dimensional space. A new set of vector coordinates--the rotated factor matrix--is then obtained. The rotated axes, now, may be rotated further into any position desired. Their mutual orientation at this point, however, is generally orthogonal. Oblique reference axes are suitable in some problems (Imbrie, 1963, p. 16).

After projection of the vectors from n to m dimensional space, some or all may be less than unit length. The square of the vector length, h, is termed the communality, h^2, of the variable.

The significance and meaning of factor solutions obtained through the procedure outlined roughly here are most easily realized from a numerical example, as shown by Imbrie (1963), who gave a clear explanation and verification. Here we shall simply state the manner in which each part of the factor analysis may be interpreted in order to arrive at a geologic model to account for the relationships among the variables being studied.

The dimensions of the common factor space (the number of dimensions in which the vectors lie), m, are determined from the successive eigenvalues. Ideally the first m eigenvalues are greater than zero, whereas succeeding eigenvalues are zero. Actually, due to random error in the data (or conversely, to insufficient data) and to nonlinear relationships disregarded in the factor analysis procedure, most of the n eigenvalues will generally be greater than zero. However, if the vectors occupy _mostly_ m dimensional space, the first m eigenvalues will be notably higher

than succeeding eigenvalues. The quantity m is interpreted as the minimum number of independent geologic processes or factors that are required to account for the covariances observed in the data. Departure of the m + 1 and succeeding eigenvalues from zero results from processes or factors that have had smaller effects on the data variation, from nonlinear effects of the factors on the data, and from random data errors.

The communalities, h^2, of the variables are equal to the fraction of variance in the corresponding variable that can be accounted for by the factor solution; the quantity $1 - h^2$ is the uniqueness or the fraction of the variance that is left unexplained. If s_{ej} is the standard error of measurement in the analytical procedure for a variable having standard deviation s_j, then the quantity $[s_j^2(1 - h^2)]^{\frac{1}{2}}$ should equal or exceed that of s_{ej}. That is, the proportion of the variance accounted for by the factor solution should not be in excess of the proportion that is real (that resulting from causes other than measurement error). The proportion of the variance not accounted for by the factor solution or by measurement error can be attributed to other sources of error, to the effects of minor geologic processes or factors (such as those that have affected only one variable or slightly affected a number of variables), or to nonlinear components in the response of the variables to the geologic processes or factors.

Although the positions of the reference axes may be entirely subjective, both the number of axes, m, and the positions of the vectors with respect to each other are derived objectively. After rotation into suitable positions, the reference axes may provide a basis for constructing a geologic model to account for the covariation observed in the initial data. This begins the subjective part of the factor analysis procedure, and is the part where geologic interpretation becomes important. Geologic reasoning is important in selecting the best reference axis system and in determining what geologic factors the axes are to represent. For example, if one vector represents mean grain size, Z_1, an axis F_1, might be rotated to coincide with this vector and named nearness to source area. A second orthogonal axis, F_2, then might be rotated to fall on a vector representing the amount of authigenic muscovite, Z_2, and named degree of

31
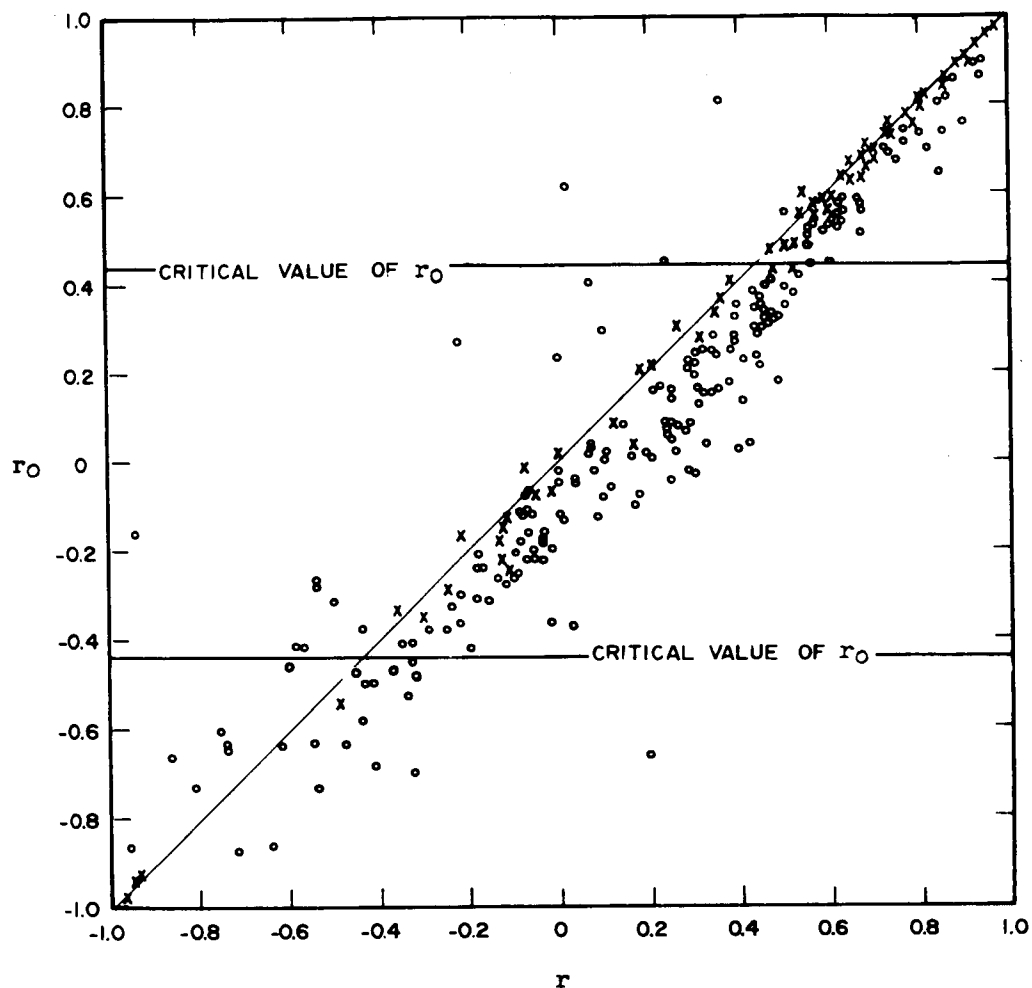
Fig. 3.--Comparison of correlation coefficients, r, derived from the bediasite data with the adjusted correlation coefficients, r_0. Circles represent correlations involving chemical constituents only. Crosses represent correlations involving physical property measurements. Correlations involving functional variables are not represented. Some points falling within clusters of others are not shown.

diagenesis. A third vector--for example, one representing total feldspar content, Z_3--may lie in the plane of the other two, midway between the two reference axes, a position indicating that this variable is controlled by both nearness to source area and degree of diagenesis. Using the co-ordinates of the vectors with respect to the rotated factor axes as coef-ficients, one can write an equation for each variable to show its rela-tion to the factors. These equations comprise the factor pattern, and for the jth variable, have the form:

$$Z_j = a_{j1}F_1 + a_{j2}F_2 + a_{j3}F_3 \ldots a_{jm}F_m. \tag{11}$$

The factor pattern for the example cited above would be:

$$Z_1 = (1) F_1 + (0) F_2$$

$$Z_2 = (0) F_1 + (1) F_2 \tag{12}$$

$$Z_3 = (0.7)F_1 + (0.7) F_2$$

The values of a (in parentheses) are the loadings or projections of the three vectors on the factor axes and are identical to regression weights. Each variable, as well as each factor, is expressed in normalized form (as units of standard deviation from the mean). Using any uncorrelated sets of N values each for F_1, F_2, F_3, ... F_m, an N x n matrix of values may be generated which will contain nearly the same relations among columns as observed in the data from which the loadings, a, were derived (if all communalities are close to 1).

The interpretation of the factor axes may be easy where variables included in the study are known to be strongly controlled by specific factors--otherwise interpretation may be difficult. Where the factors believed to have been important are not independent, the reference axes should not be orthogonal. If the factors are closely allied (as, for example, fracturing and mineralization) the angle between the axes repre-senting them should be small. Where the processes are almost perfectly correlated (as, for example, fracturing and faulting), they may be repre-sented by a single axis.

The factor pattern, then, comprises a mathematically expressed

geologic model that can account for the covariation observed among variables in the data studied. The model, of course, is not unique; it is only one of any number of equally sufficient models that could be proposed. Factor models are, in a sense, minimum models, for they explain covariation in as few terms as possible, ignoring any minor factors and nonlinear effects that may be present; the underlying natural systems may be complex, probably only rarely are they less complex.

Factor analysis of the bediasite data

As described previously, the factor analysis procedures commonly begin with a matrix of correlation coefficients such as the r values in table 2, although other measures of association or relatedness are also used. It has been shown that the r values derived from a compositional data array may be strongly affected by its numerical structure and that a better measure of petrogenetic association is the departure of r from its corresponding r_m. An absolute measure of association, r_o, which may be called the adjusted correlation coefficient, is based on this departure in the following manner:

$$Zo = Z - Z_m \tag{13}$$

$$= \left[0.5 \ln \left(\frac{1 + r}{1 - r} \right) \right] - \left[0.5 \ln \left(\frac{1 + r_m}{1 - r_m} \right) \right] \tag{14}$$

$$r_o = \frac{e^{2Z_o} - 1}{e^{2Z_o} + 1} \tag{15}$$

(Tables of Z for values of r are widely available. See, for example, Fisher and Yates, 1953, p. 54.) Values of r_o for the bediasite data are given in table 2, and compared graphically with the corresponding r values in figure 3. The value of r_o is a measure of the amount of correlation between variables beyond that with can be ascribed to the numerical structure of the data, particularly the constant row sum (closure) and the structure of the functional variables. Values of r_o can be meaningfully compared with zero; those derived from the bediasite data with absolute value in excess of 0.44 are significant at the 95 percent confidence level. As is clear from figure 3 and table 2, most correlations,

r, have been adjusted to r_o in a negative direction. Those involving SiO_2, however, became more positive.

The three correlation matrices in table 2 (r, r_m, and r_o) were each processed through the factor analysis procedures (correlations involving functional variables were not used); eigenvalues for the three matrices are given in figure 2. The first eigenvalue from the r_m matrix, where correlation is due almost entirely to closure effects (only one factor), is near 5; all successive eigenvalues are small. The corresponding eigenvalues for the r and r_o matrices are very similar, indicating that in this instance r is generally not greatly affected by closure. In each case the number of dimensions, m, of the common factor space appears to be 3, although arguments could be given for m = 2 or m = 5.

Whether m is taken as 2, 3, or 5, it is apparent from the eigenvalues plotted in figure 2 that the natural system which controlled compositional variations in the tektites need not have been highly complex. Most of the covariation among measured variables could be accounted for by two to five independent factors.

After rotation of three factor axes, according to the varimax method, the 25 vectors were projected into a three-dimensional space. Most projected vectors were thereby reduced in length from unity to h, where h^2 is the derived communality of the respective variable. Values of h^2 derived using the r_o matrix are given in table 1 (column 10). Those from the r matrix are correspondingly similar. With few exceptions, the unique portion of the variance for each variable is greater than the variance of the analytical error (compare columns 9 and 11, table 1). The exceptions (for variables 3, 9, 16) are not glaring and are attributed to estimation errors in s_j, s_{ej}, and h^2. The total communality for the factor solution is 0.70, indicating that 70 percent of the total variance in the bediasite data can be accounted for by three independent geologic factors.

When the vectors are restored to unit length within the three-dimensional common factor space their relative positions can be conveniently displayed on a stereogram, a device well known to geologists. Stereograms showing the vector positions indicated by the rotated vector coordinates from the r and r_o matrices are given in figure 4. The vector system
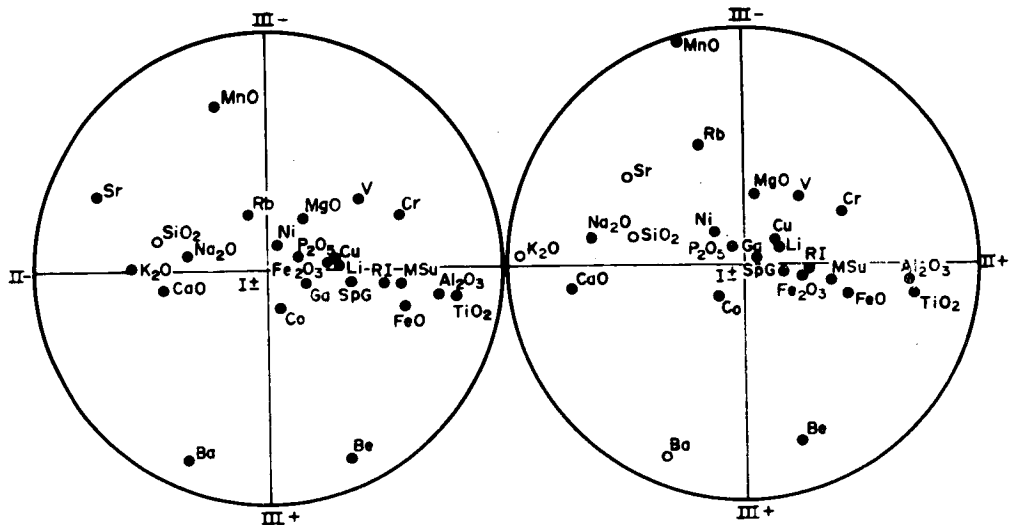
Fig. 4.--Stereograms showing vector orientations within three-factor space, derived from the r (left) and r_0 (right) matrices (table 2). Solid points are plotted on the lower hemisphere. Open circles are plotted on the upper hemisphere.
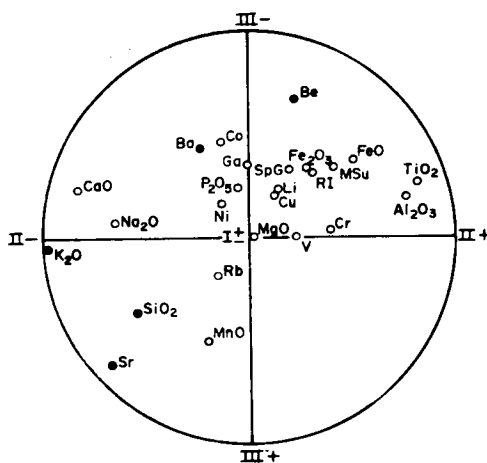
Fig. 5.--Stereogram showing vector orientations within three-factor space with respect to new reference axes, derived from the r_0 matrix. Solid points are plotted on the lower hemisphere. Open circles are plotted on the upper hemisphere.

derived from the r matrix has been rotated into a position roughly comparable to that of the vector system derived from the r_o matrix; this renders the two systems more easily comparable. It is apparent from figure 4 that here the effects of closure are not reflected to any large extent in the rotated factor matrices.

Although the factor solutions from the r and r_o matrices are not greatly different, we focused our attempts at geologic interpretation on that from the r_o matrix--because this solution is based on correlation beyond that which can be ascribed to closure effects. The reference axis positions derived directly from the varimax procedure (figure 4B) did not prove subject to satisfactory interpretation, and the axes were further rotated into the new positions shown in figure 5.

Selection of new positions for the reference axes (figure 5) was based on consideration of factors that may have had important effects on the bediasite compositions. Two kinds of factors seemed important: (1) parent materials from which the bediasites were derived, and (2) processes that acted on the parent materials to alter their compositions during tektite formation. The principal parent material is thought to have been grossly similar, in bulk composition, to a granophyre or average "low-calcium granite." This possibility is evident from a comparison of the compositions given in table 1. It is not likely that this principal parent material was of uniform composition; it undoubtedly varied at least slightly from one locality to another due to slightly varying degrees of magmatic differentiation. Another parent material likely to have been important, if tektites are of lunar origin, is meteoritic matter which may be widely and irregularly distributed on the moon's surface. Addition to the principal parent material of meteoritic matter compositionally similar to chondritic meteorites found on the earth could explain the comparatively higher concentrations of magnesium, iron, nickel, and other basic elements in the bediasite specimens (table 1).

Processes likely to have been important in altering tektite compositions during their formation by meteoritic impact include volatilization of selected elements and possibly the addition of other elements from incorporation of the impacting body itself. The two processes are likely

37

to have had highly correlated effects, each being more intense close to the point of impact, and therefore cannot be distinguished as separate factors. The compositional changes that would result are probably much the same as those that would be caused by assimilation of a basic rock in a granitic melt--an increase in mafic components and a decrease in silica and alkali metals.

With the factor axes rotated into their new positions, as shown in figure 5, the geologic factors they represent can be interpreted in accordance with those factors thought to have been important. Axis I is interpreted to represent incorporation of chondritic meteoritic material into a principal parent material. This factor, then, is the dominant control on variation in MgO, V, Ni, Rb, P_2O_5, Li, Ga, and Cr contents of the bediasites and also has important effects on their refractive indices, specific gravities, magnetic susceptibilities, and iron contents. The vectors representing all these variables have high to moderate positive projections on axis I (figure 5).

Axis II is interpreted to represent nearness to point of impact, or a combined factor representing volatilization and addition of material from the impacting body. The negative correlation of this factor with K_2O, Na_2O, CaO, SiO_2, and Sr is considered to reflect the effects of volatilization, even though not all these elements are regarded as particularly volatile when present as oxides or silicates. The order of volatilization for the major elements in the D-C arc, as given by Ahrens and Taylor (1961, p. 82), is as follows: Na, K > Mn > Si, Fe > Mg > Al, Ca > Ti. Two of the more refractory elements, TiO_2 and Al_2O_3, have high positive projections on axis II and may be enriched in the bediasites on volatilization of less refractory constituents. Other constituents, such as FeO, Cr, and Fe_2O_3, may be enriched in the specimens from nearer the point of impact by addition from the impacting body. The presence of meteoritic iron in tektites from other areas seems evident from studies by Chao and others (1964). The absence of a high positive projection of the nickel vector on axis II cannot be fully explained at present. As pointed out previously, the nickel content of the bediasites, according to the model presented here, is controlled largely by the addition of

38

chondritic material. In any case, the iron and nickel contents of the bediasites are not highly correlated (table 2) and probably were controlled mostly by unrelated geochemical factors.

As to its control on compositional variability, the geologic factor represented by axis III is the least important of the three-factor model. None of the vectors in figure 5 lies particularly close to this axis, although many of them have moderate projections on it. The axis is interpreted to represent the degree of differentiation in the principal parent material, as reflected by the relative sparsity of such accessory minerals as biotite and amphibole. According to this model, variation in the degree of differentiation was not extreme over the bediasite source locality, but did exhibit some control on variation of such constituents as Be, Mn, Sr, SiO_2, and others to a lesser extent. Most basic constituents have minor to moderate negative projection on axis III, whereas SiO_2 and a few other elements have positive projections on this axis.

The model proposed here, therefore, includes three independent geologic factors. The distribution of meteoritic debris on the lunar surface is almost certainly independent of the degree of differentiation that has taken place in the rocks on which it occurs, and neither of these factors is expected to have any bearing on the degree of alteration in the materials with volatilization or enrichment on meteoritic impact. Most basic constituents in the bediasites, as well as the three physical property variables, are related positively to the impact and chondritic material factors, and negatively related to the differentiation factor. The interpretation of the factor axes seems reasonable in view of what is now known about tektite formation, and the response of the variables to the interpreted factors, as shown in figure 5, is for the most part consistent with the known properties of the elements in terrestrial rocks and meteoritic materials. However, these interpretations are subject to change when more is known of lunar geologic conditions and the processes that lead to tektite formation. More important here is the fact that the three-factor model is sufficient to account for approximately 70 percent of the variation in the bediasite compositional data; much of the remaining 30 percent can be attributed to analytical error. Thus, a rather few

geologic processes are adequate to explain the seemingly complex relations among variables as indicated by the correlations listed in table 2.

Concluding remarks

The attention that Chayes (1960, 1962, 1964) has given to the closed array problem in petrology has resulted in both an awareness of the problem and a basis for empirical solutions. Our treatment was possible because it was rather easy to construct arrays of random deviates adjusted to have the same mean, variance, and closure properties as the data we were studying. This may not always be possible, but the extension of Chayes' basic technique, given in equations (3) through (7), should be generally useful for this purpose, especially where nonnegative solutions to (7) exist.

In attempting to assess the effects of closure it is natural to think in terms of open variables that have been forced into a closed array because it is customary and meaningful for us to do so. This trend of thought is difficult in most all problems and may be a futile effort. According to Chayes, Sarmanov and Vistelius (1958) assumed the existence of an underlying system of open variables, but Chayes (1960, p. 4189) himself questioned the necessity for such a system. The entire concept of underlying open variables is highly elusive.

Whether the system of equations in (7) has solutions that are entirely positive seems deserving of careful consideration with respect to the existence of underlying open variables. Negative variances derived from (7) indicate that there can be no open array that will yield on closure the exact means and variances observed in the real data. Whether this observation has any geologic significance is uncertain. The problem must receive much more study.

Testing of individual correlation values against corresponding values that resulted almost solely from the effects of closure enabled us to assess the degree of petrogenetic association required to account for each observed correlation. It is possible to determine whether the effects of closure alone could account for the correlation. However, we are not sure that the problem is this simple. The fact that closure could account

for a correlation is, by itself, no adequate assurance that it did, especially where the open variables cannot be defined in a petrologic sense. On the other hand, we are certain that the necessary practice of collecting geochemical data on a unit weight basis imposes restrictions on its variability. Removal of these restrictions through derivation of adjusted correlation coefficients allows us to examine an underlying system of open variables, even though the system may be entirely conceptual. There is no doubt that highly positive or highly negative values of r derived directly from the original data do not necessarily indicate petrogenetic association, regardless of whether underlying open variables can be defined petrologically.

These rather obscure considerations may raise questions regarding the meaning and importance of the r_o values derived by adjusting the original correlation coefficients for estimated effects of closure. It probably would not be proper to refer to r_o as an estimate of correlation in an underlying system of open variables; it certainly cannot be strongly defended at this time. The r_o value should be regarded as a measure of correlation beyond that to be expected from the numerical structure of the data; it can be compared directly with zero in order to interpret the probable degree of petrogenetic association among variables. In this context then, the r_o matrix, rather than the original r matrix, was interpreted after the factor solutions were derived. It was shown, however, that although many of the r_o values differ quite markedly from corresponding r values, the factor solutions in general were not greatly different.

The apparently large effects of closure on some of the correlations involving minor chemical constituents was not anticipated. The minor elements were represented in the simulation studies because they are not clearly distinct from the elements regarded as major; the distinction made in table 1 is entirely arbitrary. Also, some of the minor elements are included in the functional variables. The suggested use of the relative standard deviation as an approximate indication of the degree to which correlations involving the variable are affected by closure deserves and needs further study.

It is important in this respect to note the importance of relative standard deviation in closure effects. Each array of closed random deviates, having specific column means and variances and intercolumn correlations, may be regarded as having originated from any member of a family of open arrays. The arrays within the family may be identified by the subscript k, where the members are $X_{ijk=1}$, $X_{ijk=2}$, $X_{ijk=3}$ ... . It is necessary that:

and that

$$\overline{X}_{jk=1} = A_1\overline{X}_{jk=2} = A_2\overline{X}_{jk=3} \ \cdots$$

$$s^2_{jk=1} = A_1^2 s^2_{jk=2} = A_2^2 s^2_{jk=3} \ \cdots$$

(16)

Corresponding means among the arrays must differ by a constant, A, and corresponding variances must differ by A^2. This can be shown from equations (30) and (31) of Chayes (1960, p. 4192). The significance of these requirements here is that they impose the condition that each member of the family of open arrays has, column for column, identical relative standard deviations. Open arrays with other relative standard deviations will yield, on closure, different correlations between columns. Thus relative deviations among columns determine the closure effects, though how or if the closure effect can be predicted from relative deviations in either the open or closed arrays is unknown.

A few petrologists have argued that compositional data arrays are not closed, because analyses generally add to some variable quantity commonly between 99 and 101 percent, rather than to 100 percent exactly. This objection actually has little bearing on the problem; the true values being estimated do add to 100 percent exactly, and the true correlations are undoubtedly affected by this constant sum. Small errors in the compositional data cause the sums to deviate slightly from 100, and have only slight effects on the estimated correlations. In any case, where the data errors relative to the variances are about equal among variables, all the correlations among variables, both major and minor elements, are affected to a similar degree.

The factor model presented to account for variations in the bediasite compositional data is highly tentative, and additional consideration and

appraisal of the bediasite data is definitely intended. We hope to study other tektite data anlayzed by the U.S. Geological Survey laboratory by this and similar techniques of multivariate analysis. An entirely satisfactory model can be derived only after this has been done.

Acknowledgments

References

Ahrens, L. H., and Taylor, S. R., 1961, Spectrochemical analysis, 2d ed.: Reading, Mass., Addison-Wesley Pub. Co., Inc., 454 p.

Barnes, V. E., 1939, North American tektites: Univ. Texas Pub. 3945, Contributions to geológy, 1939, pt. 2, p. 477-582.

Cattell, R. B., 1965, Factor analysis: An introduction to essentials. I. The purpose and underlying models: Biometrics, v. 21, no. 1, p. 190-215.

Chao, E. C. T., 1963, The petrographic and chemical characteristics of tektites, in O'Keefe, J. A., ed., Tektites: Chicago, Univ. Chicago Press, p. 51-94.

Chao, E. C. T., Dwornik, E. J., and Littler, Janet, 1964, New data on the nickel-iron spherules from Southeast Asian tektites and their implications: Geochim. et Cosmochim. Acta. v. 28, no. 6, p. 971-980.

Chapman, D. R., 1964, On the unity of origin of the Australian tektites: Geochim. et Cosmochim. Acta, v. 28, no. 6, p. 841-880.

Chayes, Felix, 1949, On ratio correlation in petrography: Jour. Geology, v. 57, no. 3, p. 239-254.

_____ 1960, On correlation between variables of constant sum: Jour. Geophys. Research, v. 65, no. 12, p. 4185-4193.

References--Continued

Chayes, Felix, 1962, Numerical correlation and petrographic variation:
    Jour. Geology, v. 70, no. 4, p. 440-452.

_____ 1964, Variance-covariance relations in some published Harker
    diagrams of volcanic suites: Jour. Petrology, v. 5, no. 2, p. 219-237.

Cuttitta, Frank, Chao, E. C.T., Carron, M. K., and Littler, Janet, 1964,
    Some physical properties and the major chemical composition of
    selected Australasian tektites: Am. Geophys. Union Trans., v. 45,
    no. 1, p. 81.

Fisher, R. A., and Yates, Frank, 1953, Statistical tables for biological,
    agricultural and medical research: New York, Hafner Pub. Co., 126 p.

Griffiths, J. C., 1964, Statistical approach to the study of potential
    oil reservoir sandstones, in Computers in the mineral industries,
    pt. 2: Stanford Univ. Pubs. Geol. Sci., v. 9, no. 2, p. 637-668.

Harbaugh, J. W., and Demirmen, Ferruh, 1964, Application of factor analy-
    sis to petrologic variation of Americus Limestone (Lower Permian),
    Kansas and Oklahoma: Kansas State Geol. Survey Special Distrib. Pub.
    15, 40 p.

Harman, H. H., 1960, Modern factor analysis: Chicago, Univ. Chicago
    Press, 471 p.

Imbrie, John, 1963, Factor and vector analysis programs for analyzing
    geologic data: Evanston, Ill., Northwestern Univ. Tech. Rept. 6
    [of ONR Task No. 389-135, Contract Nonr 1228(26), Office of Naval
    Research, Geography Branch], 83 p.

Imbrie, John, and Purdy, E. G., 1962, Classification of modern Bahamian
    carbonate sediments, in Classification of carbonate rocks, a
    symposium: Am. Assoc. Petroleum Geologists Mem. 1, p. 253-272.

Manson, Vincent, and Imbrie, John, 1964, Fortran program for factor and
    vector analysis of geologic data using an IBM 7090 or 7094/1401 com-
    puter system: Kansas State Geol. Survey Special Distrib. Pub. 13,
    46 p.

Reed, L. J., 1921, On the correlation between any two functions and its
    application to the general case of spurious correlation: Washington
    Acad. Sci. Jour., v. 11, p. 449-455.

References--Continued

Sarmanov, O. V., and Vistelius, A. B., 1958, On the correlation of percentage values: Doklady Akad. Nauk SSSR, v. 126, p. 22-25 [in Russian].

Schnetzler, C. C., and Pinson, W. H., Jr., 1963, The chemical composition of tektites, in O'Keefe, J. A., ed., Tektites: Chicago, Univ. Chicago Press, p. 95-129.

Schüller, A. and Ottemann, J., 1963, Vergleichende Geochemie und Petrographie metoritischer und vulkanischer Gläser (Ein Beitrag zum Riesproblem): Neues Jahrbuch für Mineralogie Abh., v. 100, p. 1-26.

Snedocor, G. W., 1956, Statistical methods, 5th ed.: Ames, Iowa, Iowa State College Press, 534 p.

Turekian, K. K., and Wedepohl, K. H., 1961, Distribution of the elements in some major units of the earth's crust: Geol. Soc. America Bull., v. 72, no. 2, p. 175-192.

SIMILAR PETROCHEMICAL GROUPINGS OF BEDIASITES
AND AUSTRALASIAN TEKTITES

by Donald B. Tatlock

A large part of any reasonable hypothesis of tektite derivation depends on a systematic petrochemical grouping of tektites based on major-element compositions. To my knowledge, no such grouping has been published, although since 1897 more than 200 analyses of bediasites and Australasian tektites have appeared in the literature.

In collating analytical data for this paper, 49 older analyses compiled by Barnes (1940) and 8 compiled by Schnetzler and Pinson (1963) have been rejected because of probable inaccuracies, relative to modern analyses, in one or more of the following: CaO, MgO (Cuttitta and others, 1962; Schnetzler and Pinson, 1963); Na_2O, K_2O, and TiO_2 (Tatlock, 1964). It is also probable that in these older analyses several MnO and total iron determinations are inaccurate. Consequently, only those analyses published since about 1960 and known to have been precisely monitored with recognized analytical standards such as G-1 and W-1 are used. These include 116 complete and 12 partial analyses of Australasian tektites (16, Barnes, 1964; 16 Cuttitta and others, 1964a; 18, Cuttitta and others, 1964b; 34, Schnetzler and Pinson, 1964; 24, Taylor, 1962; 19, Taylor and Sachs, 1964; 1, Wilford and Barnes, 1964) and 23 complete analyses of bediasites representing a wide range in specific gravity and refractive index (22, Chao, 1963; and 1, Schnetzler and Pinson, 1963). One unpublished analysis of a javanite (specimen JS-71, specific gravity 2.558, Dean R. Chapman and Frank Cuttitta, written communication, 1965) is also used in this paper.

A study of these modern analyses strongly suggests that bediasites and Australasian tektites are derived from chemically unaltered igneous materials, and not from sediments or any random mixture of terrestrial materials, as hypothesized by Barnes (1940), Taylor and

Sachs (1964), and many other workers. Both tektites and any differentiated series of salic igneous rocks, when compared with sediments, display:

(1) a highly significant positive correlation of Al_2O_3 with TiO_2, of MgO with total iron as FeO, and, except for javanites, of both Al_2O_3 and TiO_2 with ($FeO + MgO$);

(2) a highly significant negative correlation of SiO_2 with TiO_2, Al_2O_3, and ($FeO + MgO$); and

(3) similar significant trends and restricted fields on commonly used petrologic ternary diagrams (fig. 1).

While any differentiated series of chemically unaltered salic igneous rocks (i.e., rocks that display no evidence of hydrothermal alteration of intense chemical weathering) will show all three of these characteristics, sedimentary materials (fig. 2) and altered igneous rocks do not.

Analyses of bediasites and Australasian tektites differ in some respects, however, from those of a differentiated series, but at the same time they display certain features characteristic of a unit of restricted compositional range (i.e., an igneous unit derived during a single magmatic event from a given melt) within an igneous series. These characteristics are:

(1) a narrow range in ratio of K_2O to Na_2O (figs. 3 and 4);

(2) a nearly constant ratio of Al_2O_3 to TiO_2 (which is about 17:1 in both bediasites and Australasian tektites);

(3) a relatively small range in ratio of MgO to total iron as FeO (this ratio does increase, however, with increasing $(FM)O$); and

(4) a narrow range in MnO whose standard derivation is less than 0.012 percent.

Again, to my knowledge, no units (i.e., formation, group, or series) of sedimentary materials or of altered igneous rocks display all of these characteristics. Among five sedimentary units I have investigated so far (Bailey, Irwin, and Jones, 1964; Murata and Erd, 1964; Reed, 1957; Sweeney and Hamlin, 1965; and Tourtelot, 1962), and for
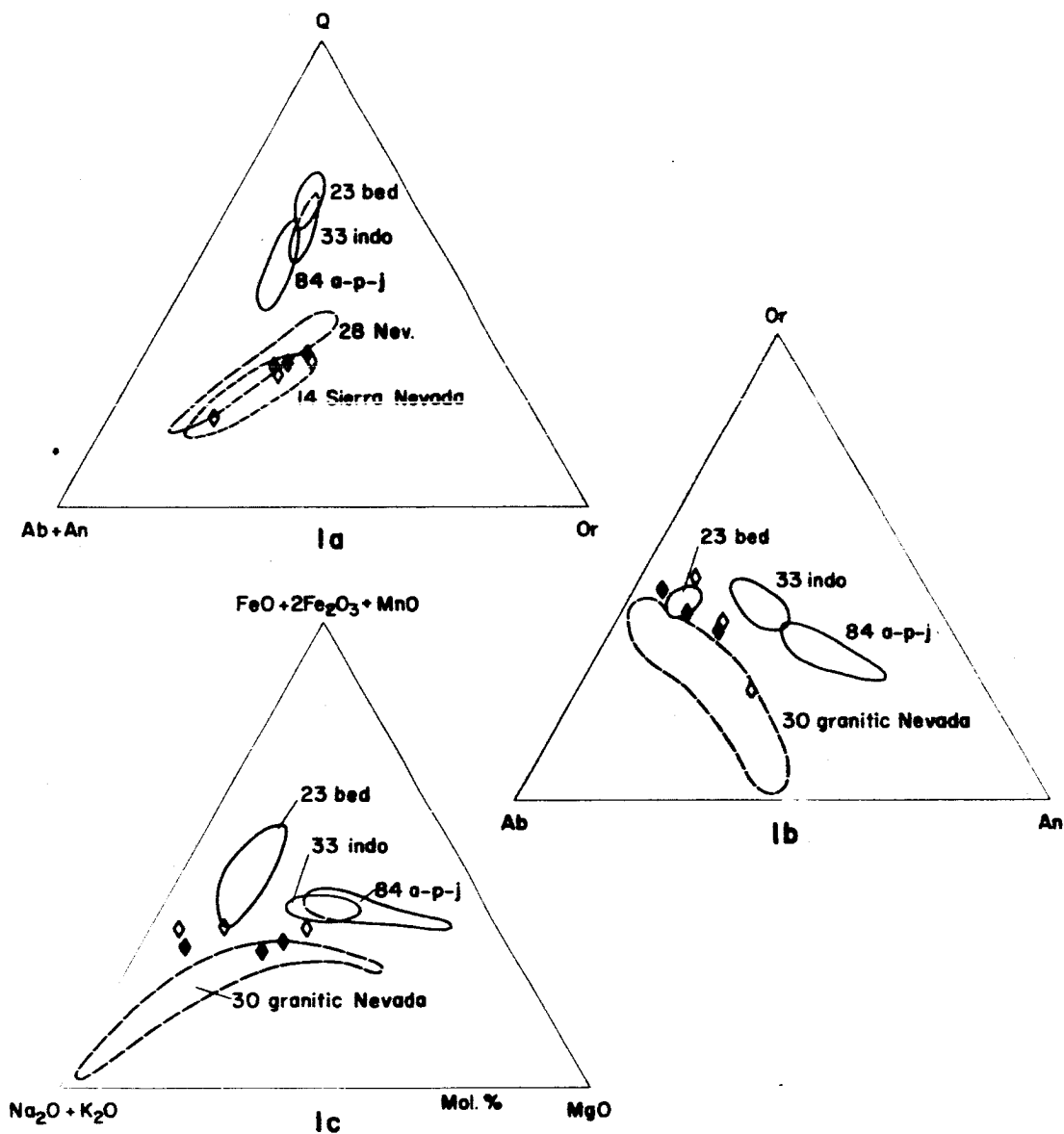
Fig. 1.--Commonly used ternary diagrams showing variation in 23 bediasites, 33 indochinites, and 84 australites-philippinites-javanites, compared with a granitic series from Pershing County, Nevada (unpublished) and from the Sierra Nevada (Bateman, 1961). Open diamonds show average hypersthene-bearing granite, hypersthene-bearing adamellite, and hypersthene-bearing granodiorite of Nockolds (1954). Solid diamonds are reconstituted tektites as described in text.
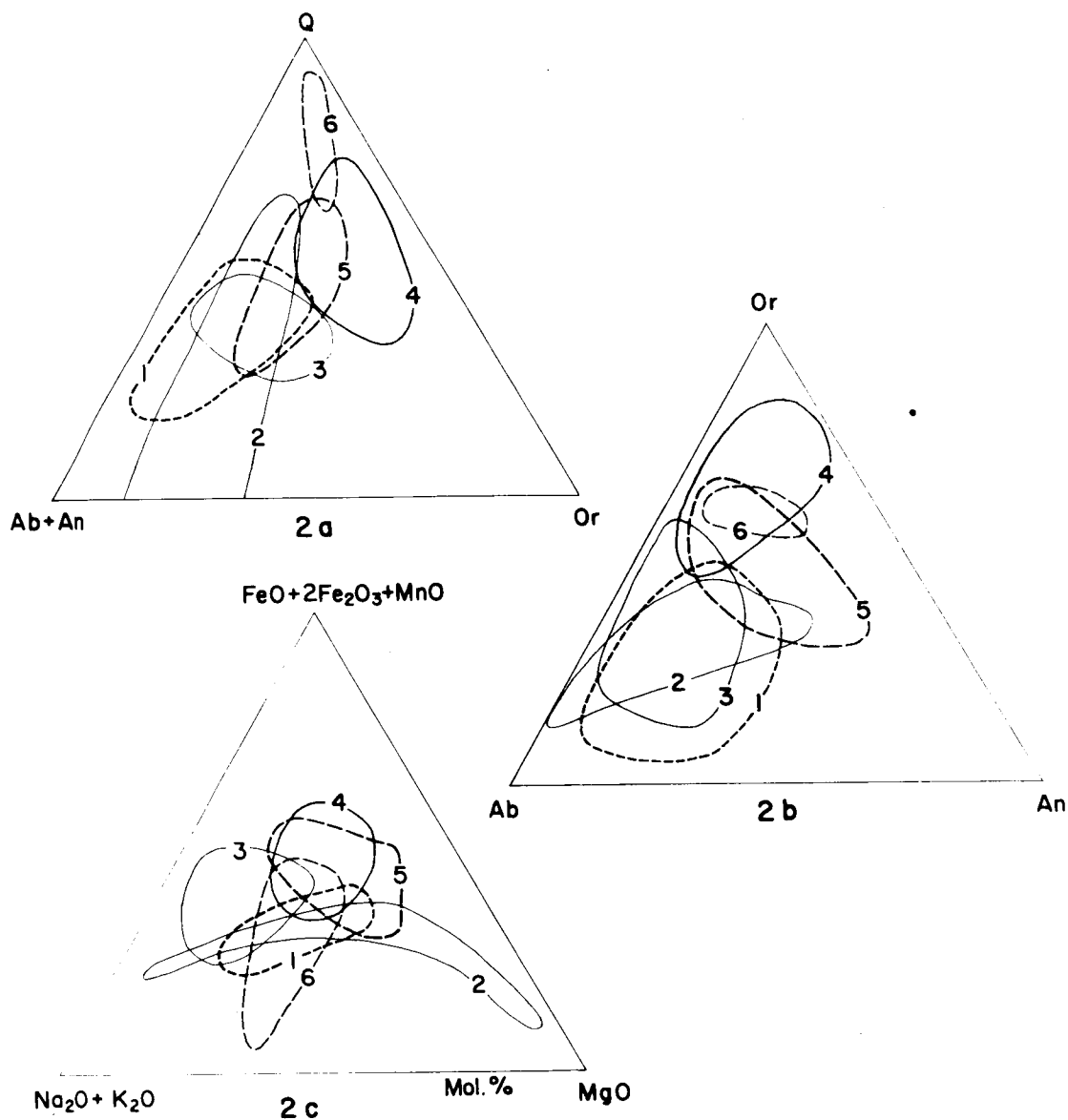
49

Fig. 2.--Commonly used ternary diagrams showing variation in (1) 25 graywackes, Franciscan Formation, Calif.; (2) 34 late Tertiary sediments from experimental mohole, Guadalupe site; (3) 8 graywackes and 7 shales from Wellington area, New Zealand; (4) 20 shales, Illinois; (5) 22 Pierre Shale and (6) 7 graywackes and quartzites, Henbury, Northern Territory, Australia. Compare with figure 1.
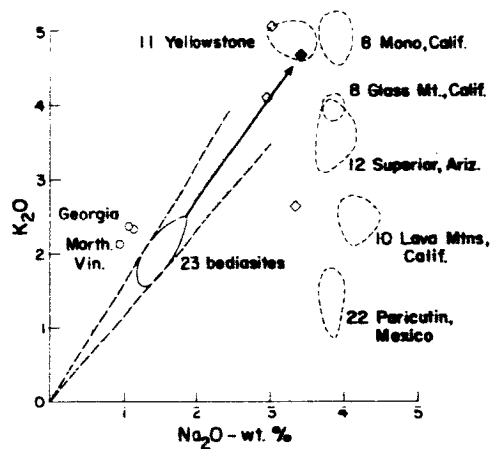
Fig. 3.--Variation of K_2O with Na_2O in 23 bediasites compared with
the variation in some late Tertiary to Recent volcanic rocks. Open
circles are tektites from Georgia and Martha's Vineyard. Solid diamond
is reconstituted bediasite. Open diamonds are average hypersthene-
bearing granitic rocks of Nockolds (1954).
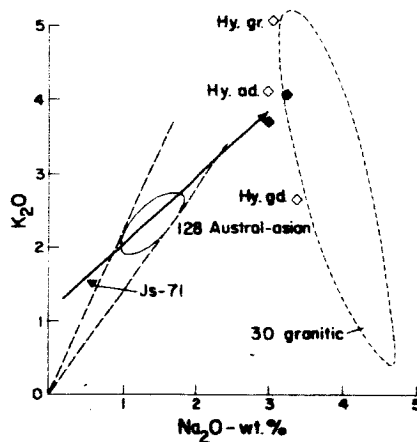
Fig. 4.--Variation of K_2O with Na_2O in 129 Australasian tektites
compared with variation in 30 rocks of a granitic series in Pershing
County, Nevada. Arrow marks trend of changing alkali ratio in tektites.
Solid diamonds are reconstituted indochinite and austral-philippinite.
Dashed straight lines show maximum and minimum alkali ratios.

51

each of which a minimum of 15 modern analyses is available (report in progress), none displays all of the three characteristics that tektites have in common with a differentiated series of salic igneous rocks, or the four they have in common with an igneous unit of restricted compositional range within a series.

Analyses of bediasites and Australasian tektites do differ, however, from those of terrestrial igneous rocks, whether of a series or of a unit within a series, in that they display:

(1) a wide range in SiO_2, Al_2O_3, $(FM)O$, and CaO, while maintaining a nearly constant ratio of Al_2O_3 to TiO_2 and a narrow range in alkali ratio (as well as low total alkali);

(2) a highly significant positive correlation of K_2O with Na_2O and, in Australasian tektites, a distinct increase in ratio of K_2O to Na_2O with decreasing total alkali (fig. 4);

(3) an extremely wide range in Al_2O_3 - $(CaO + Na_2O + K_2O)$ reflected as normative corundum or wollastonite--a range greater by an order of magnitude than is generally found in unaltered salic igneous units;

(4) an excessively high silica content relative to total $(FeO + MgO + CaO)$; and

(5) compared to a differentiated igneous series, no significant correlation of CaO with SiO_2, Al_2O_3, or $(FM)O$.

Points 3, 4, and 5 are among the chief facts used by some investigators to hypothesize a sedimentary origin for tektites.

Except, possibly, for the poor correlation of CaO with various constituents, all 12 of the above-mentioned characteristics of tektites (i.e., three common to a differentiated series, four common to a unit of restricted compositional range within a series, and five different from igneous differentiates) are seemingly compatible with the hypothesis that tektite compositions result from the alteration of an igneous source material of rather restricted compositional range by some sort of "fusion (or volatilization) differentiation" (Chao, 1963; Walter and Carron, 1964), resulting, probably, from meteoritic impact (Walter, 1965) on the moon (Chapman and Larson, 1963).

52

Some of the similarities as well as differences between tektites and igneous rocks are shown in figures 1-6, in which solid diamonds indicate the average normal bediasite, indochinite, and austral-philippinite (fig. 7) to which sufficient alkali has been added (and the analyses normalized) to approximate that contained in hypersthene-bearing terrestrial salic igneous rocks. The average hypersthene-bearing granite, hypersthene adamellite, and hypersthene granodiorite of Nockolds (1954) are plotted for comparison (open diamonds). On the ternary plot Q:Or:(Ab + An) (fig. 1a), the elongate fields of bedia-sites and Australasian tektites are subparallel to those of a differentiated series of terrestrial igneous rocks, chiefly because of their low alkali content, which allows for high excess silica (normative quartz). In figure 1b the fields of normative feldspar proportions of tektites are, again because of low alkali content, subparallel to the field of a differentiated series. Figure 1c shows the tendency for the alkali oxides to decrease with increasing FeO and MgO, just as in igneous differentiation trends. However, the rate of increase in ratio of MgO to FeO with increasing total (FM)O tends to be less in tektites than in igneous differentiates, and a narrow range in alkali ratio is maintained. In the three ternary plots discussed so far, the similarities in trends in igneous rock differentiation and in tektite "differentiation" are clear. The same plots of sedimentary rocks (fig. 2) invariably show greater scatter and no well-defined trends.

Figure 5 emphasizes the wide range in Al_2O_3 - (CaO + Na_2O + K_2O) found in tektites relative to that in unaltered salic igneous rocks. It emphasizes also the narrow range in ratio of K_2O to Na_2O which closely matches that of individual units of unaltered igneous rocks (figs. 3 and 4). In figure 5 all analyses of bediasites plot in the so-called argillic field, which suggests that, if bediasites were to crystallize in the presence of water, all K_2O would be contained in mica, which would make up at least 20 percent of the average crystal-lized bediasite; there would be no k-feldspar, and excess alumina would occur as kaolinite or andalusite. If, however, sufficient alkali (presumably lost by volatilization) were added to the average bediasite

to use up all excess Al_2O_3 while maintaining the original alkali ratio, the resulting analysis recalculated to 100 percent would closely match the average hypersthene-bearing granite of Nockolds (1954). In this regard it is of interest that the range in the quantity Al_2O_3 - (CaO + Na_2O + K_2O) is the same in both bediasites and Australasian tektites, and, as mentioned earlier, nearly an order of magnitude greater than in a given unit of unaltered salic igneous rock. This, combined with the narrow range in ratio of K_2O to Na_2O and of Al_2O_3 to TiO_2, further suggests a similarity in genesis of tektites of widely different age.

In summary thus far, we can say that both tektites and igneous rocks display marked regularity in trends and remarkably little scatter on various petrochemical plots; sedimentary rocks do not. While it may be true that average compositions of certain sedimentary units closely approach the composition of tektites, plots of individual analyses comprising the averages tend to display wide scatter, a fact not emphasized by those who hypothesize a sedimentary origin for tektites. Furthermore, features that distinguish tektite analyses from those of igneous differentiates, as well as the characteristics that both have in common, are all compatible, a priori, with the hypothesis that tektites are derived from an unaltered igneous source material of restricted compositional range by volatilization differentiation (Chao, 1963).

A petrochemical grouping of tektites for hypothesizing genesis

Considering the seemingly erratic behavior of CaO with respect to FeO and MgO in tektites, the wide range in Al_2O_3 - (CaO + Na_2O + K_2O) and in (FM)O, and the narrow range in ratio of the alkalis, any volatilization differentiation trends, as opposed to magmatic trends, should be discernible on an ACF plot which considers all major constituents except SiO_2.

In figure 6, the plots of 117 analyses of Australasian tektites and of 23 bediasites are compared on an ACF diagram with those of 30 plutonic rocks ranging from diorite to granite, and with some hypersthene-bearing granitic rocks of Nockolds (1954). The tektites display
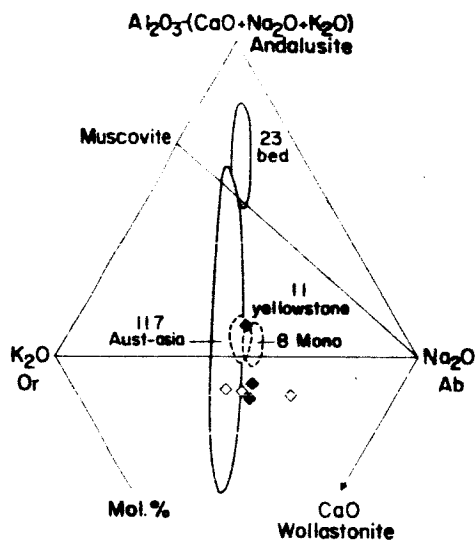
Fig. 5.--Variation of Al_2O_3 - $(CaO + Na_2O + K_2O):Na_2O:K_2O$ in 23 bediasites and 117 Australasian tektites compared with 11 rhyolitic rocks from the Yellowstone Plateau and 8 from Mono Craters, California. Diamonds same as in figure 1.
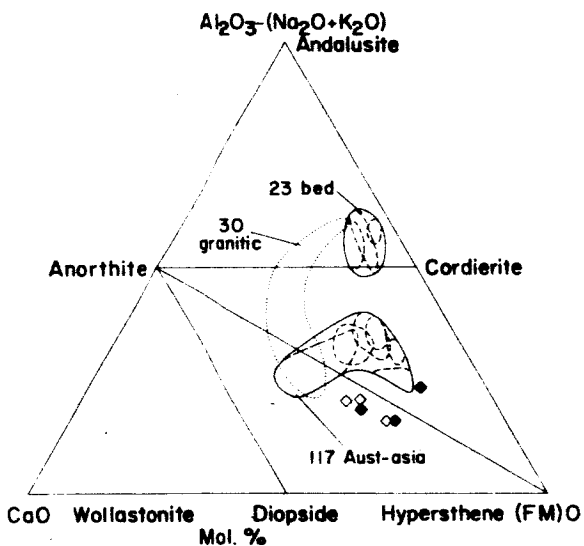

Fig. 6.--ACF plot of 23 bediasites and 117 Australasian tektites compared with 30 granitic rocks (dotted field) ranging from diorite to granite, Pershing County, Nevada. Dashed fields within the overall tektite fields are the various high FM, normal, and low alumina groups referred to in figure 7.

remarkably little scatter, and compositional trends, especially in the
bediasites, are not readily apparent. The trend of the Australasian
tektites is obviously different, however, from that of terrestrial
igneous differentiates. If the ACF plot is modified as in figure 7, with
F as the ordinate and the ratio of C to A as the abscissa, then distinct
chemical groupings, and trends within each group, become apparent.

In figure 7, of the 117 complete analyses of Australasian tektites,
115 fall into six major groups. The three groups with ratios of C to A
ranging from about 0.35 to 0.55 consist entirely of indochinites (includ-
ing thailandites). These I have termed (1) high FM, (2) normal, and (3)
low alumina indochinites. The remaining three groups of Australasian
tektites, all having higher ratios of C to A than the indochinites, I
have termed (1) high FM, (2) normal, and (3) low alumina austral-philip-
pinites. The low alumina group has been subdivided into a peraluminous
group (over-saturated with respect to alumina) and a metaluminous group
(undersaturated). Similarly, the high FM group has been subdivided on
the basis of (FM)0 content. The high FM group consists of nine javanites
and one Brunei tektite. The normal group consists of 16 australites and
30 philippinites, and the low alumina group, of 25 australites and 1
philippinite. The bediasites, with a very low ratio of C to A (very
high normative corundum), display a similar pattern of high FM, normal,
and low alumina groups.

Among the Australasian tektites, the two low alumina groups tend
to display a regular transition from one to the other (figs. 7-9).
Tektites belonging to the normal austral-philippinite group are distin-
guished from those of the low alumina groups in having (Al_2O_3 - CaO) >
0.060 (molecular amount) and (FM)0 > 0.100; they are distinguished from
normal and high FM indochinites in having CaO > 2.40 percent, and from
high FM austral-philippinites (javanites) in having (FM)0 < 0.140 while
Al_2O_3 exceeds 12.00 percent. The two high FM groups tend to have low-
er CaO and higher MgO than their respective normal groups. Furthermore,
javanites have a higher CaO content than do the indochinites; and for
this reason it is probable that they are chemically more nearly related
to austral-philippinites than to indochinites. One australite from
Lake Wilson and one philippinite from Isabella (fig. 7) may possibly
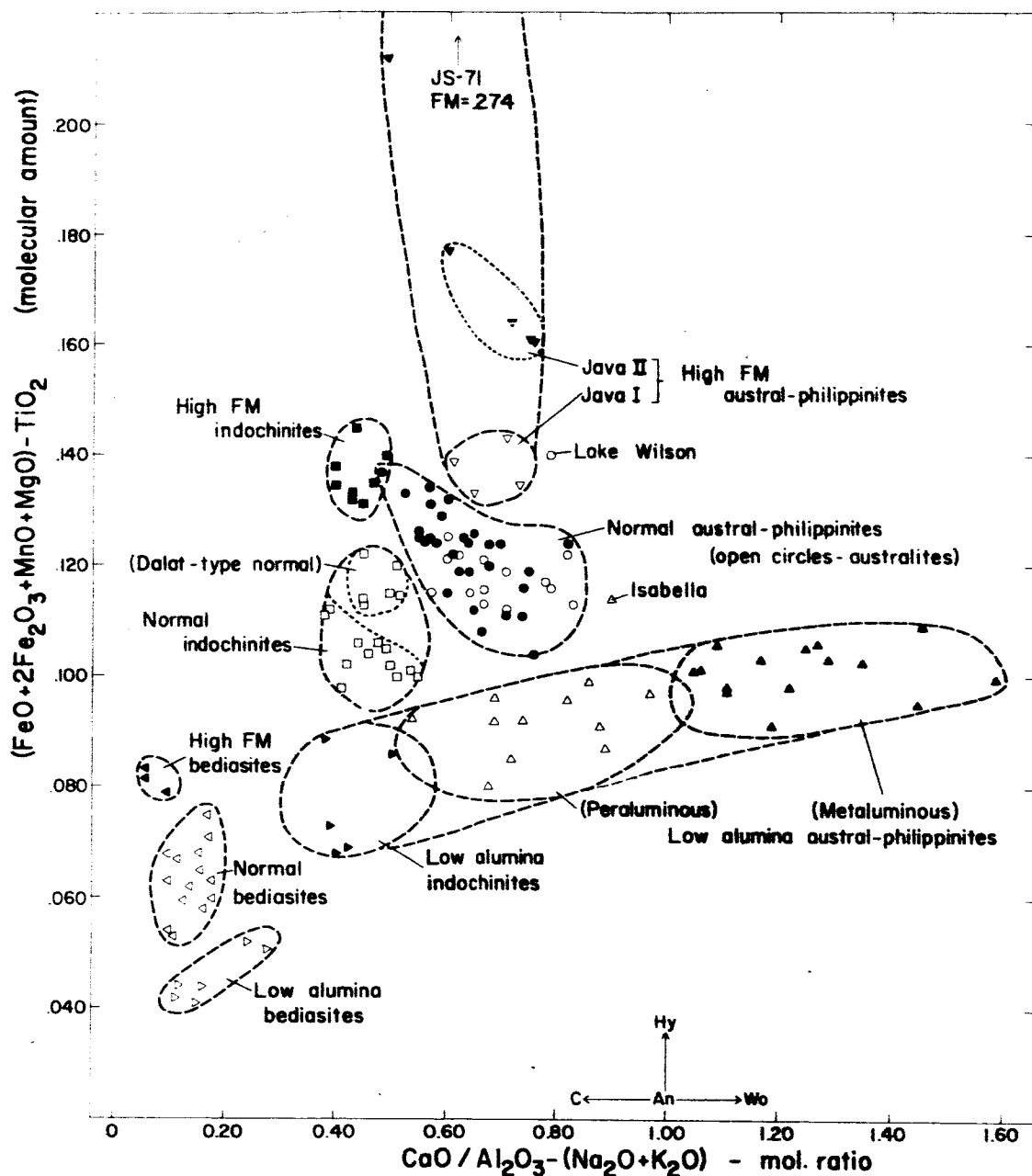mark a group that is transitional between low alumina and high FM

Fig. 7.--Modified ACF plot showing variation of (FM)0 with respect to the ratio of CaO to Al_2O_3 - (Na_2O + K_2O) in 23 bediasites and 117 Australasian tektites. Values of C/A > 1 indicate undersaturation with respect to alumina (metaluminous).

austral-philippinites; it is somewhat surprising that more analyses do
not plot in this part of the diagram.

Several plots other than the modified ACF plot of figure 7 show
similar grouping patterns among bediasites, indochinites, and austral-
philippinites. These include (FM)O versus CaO (fig. 8), Al_2O_3 versus
$(Al_2O_3 - CaO)$, Al_2O_3 versus (FM)O, and (FM)O versus $(Al_2O_3 - CaO)$.
However, the modified ACF plot effects the best separation of groups
while utilizing all major constituents except SiO_2. In figure 9,
plots showing the variation of SiO_2 with CaO in bediasites and Austral-
asian tektites are compared. Again, the similarity in grouping patterns,
especially of the low alumina and normal groups, is striking.

The normal groups

The three normal groups of bediasites, indochinites, and austral-
philippinites are marked by small standard deviations of all major con-
stituents, equivalent to the deviations calculated from groups of analy-
ses of unaltered igneous units such as, for example, an ash-flow sequence
of quartz latitic composition. Tektites belonging to the normal groups
are probably only slightly "differentiated" with respect to their igneous
source material, and except for low total alkali (but higher than in
the low alumina and high FM groups) and hence somewhat too high silica,
are just within the realm of igneous products as we know them terrestrially.

All three normal groups have a similar, relatively wide range in
normative corundum (excess alumina). The normal bediasite and austral-
philippinite groups display a highly significant negative correlation
between normative corundum and total alkali oxide, thus supporting the
hypothesis that the alkalis have been volatilized relative to aluminum.
This correlation is not as highly significant in the normal indochinites,
but will probably become so as more indochinites (and thailandites)
displaying a wider range in specific gravity and refractive index are
analyzed. Among altered terrestrial igneous rocks, a wide range in
normative corundum (or excess alumina) is most commonly a function of
differential loss of alkalis through leaching (hydrothermal alteration),
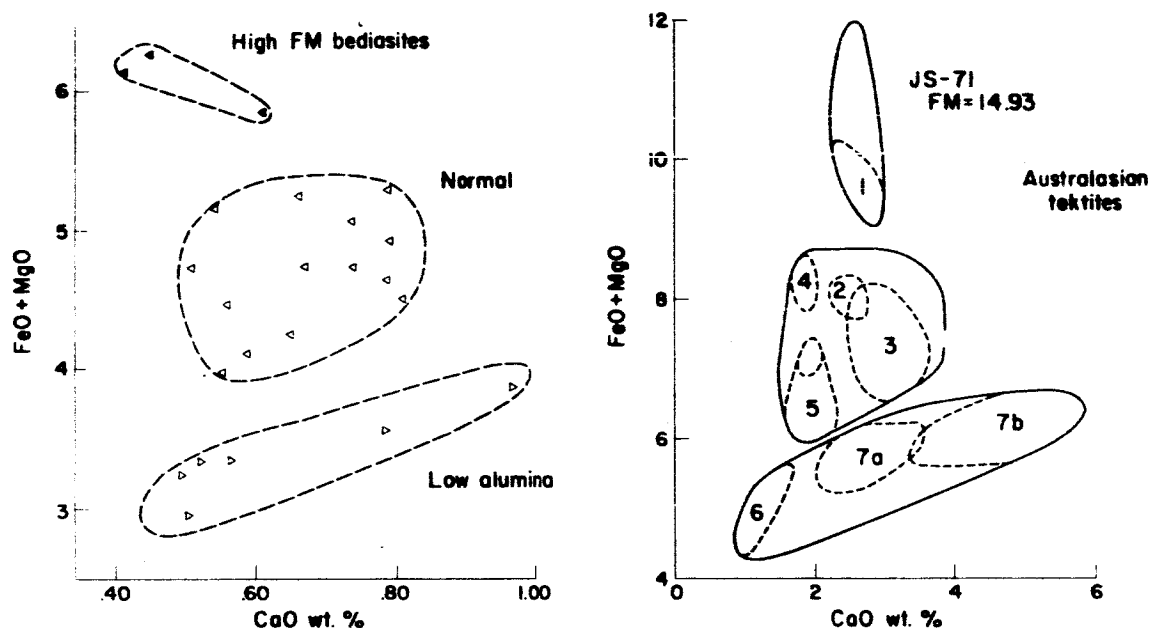and a wide range in alkali ratios invariably results. In tektites,

Fig. 8.--Comparison of variation of (MgO plus total iron as FeO) with respect to CaO in 23 bediasites and 118 Australasian tektites, showing gross similarities in grouping patterns. Numbered fields in Australasian plot are (1) Java II, (2) java I, (3) normal austral-philippinites, (4) high FM indochinites, (5) normal indochinites, including Dalat-type normal, (6) low alumina indochinites, and (7) low alumina austral-philippinites.
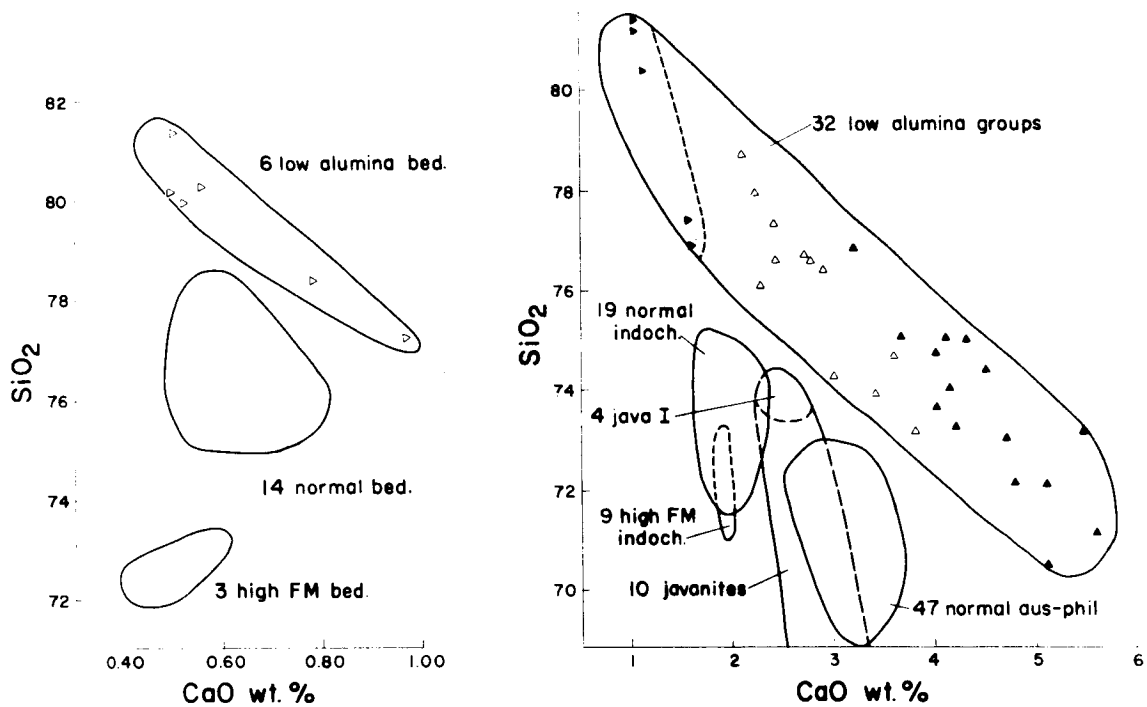
Fig. 9.--Comparison of SiO_2 with respect to CaO in 23 bediasites and 117 Australasian tektites, showing similarities in grouping patterns.

alkali ratios display a remarkably narrow range; and aluminum, of course, is presumably less volatile than the alkali metals.

Iron and magnesium, possibly among the least volatile of major constituents, must also be considered in any hypothetical volatilization differentiation process. In all three normal groups we find a significant negative correlation between Al_2O_3 - $(CaO + Na_2O + K_2O)$ and the ratio of $(Na_2O + K_2O)$ to $(FM)O$. An even more significant negative correlation is displayed in the normal austral-philippinites if normative corundum (excess alumina) is plotted against the ratio of Na_2O to MgO, presumably the most and the least volatile constituents, respectively (fig. 10). In figure 11, the variation of normative corundum with respect to the ratio of $(Na_2O + K_2O)$ to $(FM)O$ in the normal (as well as in the low alumina, and high FM) group of bediasites is shown.

In each of the correlations cited, except for the indochinites, there is less than 1 chance in 1000 that correlation would arise by chance. It should be stressed that in unaltered terrestrial igneous rocks, in contrast to tektites, the correlation of Al_2O_3 - $(CaO + Na_2O + K_2O)$ with total alkali (and with alkali/$(FM)O$) is positive.

The high FM groups

The high FM austral-philippinites (javanites) display a wide range in SiO_2, $(FM)O$, and $(Na_2O + K_2O)$, and a tendency toward a higher ratio of K_2O to Na_2O with increasing $(FM)O$ and decreasing total alkali. Alumina and CaO tend to show an irregular increase with increasing $(FM)O$.

The group can be divided petrochemically on the basis of $(FM)O$ content into two subgroups (java I and java II, fig. 8), which are reflected in the population polygons of specific gravity for java tektites(Chapman and others, 1964). The java I group seems to bear the same relationship to the normal austral-philippinites that the high FM indochinites bear to normal indochinites. Both are marked by low deviations of all constituents, and by lower CaO and Al_2O_3, and higher $(FM)O$ (chiefly as a function of increased MgO) than their respective normal groups. Javanites, however, do have a higher CaO content and a higher ratio of MgO to FeO than do high FM indochinites. In these

respects the javanites and high FM indochinites parallel their respective normal groups. Because of this parallelism it is probable that javanites are not related to the indochinites, as has been suggested by Cuttitta and others (1964b) on the basis of ratios of Cr to Ni.

The three analyses of high FM bediasites show decreasing SiO_2, $(Na_2O + K_2O)$, and CaO with increasing (FM)O, as do the Australasian high FM groups (except for java II). They differ from the latter, however, in showing a more.regular increase in Al_2O_3 with decreasing SiO_2 and increasing (FM)O.

The low alumina groups

The low alumina austral-philippinites display significant negative correlations between silica and all other major constituents including CaO (fig. 9). The low alumina bediasites, on the basis of only six analyses, also tend to display these correlations. The low alumina indochinites cannot be intelligently discussed until more indochinites displaying a wider range in specific gravity and refractive index are analyzed.

Why the low alumina groups should trend at nearly right angles to the trend of the normal and high FM groups(fig. 7) is not yet clear to me. In both the low alumina bediasite and austral-philippinite groups, CaO passes through a twofold increase. It has been suggested by Taylor (1962) and Taylor and Sachs (1964) that the high CaO content of some australites (low alumina austral-philippinites) results from contamination with a CaO-rich material. This I discount because: (1) If mixing with relatively pure limestone had taken place, we should expect a decrease in (FM)O, Al_2O_3, and $(Na_2O + K_2O)$ in the metaluminous group relative to the low lime peraluminous group (fig. 7); actually a significant increase is seen in (FM)O, and a slight increase in Al_2O_3 and $(Na_2O + K_2O)$. (2) If contamination resulted from mixing with an anorthite-rich material (anorthosite, for example), we should expect a substantial increase not only in CaO, but also in Al_2O_3 and Na_2O, with a consequent decrease in (FM)O and in the ratio of TiO_2 to Al_2O_3 and of K_2O to Na_2O. The same arguments with regard to mixing obtain
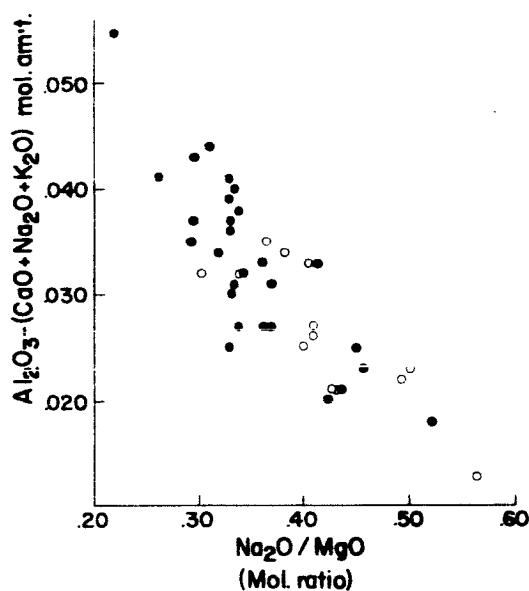
Fig. 10.--Variation of normative corundum (excess alumina) with respect to the ratio of Na_2O to MgO in normal austral-philippinites. Open circles are australites.
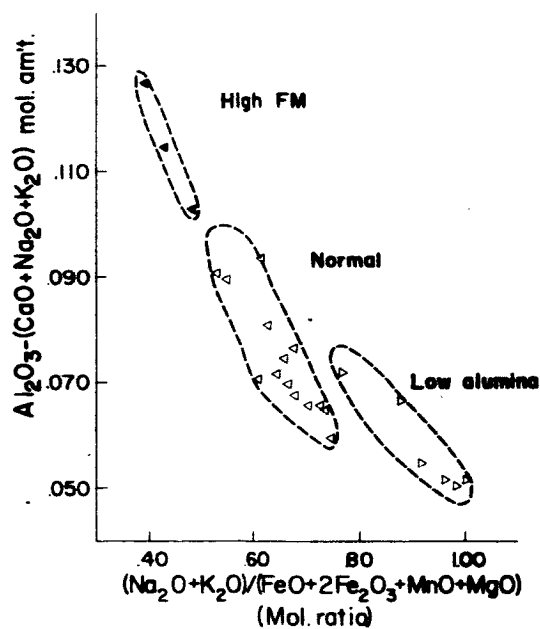

Fig. 11.--Variation of normative corundum with respect to the ratio of $(Na_2O + K_2O)$ to $(FM)O$ in high FM, normal, and low alumina bediasites.

for the low alumina bediasites in which CaO displays significant positive correlation with (FM)O, Al_2O_3, and $(Na_2O + K_2O)$.

The similarity in trends (figs. 7-9) of the low alumina groups in both bediasites and Australasian tektites suggests that some fundamental process, possibly of "volatilization differentiation," is at work; it would be fortuitous if contamination with CaO had affected tektites of widely different age and composition in so similar a manner.

Judging from the similarities in grouping patterns among bediasites, indochinites, and austral-philippinites (including javanites) (fig. 7), it might be hypothesized that Australasian tektites were derived from two similar but distinct igneous source materials, both included in a single lunar impact area. However, a detailed discussion of the various groups must be reserved for a more comprehensive paper in which individual analyses are presented.

Geographic distribution of the various
Australasian petrochemical groups

The petrochemical groupings of Australasian tektites (fig. 7) tend to parallel the different compositional populations found in various areas of Australasia. The locations and petrochemical groupings are cross-referenced in figures 12 and 13. Included in this discussion of geographic distribution are nine partial analyses, three of which belong to the normal group of austral-philippinites and six to the low alumina group. Three partial analyses could not be grouped without a knowledge of their alumina content, and no location is given for one metaluminous australite analyzed by Schnetzler and Pinson (1964).

The petrochemical groupings tend also to parallel the population spectrums of tektite specific gravity in the various areas (Chapman and others, 1964). Thus, a wide spectrum for both specific gravity and chemical make-up are found in tektites extending from the Victoria area to the Charlotte Waters area in Australia. Twenty-six of the 29 analyzed tektites from this area plot in the low alumina group of austral-philippinites. A further breakdown of this area reveals that in the Charlotte Waters area 12 of 18 tektites belonging to the low alumina group are metaluminous (fig. 7); the remaining six are

64

peraluminous while only one is normal, thereby possibly accounting in large part for the two rather distinct population polygons of specific gravity for the Charlotte Waters area (Chapman and others, 1964).

Similarly, the relatively wide range in chemical make-up of the javanites is reflected in their wide spectrum of specific gravity; here, as at Charlotte Waters, two distinct populations are revealed. In Java, however, the wide spectrum is probably chiefly a function of wide range in $(\overline{FM})O$ and SiO_2, whereas at Charlotte Waters it is chiefly a function of wide range in CaO and SiO_2.

Probably the most convincing evidence regarding correlation between chemical composition and specific gravity is provided by the almost identical chemical compositions and population polygons of specific gravity (Chapman and others, 1964) for tektites in the Kalgoorlie area of western Australia and in the Philippine Islands. In both these areas the vast majority of analyzed tektites belong to the normal group of austral-philippinites, although both populations also contain some belonging to the low alumina group.

Among the indochinites, we find that all those belonging to the high FM group seem to be confined to a narrow zone extending from South Vietnam, through the island of Hainan, and onto the southeast coast of China (fig. 12). Included in this area, also, are six normal indochinites containing somewhat higher (FM)0 than the normal indochinites found in Thailand. These six (fig. 7) I have tentatively termed the "Dalat-type normal" indochinites; they may bear the same relationship to normal indochinites that java I tektites bear to normal austral-philippinites, in which case the high FM indochinites would be the counterpart of java II tektites. The "Dalat-type normal" indochinites probably contain considerably more Cr and Ni than do the remaining normal indochinites.

Some normal austral-philippinites have compositions that are transitional toward high FM indochinites (fig. 7). This has been suggested also by the specific gravity studies of Chapman and others (1964). Similarly, one australite from Lake Wilson and one philippinite from Isabella seem to mark a possible transitional group between metaluminous
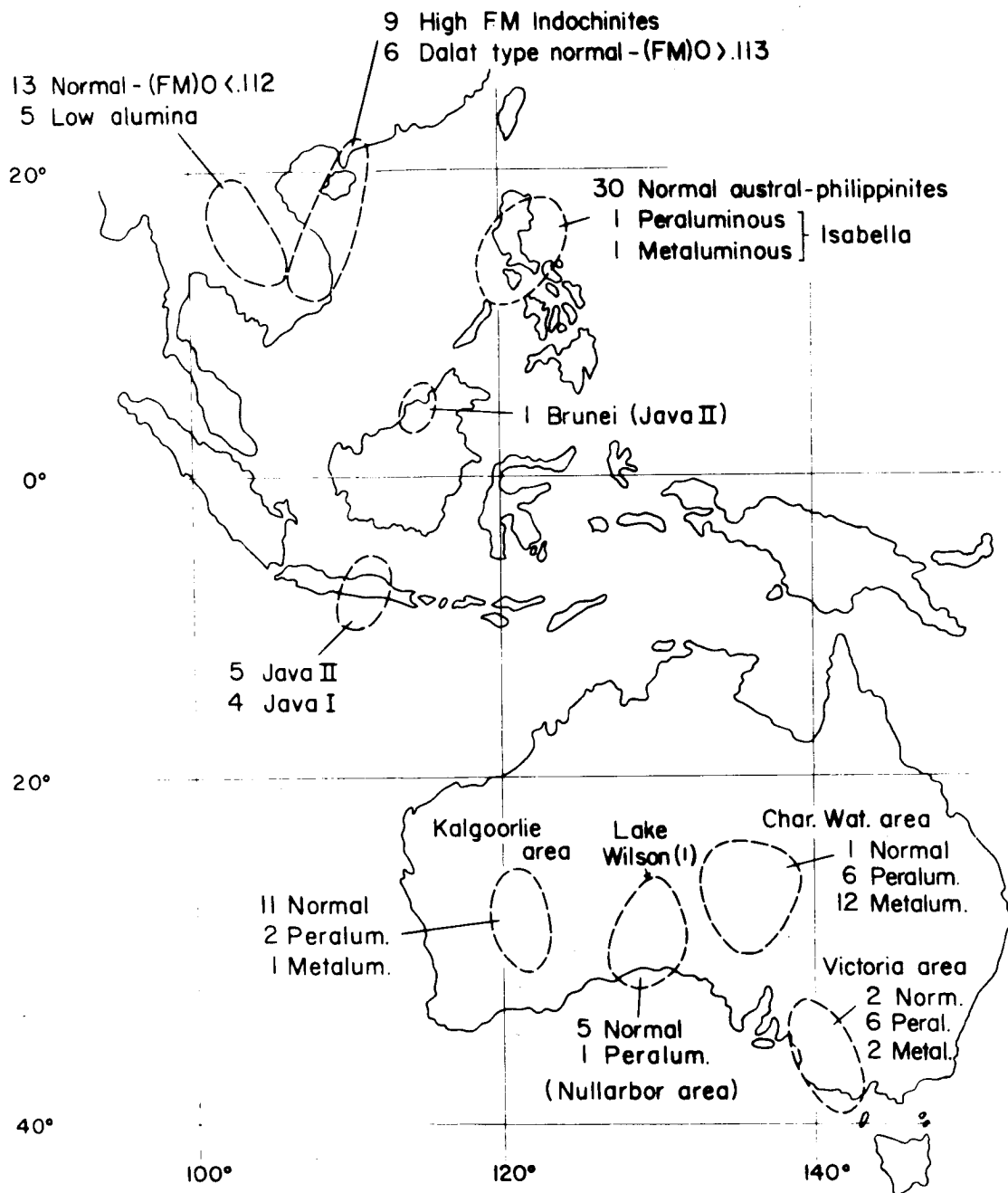
9 High FM Indochinites
6 Dalat type normal-(FM)O > .113

13 Normal-(FM)O < .112
5 Low alumina

20°

30 Normal austral-philippinites
1 Peraluminous ⎤
1 Metaluminous ⎦ Isabella

1 Brunei (Java Ⅱ)

0°

5 Java Ⅱ
4 Java I

20°

Kalgoorlie area   Lake Wilson (1)   Char. Wat. area
1 Normal
6 Peralum.
12 Metalum.

11 Normal
2 Peralum.
1 Metalum.

Victoria area
2 Norm.
6 Peral.
2 Metal.

5 Normal
1 Peralum.
(Nullarbor area)

40°

100°   120°   140°

Fig. 12.--Geographic distribution of 125 Australasian tektites according to their petrochemical groups as outlined on the modified ACF plot of figure 7. Includes 9 partial analyses. May be cross-referenced with figure 13.
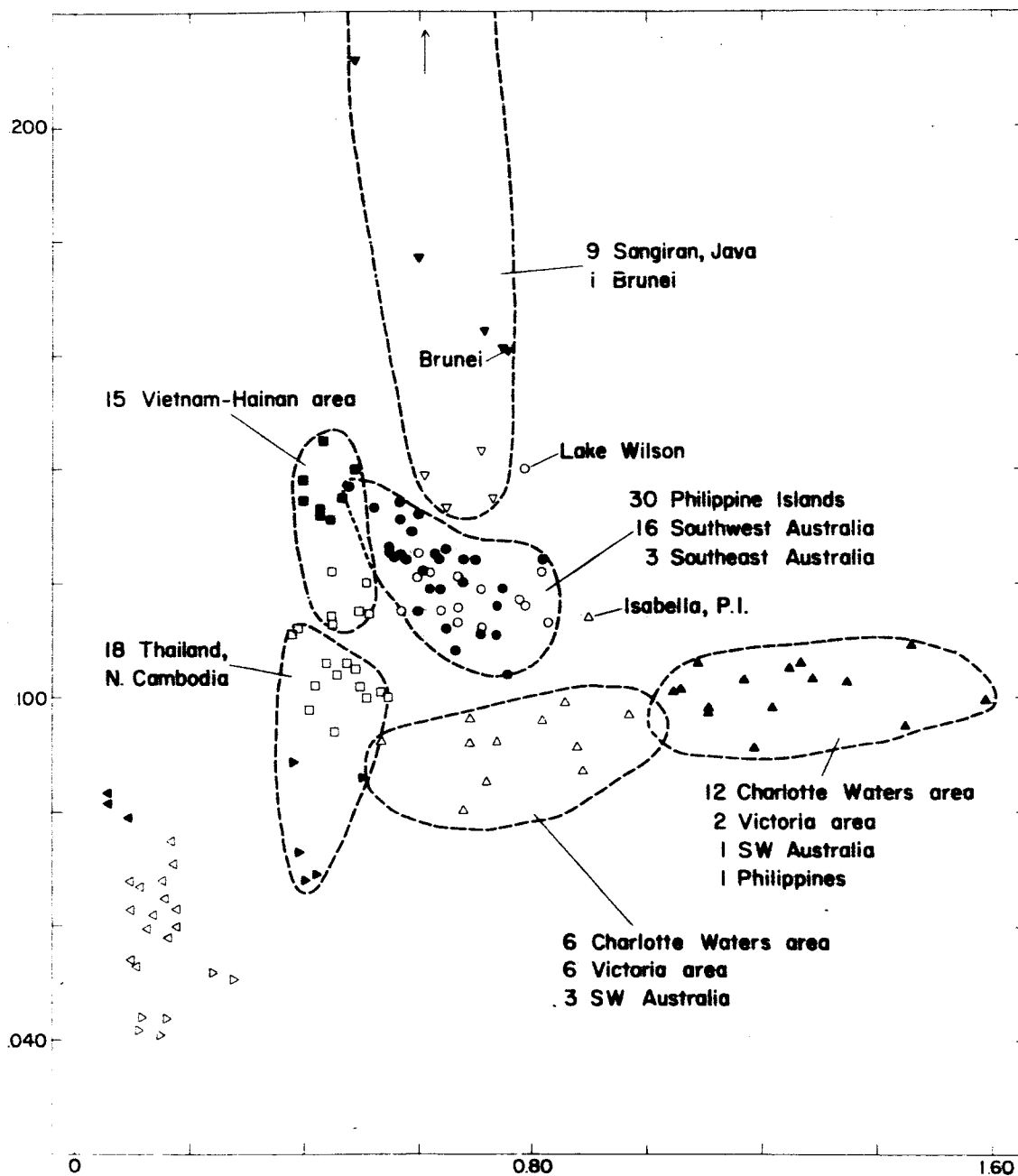
Fig. 13.--Modified ACF plot, as in figure 7, designating the geographic distribution of Australasian tektites within each petrochemical group. May be cross-referenced with figure 12.

67

low alumina austral-philippinites and high FM (java I) austral-philippinites. Transitional compositions might also be hypothesized between low alumina indochinites and peraluminous low alumina austral-philippinites.

Summary and conclusions

Modern major element analyses of bediasites and Australasian tektites strongly indicate a derivation from chemically unaltered salic igneous material of narrow compositional range, by a process of volatilization differentiation. Both tektites and terrestrial igneous rocks display highly significant correlations among various pairs of major constituents; these correlations, as a group, are not found in sedimentary units or among altered igneous rocks. Moreover, tektites maintain a remarkably small range in ratio between K_2O and Na_2O, Al_2O_3 and TiO_2, and (relative to igneous rocks showing a similar range in (FM)O) between MgO and total iron as FeO; they display, also, a small range in MnO. These features, as a group, are not characteristic of sedimentary units, but they are characteristic of a given igneous unit within a differentiated series of unaltered salic rocks.

Tektites differ from igneous rocks, however, chiefly in their (1) wide range in the quantity Al_2O_3 - (CaO + Na_2O + K_2O); (2) highly significant positive correlation of K_2O with Na_2O; (3) wide range in (FM)O and SiO_2 while maintaining a narrow range in ratio of K_2O to Na_2O and of Al_2O_3 to TiO_2; and (4) in having a seemingly erratic CaO content, especially in australites and bediasites. These characteristics make possible, on a modified ACF plot (fig. 7), an effective separation of bediasites, indochinites (including thailandites), and austral-philippinites (including javanites) into three similar grouping patterns, each of which is made up of a high FM, a normal, and a low alumina group. The similar grouping patterns suggest that indochinites and austral-philippinites were derived during a single fusion process from two igneous source materials, differing only slightly in composition, and contained in a single lunar impact area.

The three normal groups, which probably account for most of the

tektite material on earth, are marked by small standard deviations of all constituents, and, except for low total alkali (and hence, somewhat too high silica), closely parallel the compositions of terrestrial hypersthene-bearing salic igneous rocks. In the normal groups, the quantity $Al_2O_3 - (CaO + Na_2O + K_2O)$ displays significant negative correlations with total alkali and with the ratio of alkali to $(FM)O$, suggesting that volatilization differentiation has played an important role in the derivation of tektite compositions. As significant volatilization of alkalis seems possible only at very low partial pressures of oxygen (Walter and Carron, 1964), a lunar source is probable. Considering the heterogeneity of the earth's surface, the great volume of rock involved in a major impact event, and the random nature of any fusion process, and also considering the regularities and similarities in "differentiation" trends among tektites in two strewn fields of widely different age, it is improbable that the source material of tektites was terrestrial.

The geographic distribution of the high FM, normal, and low alumina groups of Australasian tektites shows there are three distinct chemical types (or fusion differentiates) on the Indochina peninsula, two in Java, two in the Philippines, and three (possibly four) in Australia. The compositions of tektites in the Kalgoorlie area of western Australia are, for the most part, indistinguishable from those in the Philippines. These findings are, in general, substantiated by the specific gravity studies of Chapman and others (1964). If it were possible to thoroughly sample and analyze tektites that were strewn into the ocean areas of Australasia, it is probable that many transitional types would be found to plot among the distinct groupings of figure 7.

References

Bailey, E. H., Irwin, W. P., and Jones, D. L., 1964, Franciscan and related rocks and their significance in the geology of western California: Calif. Div. Mines and Geology Bull. 183.

Barnes, V. E., 1940, North American tektites: Univ. Texas Pubs. 3945, p. 477-582.

Barnes, V. E., 1964, Variation of petrographic and chemical charac-
teristics of indochinite tektites within their strewn field:
Geochim. et Cosmochim. Acta, v. 28, p. 893-913.

Bateman, P. C., 1961, Granitic formations in the east-central Sierra
Nevada near Bishop, California: Geol. Soc. America Bull. 72,
p. 1521-1537.

Chao, E. C. T., 1963, The petrographic and chemical characteristics
of tektites, in O'Keefe [ed.], Tektites: Chicago, Univ. Chicago
Press, p. 51-94.

Chapman, D. R., and Larson, H. K., 1963, On the lunar origin of tek-
tites: J. Geophys. Research, v. 68, p. 4305-4358.

Chapman, D. R., Larson, H. K., and Scheiber, L. C., 1964, Population
polygons of tektite specific gravity for various localities in
Australasia: Geochim. et Cosmochim. Acta, v. 28, p. 821-839.

Cuttitta, Frank, Carron, M. K., Fletcher, J. D., and Chao, E. C. T.,
1962, Chemical composition of bediasites and philippinites, in
Astrogeologic Studies Semiannual Prog. Rept., February to August,
1961, U.S. Geol. Survey open-file report, p. 15-36.

Cuttitta, Frank, Chao, E. C. T., Carron, M. K., Littler, J., Fletcher,
J. D., and Annell, C., 1964a, Some physical properties and the
chemical composition of Australasian tektites, in Astrogeologic
Studies Annual Prog. Rept., August 1962 - July 1963, Pt.C,
U.S. Geol. Survey open-file report, p. 1-52.

Cuttitta, Frank, Chao, E. C. T., and Carron, M. K., 1964b, The chemical
composition of selected indochinites and philippinites, in Astro-
geologic Studies Annual Prog. Rept., July 1963 - July 1964, Pt.C,
U.S. Geol. Survey open-file report, p. 65-75.

Murata, K. J., and Erd, R. C., 1964, Composition of sediments from the
experimental mohole project (Guadalupe site): Jour. Sed. Petrology,
v. 34, p. 633-655.

Nockolds, S.R., 1954, Average chemical compositions of some igneous
rocks: Geol. Soc. America Bull. 65, p. 1007-1032.

References--Continued

Reed, J. J., 1957, Petrology of the lower Mesozoic rocks of the
Wellington district: New Zealand Geol. Survey Bull. 57.

Schnetzler, C. C., and Pinson, W. H., Jr., 1963, The chemical com-
position of tektites, in O'Keefe, J. [ed.], Tektites, Chicago,
Univ. Chicago Press, p. 95-129.

_____ 1964, A report on some recent major element analyses of tek-
tites: Geochim. et Cosmochim. Acta, v. 28, p. 793-806.

Sweeney, J. W., and Hamlin, H. P., 1965, Lightweight aggregates, ex-
pansion properties of selected Illinois shales and clays: U.S.
Bur. Mines Rept. Inv. 6614, 34 p.

Tatlock, D. B., 1964, Some alkali and titania analyses of tektites be-
fore and after G-1 precision monitoring, in Astrogeologic Studies
Annual Prog. Rept., July 1963 - July 1964, Pt.C, U.S. Geol.
Survey open-file report, p. 97-109.

Taylor, S. R., 1962, The chemical composition of australites:
Geochim. et Cosmochim. Acta, v. 26, p. 685-722.

Taylor, S. R., and Sachs, Maureen, 1964, Geochemical evidence for the
origin of australites: Geochim. et Cosmochim. Acta, v. 28,
p. 235-264.

Tourtelot, H. A., 1962, Preliminary investigation of the geologic setting
and chemical composition of the Pierre Shale Great Plains region:
U.S. Geol. Survey Prof. Paper 390, 74 p.

Walter, L. S., 1965, Coesite discovered in tektites: Science, v. 147,
p. 1029-1032.

Walter, L. S., and Carron, M. K., 1964, Vapor pressure and vapor
fractionation of silicate melts of tektite composition: Geochim.
et Cosmochim. Acta, v. 28, p. 937-952.

Wilford, G. E., and Barnes, V. E., 1964, Brunei tektites [abs.]: Am.
Geophys. Union Trans, p. 82.

ABUNDANCES OF SOME LITHOPHILE ELEMENTS
IN BASALTIC METEORITES, HYPERSTHENE ACHONDRITES
AND DIOPSIDE ACHONDRITES

by Michael B. Duke

Introduction

Minor-element contents have been determined by optical emission spectroscopy for whole rocks, separated plagioclase and pyroxene from several basaltic meteorites, hypersthene achondrites and diopside achondrites. These data and published minor-element data for basaltic meteorites (eucrites, howardites, and the silicate phase of many meso-siderites) show variations as functions of the major variable $Fe/Fe + Mg$ that are consistent with an origin by magmatic differentiation as proposed by Duke (1963) and Duke and Silver (in preparation). For all elements studied but the alkali metals, the minor-element abundances in basaltic meteorites with $Fe/Fe + Mg < 0.3$ seem similar to chondrites ($Fe/Fe + Mg \sim 0.2$), whereas basaltic meteorites with $Fe/Fe + Mg > 0.5$ show marked differences of many minor-element concentrations with respect to chondrites. Some compositional properties of the basaltic meteorite parent material are inferred from these data.

Minor-element contents of pyroxenes from two hypersthene achondrites are similar to the basaltic meteorite pyroxenes, whereas the pyroxenes of a diopside achondrite and the Sherghotty basaltic achondrite are distinct, especially in their contents of siderophile elements.

New emission spectrographic data

New emission spectrographic analyses of separated plagioclase and pyroxene and of total meteorite samples are given in tables 1-3. The analyses were made in two laboratories: the spectrographic laboratory of the Division of Geological Sciences of the California Institute of Technology, E. Bingham, analyst, and the spectrographic laboratory of the U.S. Geological Survey in Washington, D.C., J. D. Fletcher, analyst.

Table 1. Minor-element abundances in pyroxenes (ppm)

	Sn	Mn	Cr	Co	Ni	Ba	Sr	V	Ti	Nb	Sc	Y	Zr	Fe/Fe + Mg
Hypersthene achondrites														
Shalka	*	4700	3200	<5	<5	<5	<10	280	29	<50	12	<20	<50	0.22
Johnstown	*	4400	*	*	*	*	*	*	*	*	17	*	*	0.22
Mesosiderite														
Crab Orchard	*	5000	*	*	*	*	*	*	*	*	25	<10	*	0.30
Eucrites														
Binda	*	6200	*	*	*	*	*	*	*	*	22	<10	*	0.32
Serra de Mage	11	6700	2250	6.2	6.2	*	4	155	130	20	32	20	<10	0.44
Moore County	89	7200	2100	6.8	4.0	3.3	3	175	290	25	42	31	<10	0.50
Sioux County	14	8400	1850	5.8	3.8	3.8	12	140	330	27	42	25	<10	0.58
Juvinas	14	7400	1650	5.7	3.7	3.6	<2	130	240	25	41	25	58	0.60
Nuevo Laredo	*	6800†	*	*	*	*	*	*	*	*	40†	31	70	0.66
Sherghottite														
Sherghotty	11	6700	1150	42	100	5.6	8	340	200	22	72	19	41	0.50
Diopside achondrite														
Nakhla	13	5100	1250	40	73	11	28	230	120	<10	33	<5	<10	0.

*Not determined.

†Neutron activation analysis by R. A. Schmitt gave Mn, 6710; Cr, 3250; Sc, 47.

Table 2. Minor-element abundances in plagioclase (ppm)

	Mn	Cr	Ni	Ba	Sr	V	Ti	Sc	Li
Mesosiderite									
Crab Orchard	*	*	*	5	100	*	*	*	*
Eucrites									
Binda	*	*	*	14	120	*	*	*	*
Serra de Mage	90	84	< 6	15	110	10	5	< 2	2
Moore County	130	57	< 5	41	130	11	7	< 2	2
Sioux County	560	390	< 5	49	130	20	51	11	10
Juvinas[†]	360	230	< 3	84	130	15	66	5	10
Nuevo Laredo[‡]	630[†]	255[†]	< 5	120	160	16	100	5[†]	20

*Not determined.

[†]Neutron activation analysis by R. A. Schmitt gave Mn, 480; Cr, 1360; Sc, 3.9.

[‡]Nb < 5 ppm; Y < 10 ppm.

Table 3. Minor-element abundances in total meteorite samples (ppm)

	Mn	Sc	Y	Ti	Zr	V	Sr	Ba	Fe/Fe + Mg
Chondrites†	2600	10	2	640	33	65	10	3.4	0.18-0.22
Mesosiderite									
Estherville	2100	16	10	800	13	130	29	5	0.20
Eucrites									
Binda	3600	19	*	930	< 20	140	37	2	0.32
Moore County	2200	18	10	1100	17	120	81	17	0.50
Sioux County	2900	30	20	2200	38	64	80	20	0.58
Juvinas	2500	32	24	1900	41	150	81	26	0.60
Pasamonte	2400	30	18	1700	36	130	70	26	0.61
Stannern	2500	33	37	3000	73	110	92	62	0.61
Nuevo Laredo	3500	40	30	3000	70	70	100	40	0.65

†From the compilation of Mason, 1962.

*Not determined.

Each sample was run at least twice in both laboratories, and several duplicate samples, unknown to the analysts, were submitted as checks on the analytical precision. Standards prepared by mixing known amounts of oxides with a "pegmatite mineral" matrix consisting primarily of quartz and feldspar, which is a good approximation to the silicate matrix of the samples, were run on the same spectrographic plates as the samples. Line intensities were evaluated by comparative densitometry. Both laboratories claim ± 15 percent to ± 20 percent precision on routine analyses. Comparison of analyses obtained on the same samples in the two laboratories showed agreement to within ± 20 percent of the mean for all elements except chromium, for which the analyses made at the California Institute of Technology were too high by a factor of about 3, and strontium, where the Survey analyses were apparently high systematically by a factor of 2 to 3. The Survey values for chromium are reported here because they agree with those obtained by wet chemical analysis (Duke, 1963) and neutron activation analysis (Schmitt and Smith, 1964); the California Institute of Technology strontium determinations are given, as they agree well with those made by Gast (1962), where comparison can be made. The spectrographic analyses for Mn made in both laboratories are in good agreement, but are systematically low by about 30 percent with respect to data obtained by neutron activation analysis (Schmitt and Smith, 1964). Other spectrographic determinations for total meteorites agree well with data compiled by Mason (1962). These values are arithmetic means of at least four determinations, two from each laboratory.

Interpretation

Fractionation between pyroxene and plagioclase

Table 4 gives typical distributions of minor elements between plagioclase and pyroxene in two basaltic meteorites. These data show the elements Sn, Mn, Cr, Co, Ni, V, Ti, Sc, Nb, Zr, and Y to be concentrated in pyroxenes and Ba and Sr to be concentrated in plagioclase. These distributions are consistent with crystal chemistry and normal distributions in terrestrial basaltic rocks.

Table 4. Typical distribution of minor elements in coexisting
plagioclase and pyroxene (ppm)

	Serra de Mage		Juvinas	
	Plagioclase	Pyroxene	Plagioclase	Pyroxene
Sn	0	11	0	14
Mn	90	6700	360	7400
Cr	84	2250	230	1650
Co	0	6.2	0	5.7
Ni	< 6	6.2	< 3	3.7
Ba	15	0	84	3.6
Sr	110	4	130	< 2
V	10	155	15	130
Ti	5	130	66	240
Sc	< 2	32	5	41
Nb	< 5	20	< 5	25
Y	< 10	20	< 10	25
Zr	0	< 10	0	58

The mineral separates were made on small amounts of starting materials and could not be entirely cleaned up in many cases. This was a more important effect for the finer-grained meteorites such as Juvinas than in the coarser-grained meteorites such as Serra de Mage. The smaller apparent magnitudes of elemental fractionations between plagioclase and pyroxene in Juvinas is undoubtedly due to the larger amounts of impurities in those mineral separates than in Serra de Mage separates.

Systematic variations of minor-element abundances

The most obvious correlations of the minor-element data are with respect to Fe/Fe + Mg, which is governed by the composition of pyroxene in the meteorites.

Duke and Silver (in preparation) have used the ratio Fe/Fe + Mg as an indicator of the degree of magmatic differentiation of basaltic meteorites. If this index is used to order the minor-element data in the analyses of mineral separates, Mn and Sc in pyroxenes tend to increase with increasing Fe/Fe + Mg, Cr in pyroxenes tends to decrease and Ba in plagioclase very definitely increases.

In total meteorite analyses, the minor-element content is a function of proportion of the minerals as well as of their compositions. The lack of a significant systematic variation of Mn in whole rock meteorite determinations, for instance, may be due to the fact that with increasing Fe/Fe + Mg, the proportion of pyroxene tends to decrease, whereas Mn in pyroxene tends to increase. Ti, which is concentrated in the mineral ilmenite, whos a general increase with increasing Fe/Fe + Mg. Ba, and to a lesser extent, Sr, which are concentrated in plagioclase, increase with increasing Fe/Fe + Mg. These variations are consistent with the model of magmatic differentiation. With respect to the correlation with Fe/Fe + Mg the whole rock Ba content of Stannern is anomalously high. The same anomalous characteristic is found for the alkali elements and for the rare-earth elements (table 5) in Stannern. Duke (1963) showed that the plagioclase of Stannern is more sodic (An80) than most other basaltic meteorites. The correlations between Ba, alkalis and La suggest that La and other rare-earth elements are concentrated in the plagioclase.

Table 5. Barium, rare-earth element uranium and alkali element concentrations in basaltic meteorites (ppm)

	Ba	La[‡]	U[§]	K[†]	Rb[†]	Cs[†]	Na$_2$O[†]	Fe/Fe + Mg
Chondrites	3.4	0.74	.02	800-900	2-4	.09-.15	0.92	0.18-0.22
Mesosiderite								
Estherville	5	1.12	*	*	*	*	0.18	0.20
Howardites								
Pavlovka	*	*	*	170	*	*	0.17	0.34
Frankfort	*	*	*	210	*	*	0.20	0.29
Eucrites								
Binda	2	*	.0226	*	*	*	0.28	0.32
Moore County	17	*	.0196	187	0.16	.005	0.45	0.50
Sioux County	20	*	.0630	322	0.18	.012	0.42	0.58
Juvinas	26	2.53	*	380	*	*	0.42	0.60
Pasamonte	26	3.21	.0542	390	0.21	.011	0.45	0.61
Stannern	62	4.89	*	690	*	*	0.60	0.61
Nuevo Laredo	40	4.03	.135	410	0.37	.018	0.57	0.66

*Not determined.

[‡]Schmitt and others, 1962, and Schmitt and others, 1963.

[†]From compilation by Mason, 1962.

[§]Lovering and Morgan, 1964; Morgan and Lovering, 1965.

Duke (1963) and Duke and Silver (in preparation) have suggested that the range of Fe/Fe + Mg in basaltic meteorites covers essentially the range from undifferentiated parent material, with Fe/Fe + Mg < 0.3 to highly differentiated rocks with Fe/Fe + Mg > 0.6. If this criterion is used here, some limits can be placed on the minor-element content of the parent material of the basaltic meteorites, which in this interpretation would be similar to the concentrations in Binda, Crab Orchard and Estherville.

These data can also be combined with independent determinations of uranium (Morgan and Lovering, 1964, 1965) and potassium to suggest possible U-K ratios in the basaltic meteorite parent material (table 5). As in the case of Ba and rare-earth elements, the data of Morgan and Lovering (1964, 1965) indicate an enrichment of U with increasing Fe/Fe + Mg, with values close to chondritic concentrations for basaltic meteorites with lower Fe/Fe + Mg (such as Binda). The enrichment of uranium is more extreme than the enrichment of potassium and it is inferred that the U-K ratio varies from about 1×10^{-4} for the undifferentiated basaltic meteorite parent material to about 3×10^{-4} for Nuevo Laredo.

The U-K ratio of 1×10^{-4} is similar to the U-K ratio proposed by Wasserburg and others (1964) for the Earth's upper mantle. This is consistent with a closer relationship of the basaltic meteorites to the Earth than to the chondrites as has been suggested recently by several authors (Wasserburg and others, 1964; Engel and others, 1965). Whereas the rare-earth element ratios seem to relate chondrites to basaltic meteorites in oxygen isotope ratios (Taylor and others, 1965), the basaltic meteorites are dissimilar to the Earth as well as to the chondrites. More data on the basaltic meteorites and the Earth's upper mantle are needed to help resolve these inconsistencies.

The basaltic meteorites are interpreted by Duke and Silver (in preparation) as the crustal rocks of their parent body. The development of the minor-element concentrations in basaltic meteorites may therefore have a direct bearing on the manner in which these elements are distributed during the early formation of planetary crusts. Based on these data, for instance, the crust of the basaltic meteorites'

parent body contains approximately 6 times the uranium content of its parent material (Estherville-like or Binda-like) and 2 times the potassium content. These fractionations and the attendant crustal enrichment of uranium in the parent body may play an important part in the determination of the long-term thermal history of the parent body.

Comparison to chondrites

Previous isolated analyses have shown certain achondrites to have much larger or lesser amounts of elements than chondrites. For example, Reed and others (1960) determined the Ba content of Nuevo Laredo to be 44 ppm. As an isolated number, it was difficult to explain. The present data show that as a function of Fe/Fe + Mg, the Ba content shows a systematic increase from the chondritic value of 4 ppm to more than 40 ppm in Nuevo Laredo. This is consistent with magmatic differentiation of a parent material with an initial Ba content similar to chondrites. The same applies to most other elements except the alkalis. The parent material must have had much smaller quantities of alkalis than the chondrites, as has been suggested previously (Duke, 1963).

Hypersthene and diopside achondrites

The Mn, Cr, and Sc contents of the pyroxenes of hypersthene achondrites are similar to those of the basaltic meteorites, and it is possible that these types are genetically related. Taylor and others (1965) showed that the oxygen isotopic ratios of hypersthene achondrites and basaltic meteorites were identical, further supporting a genetic relationship.

The pyroxene of the diopside achondrite, Nakhla, is similar in minor-element content to that of Sherghotty, an atypical basaltic meteorite, and these pyroxenes are distinctly different from other basaltic meteorite pyroxenes.

The most obvious differences are in the siderophile elements, Co and Ni, which are much more abundant in the pyroxenes of Nakhla and Sherghotty. This feature is correlated with the presence of primary magnetite and the absence of metallic iron in these two meteorites. Higher partial pressures of oxygen during the magmatic crystallization

of Nakhla and Sherghotty may have prevented the separation of a metallic phase with consequent scavenging of nickel and cobalt as suggested for the basaltic meteorites by Duke (1965).

Acknowledgments

References*

Duke, M. B. (1963), Petrology of the basaltic achondrite meteorites: Ph. D. dissertation, California Institute of Technology.

_____ (1965), Metallic iron in basaltic achondrites: Jour. Geophys. Research, v. 70, p. 1523-1527.

Engel, A. E. J., Engel, C. G., and Havens, R. G. (1965), Chemical characteristics of oceanic basalts and the upper mantle: Geol. Soc. America Bull., v. 76, p. 719-734.

Gast, P. W. (1962), The isotopic composition of strontium and the age of stone meteorites-I: Geochim. et Cosmochim. Acta, v. 26, p. 927-944.

Lovering, J. F., and Morgan, J. W. (1964), Uranium and thorium abundances in stony meteorites-1. The chondritic meteorites: Jour. Geophys. Research, v. 69, p. 1979-1988.

Mason, B. H. (1962), Meteorites: New York, John Wiley & Sons, 274p.

Morgan, J. W., and Lovering, J. F. (1964), Uranium and thorium abundances in stony meteorites-2. The achondritic meteorites: Jour. Geophys. Research, v. 69, p. 1989-1994.

_____ (1965), Uranium and thorium in the Nuevo Laredo achondrite: Jour. Geophys. Research, v. 70, p. 2002.

Reed, G. W., Kigoshi, K., and Turkevich, A. (1960), Determinations of concentration of heavy elements in meteorites by activation analysis: Geochim. et Cosmochim. Acta, v. 20, p. 122-140.

Schmitt, R. A., and Smith, R. H. (1964), Abundances of Na, Sc, Cr, Mn, Fe, Co and Cu in 18 meteorites and 146 individual chondrules: Gen. Atomic Quart. Prog. Rept. GA-4997.

Schmitt, R. A., Smith, R. H., Lasch, J. E., Olehy, D. A., Perry, K. I., and Mosen, A. W. (1962), A program of research for the determination of rare-earth elemental abundances in meteorites: Gen. Atomic Quart. Prog. Rept. GA-3411.

Schmitt, R. A., Smith, R. H., and Olehy, D. A. (1963), Rare-earth, yttrium and scandium abundances in meteoritic and terrestrial matter: Gen. Atomic Quart. Prog. Rept. GA-4221.

Taylor, H. P., Jr., Duke, M. B., Silver, L. T., and Epstein, S. (1965), Oxygen isotope studies of minerals in stony meteorites: Geochim. et Cosmochim. Acta, v. 29, p. 489-512.

Wasserburg, G. J., MacDonald, G. J. F., Hoyle, F., and Fowler, W. A. (1964), Relative contributions of uranium, thorium and potassium to heat production of the earth: Science, v. 143, p. 465-467.

A PROPOSED ORIGIN FOR COHENITE

by Robin Brett

Introduction

Cohenite $(Fe,Ni)_3C$ occurs in metallic and stony meteorites, and in terrestrial deposits of native iron. It is the natural equivalent to cementite (Fe_3C), from which it differs only by containing nickel and a trace of cobalt.

Cohenite, like cementite, is metastable at all temperatures at 1 atm pressure and decomposes in measurable times at elevated temperatures. Its occurrence in meteorites therefore suggested to Ringwood (1960) that it formed at pressures of 25 kb or more. This would require a parent body of at least lunar dimensions. Since the appearance of Ringwood's paper, the literature on cohenite has been active.

In view of the current interest in cohenite and of the broad implications of a high pressure origin, a thorough study of its occurrence, decomposition kinetics, and phase equilibria has been attempted.

Controversial literature exists on the origin of cohenite. Leading contributors have been Ringwood (1960, 1965) and Ringwood and Seabrook (1962), who argue a high-pressure origin for the phase, largely on thermodynamic grounds, and Lipschutz and Anders (1961, 1964), who opposed Ringwood initially with the argument that phosphorus stabilizes cohenite at 1 atm and more recently with the suggestion that previous thermodynamic and phase equilibria studies on the system Fe-C are incorrect, so that cohenite is stable at neither high nor low pressures. Ringwood and Seabrook (1962) and Ringwood (1965) have refuted the objection of Lipschutz and Anders.

The occurrence and composition of cohenite

Structure and composition

Cohenite is orthorhombic, space group Pbnm (Palache and others, 1944), and contains 0.5 to 3 wt. percent nickel (Lovering, 1964; Brown and Lipschutz, 1965). On the basis of published analyses, it is unlikely that the cobalt content exceeds 1 wt. percent or that the carbon content deviates much from the stoichiometric ratio.

Terrestrial occurrence

Cohenite is found in the native iron of Ovifak, Disko Island, Greenland (Löfquist and Benedicks, 1941; Lovering, 1964), which occurs as segregations in a series of basalt flows. Abundant graphite accompanies the iron and cohenite.

Lovering (1964) states that the overall composition of the metallic masses at Ovifak approximates the composition of a hypereutectoid steel containing about 3 wt. percent carbon, 1.7 wt. percent nickel, 0.6 wt. percent cobalt, and 0.2 wt. percent copper. Cohenite also occurs in the native iron of the glassy basalt flows at Bühl in Germany (Ramdohr, 1953).

Meteoritic occurrences

Stony meteorites.--Cohenite has been reported in the enstatite chondrites Abee (Dawson and others, 1960), Indarch (Ramdohr, 1964), and St. Mark's (P. Ramdohr, written communication, 1965). Ramdohr (1963) states that cohenite is rare in the stones and generally occurs with kamacite (α-Fe, Ni) in a structure that is partly pearlitic. The metal in Abee contains 4.5 wt. percent nickel, and 0.2 wt. percent carbon (Dawson and others, 1960). Electron-probe analyses of the metallic portion of St. Mark's by K. Fredriksson (oral communication, 1965) are as follows:

Fe	91.0	89.9
Ni	4.0	6.3
Si	3.2	3.5
Co	tr.	tr.
C	n.d.	n.d.

The metal in Indarch contains 6.7 wt. percent nickel, if it is assumed
that all the nickel is in the metal phase and the data of Wiik (1956)
are used.

Iron meteorites.--Cohenite has been confirmed in the 26 iron meteor-
ites listed in table 1. The mineral has been reported in other meteorites;
but E. P. Henderson and S. H. Perry (unpublished manuscript) state that
all other reported occurrences require confirmation.

Twenty-one of the 26 meteorites in which cohenite has been con-
firmed have nickel contents between 6 and 8 wt. percent, and 20 of these
21 are coarse octahedrites. Less than one in three analyzed iron meteor-
ites have nickel contents within this limited range of composition (Yavnel,
1958). Thus it would appear that the distribution of meteorites that con-
tain cohenite is not random and that cohenite, with certain exceptions, is
restricted to meteorites containing between 6 and 8 wt. percent nickel.

In the octahedrites, cohenite occurs almost exclusively in irregular,
scalloped and rounded grains, up to a few millimeters maximum length,
elongated along kamacite lamellae (fig. 1). It is rarely found in contact
with taenite (E. P. Henderson and S. H. Perry, unpublished manuscript).
Rims of cohenite may surround small schreibersite $[(Fe, Ni)_2P]$ bodies,
as in the Canyon Diablo meteorite. Cohenite also occurs as rims around
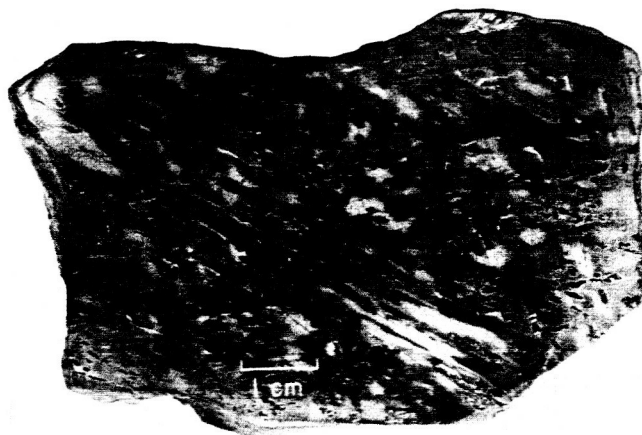
Fig. 1.--Etched surface of Canyon Diablo meteorite showing unusually
large amounts of scalloped cohenite roughly aligned along kamacite lamel-
lae. Point counting reveals carbon content of about 0.6 wt. percent,
extremely high for iron meteorites. (Photo by the late S. H. Perry.)

Table 1. Iron meteorites in which cohenite has been confirmed

Meteorite	Type[*]	Approx. Ni[†]	Cohenite confirmed by
Bendego	Og	6.5 - 7.0	Mason, 1962
Breece	Om	9.0 - 9.5	Henderson and Perry, 1958
Canyon Diablo	Og	7-8	Mason, 1962
Chesterville	NPA	5-6	Perry, 1944
Coolac	Og	6.5 - 7.0	Mason, 1962
Cosby Creek	Og	6.5 - 7.0	" "
Cranbourne	Og	6-8	" "
Gun Creek	Om	6-7	E. P. Henderson (oral comm., 1965)
Lexington Co.	Og	7.0 - 7.5[‡]	Mason, 1962
Locust Grove	NPA	5.5 - 6.0	Perry, 1944
Magura	Og	7 - 7.5	Mason, 1962
Mooranoppin	Og	7 - 7.5	" "
Mt. Ayliff	Og	6.5 - 7.0	" "
Mt. Stirling	Og	6.5 - 7.0	" "
Navajo	NPA	5-6	" "
Odessa	Og	7-8	" "
Pittsburg	Og	6.5 - 7.0[§]	" "
Rosario	Og	?	" "
St. Francois Co.	Og	6.5 - 7.0	" "
Seligman	Og	6.5 - 7.0[‡]	" "
Seymour	Og	?	E. P. Henderson (oral comm., 1965)
Smithville	Og	7.0 - 7.5	Mason, 1962
Tambo Quemada	Om	9.5 - 10[‡]	Perry, 1942-53
Wichita Co.	Og	7.5 - 8.0	" "
Yenberrie	Og	7.0 - 7.5[‡]	" "
Youndegin	Og	6-7	" "

[*]The revised classification of Lovering and others (1957) has been used.

[†]Nickel analyses are from Prior (1953), except where noted. Analyses are given as a range to the nearest 0.5 wt. percent.

[‡]E. P. Henderson, unpublished data.

[§]Henderson and Perry, 1958.

graphite inclusions (El Goresey, 1965). Perry (1944) states that cohenite is confined to areas rich in carbon compared to the bulk of the meteorite.

The occurrence of cohenite in the nickel-poor ataxites Navajo, Locust Grove, and Chesterville, and the medium octahedrites, Breece and Tambo Quemada differs from the above. In Locust Grove, Chesterville, and Tambo Quemada the cohenite occurs in a fine-grained eutectic texture consisting of metal, schreibersite, and cohenite (Perry, 1944). Dendritic forms, indicative of rapid cooling, are common.

Perry (1942-53) states that the cohenite in Navajo is extremely fine grained. In Breece, cohenite is sparse and very fine grained; it could not be detected microscopically, but only by leaching and subsequent x-ray methods (Henderson and Perry, 1958).

Carbon in meteorites

It is clear that the carbon content of an alloy is important in cohenite formation. The graphite and carbon contents of meteorites are therefore discussed below. It would appear that meteorites containing cohenite are high in carbon.

Observations by Heide and others (1932), Perry (1944), Nininger (1952), E. P. Henderson (oral communication, 1965) and the present writer leave little doubt that carbon commonly occurs in the iron meteorites both as macroscopic nodules and microscopic inclusions. Carbon analyses of iron meteorites are probably not representative of the true carbon distribution because of the extremely patchy occurrence of graphite nodules. Published carbon analyses for iron meteorites range from zero to over half a percent. Buddhue (1946), from a compilation of previous analyses, gives 0.2 wt. percent as the average carbon content of hexahedrites and octahedrites. Buddhue's analyses show that all classes of iron meteorites may contain carbon. Perry (1944) states that Dungannon, Canyon Diablo, Savannah, Seelasgen, and Cosby's Creek all have high carbon contents of between 0.4 and 0.55 wt. percent. It is noteworthy that two of these five meteorites with high carbon contents also are known to contain cohenite.

The system Fe-Ni-C

To speculate on the origin of cohenite it is necessary to review the published literature on the formation of phases in the Fe-Ni-C system. The three binaries constituting the ternary system have been investigated in some detail; however, few studies have been made of the ternary system, so far as the writer is aware. The lack of study is not due to unimportance of the system, but rather to experimental difficulty. Reaction rates in the binary system Fe-Ni are extremely slow, and both the systems Fe-C and Fe-Ni are beset with problems caused by the appearance of metastable phases. The present ternary phase diagrams have therefore been compiled entirely by extrapolation of data from the bounding binary systems. The extrapolation in the composition region of interest is of a fraction of a weight percent only, and therefore is justifiable.

Assemblages involving cohenite are metastable and decompose in time to the assemblage metal + graphite. Cohenite may be treated as a stable phase in the diagrams by analogy with cementite in the system Fe-C, in which metastable equilibria involving cohenite are reversible.

System Fe-C

Fe_3C is metastable at all temperatures at low pressures, but nucleates in preference to the stable Fe + C (fig. 2). On prolonged annealing, cementite decomposes. The carbides Fe_2C (Hofer and others, 1949), Fe_2C_3 (Herbstein and Snyman, 1964), Fe_3C_2 (Senateur and others, 1962), and Fe_4C (Pinsker and Kaverin, 1956) have been reported, but they are unstable with respect to Fe_3C.

Kaufman (1965) has summarized data on the system at high pressures. The eutectoid composition becomes more iron rich with pressure, so that the solubility of carbon in α-Fe decreases with pressure. In addition, both the temperature of the eutectoid and the γ-α transition decrease with pressure. The revised high-pressure diagram of Lipschutz and Anders (1964) may be disregarded as shown by Ringwood (1965). Similarly, the P-T diagram presented by Olsen (1964) has been neglected in the present study, as it is inconsistent with the well-established 1-atm
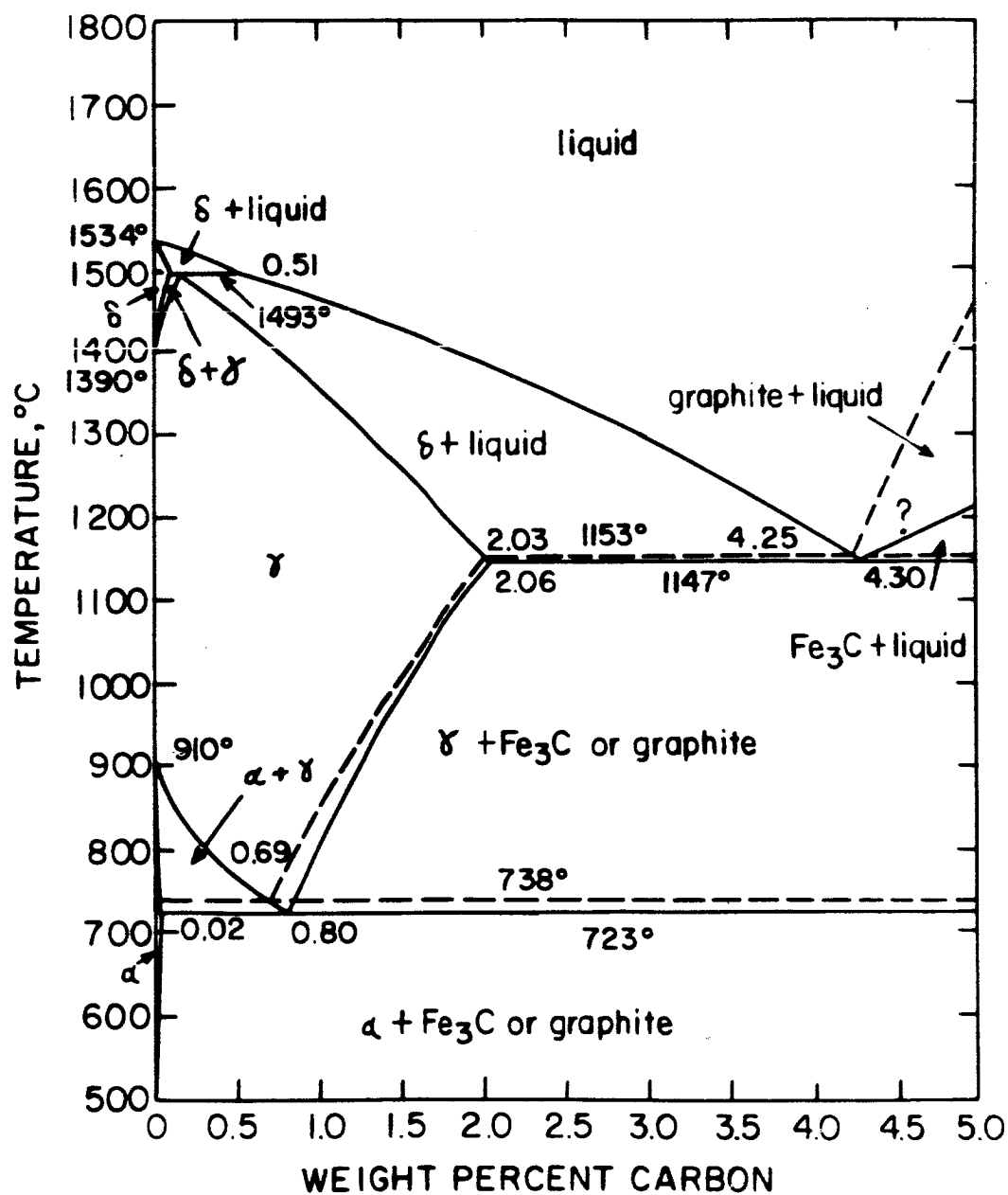
Fig. 2.--Portion of the temperature-composition diagram Fe-C at 1 atm (after Hansen and Anderko, 1958). Solid lines represent metastable equilibria, dashed lines true equilibria. α = kamacite, γ = taenite.

pressure phase diagram (Hansen and Anderko, 1958) and with the high-pressure data summarized by Kaufman (1965). The stability field of Fe_3C in the hypoeutectoid region is that shown by Lipschutz and Anders (1964, figure 3).

System Fe-Ni

Equilibria in the system Fe-Ni are shown in figure 3 after Goldstein and Ogilvie (1965a).

The Fe-Ni diagram has been calculated from thermodynamic data for high pressures by Kaufman and Ringwood (1961) and Ringwood and Kaufman (1962).

System Ni-C

The low-temperature, nickel-rich portion of the diagram is shown in figure 4. The solubility of carbon in nickel at 700° C is 0.08 wt. percent according to Lander and others; hence by extrapolation, is a few hundredths of 1 percent at lower temperatures.

Nickel carbide (Ni_3C) is not stable at any temperature at low pressures (Hofer and others, 1950). The system has not been investigated at high pressures.

System Fe-Ni-C

The isothermal sections drawn in figures 5 and 6 are based on the preceding data on the three binary systems and from the results of Heller and Branner (1964), who found that for alloy compositions from Fe_{100} to $Fe_{95}Ni_5$, nickel has no detectable influence on the solubility of carbon in kamacite (α - Fe,Ni). The results of Samuel and others (1955) have not been used, as they are inconsistent with the well-established iron-carbon temperature-composition diagram.

In drawing the sections, the following assumptions have been made:

1. The nickel content of cohenite in equilibrium with kamacite and taenite is assumed to be approximately 3 wt. percent, in keeping with natural occurrence.

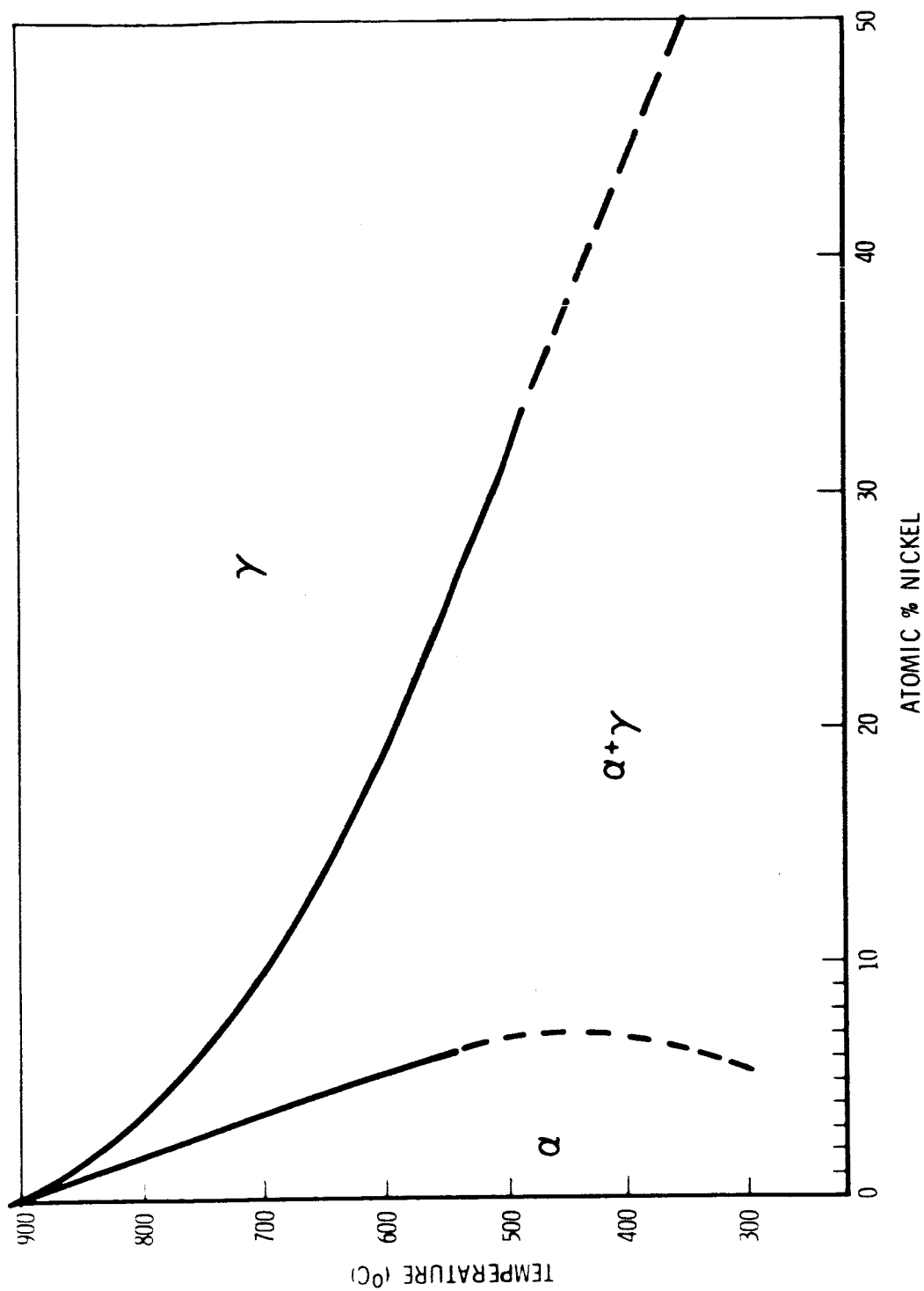2. All boundaries of solid solution fields are assumed linear

Fig. 3.--Temperature-composition diagram of the system Fe-Ni (after Goldstein and Ogilvie, 1965a). α = kamacite, γ = taenite.
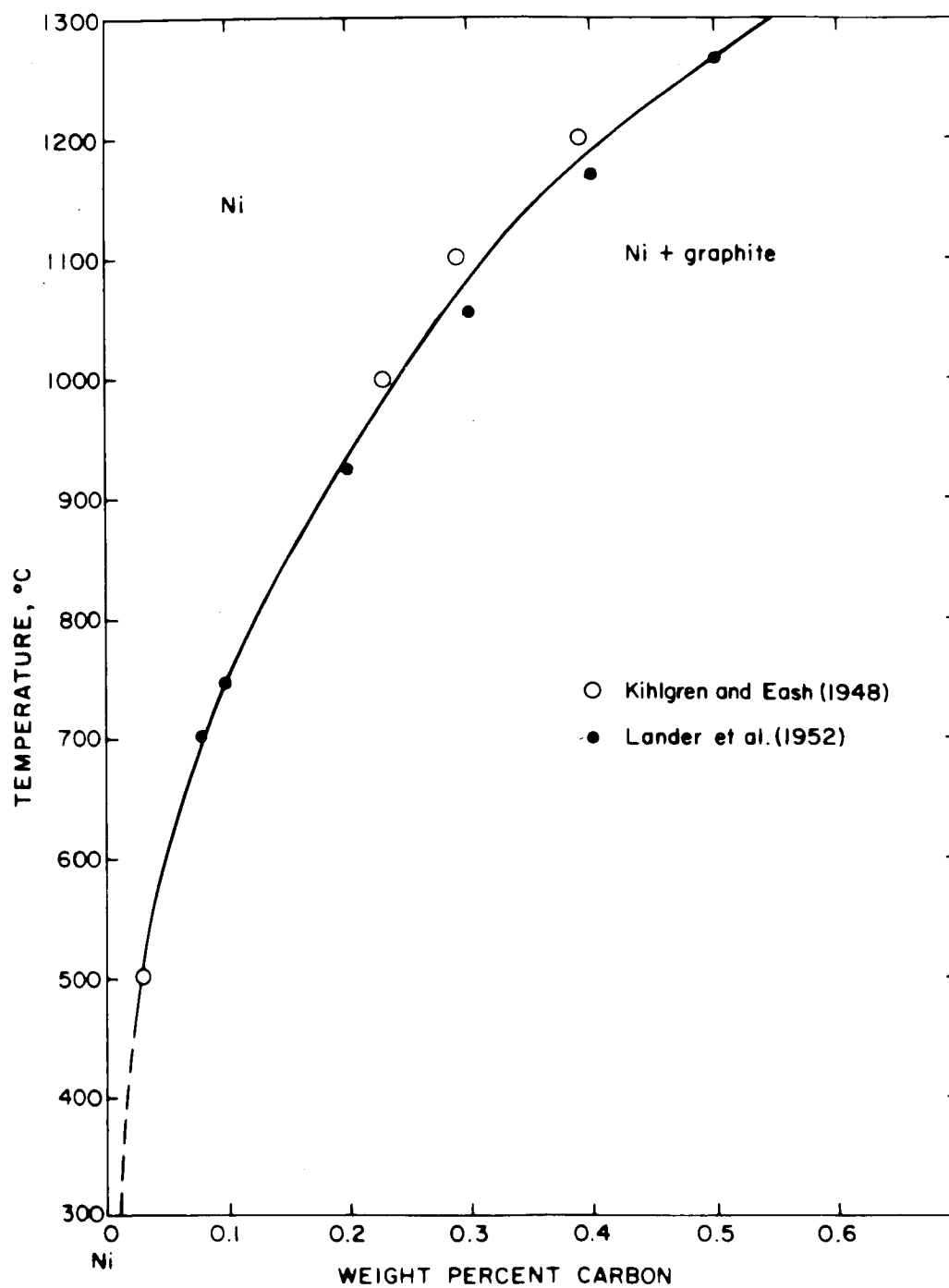
Fig. 4.--Part of the temperature-composition diagram of the system
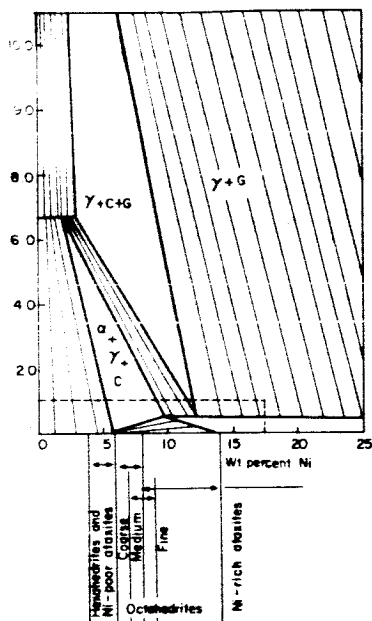Ni-C (from the data of Kihlgren and Eash, 1948; and Lander and others, 1952).

Fig. 5 (left).--Isothermal section of the system Fe-Ni-C at 650° C, in which the metastable phase cohenite is included. α = kamacite; γ = taenite; G = graphite; C = cohenite. Composition ranges of iron meteorites are shown. Dashed line indicates composition range of figure 6.

Fig. 6 (below).--Isothermal sections of part of the system Fe-Ni-C in which the metastable phase cohenite is included. Symbols as in figure 5. Arrows from 0 to 0.5 wt. percent carbon indicate range of carbon in iron meteorites.
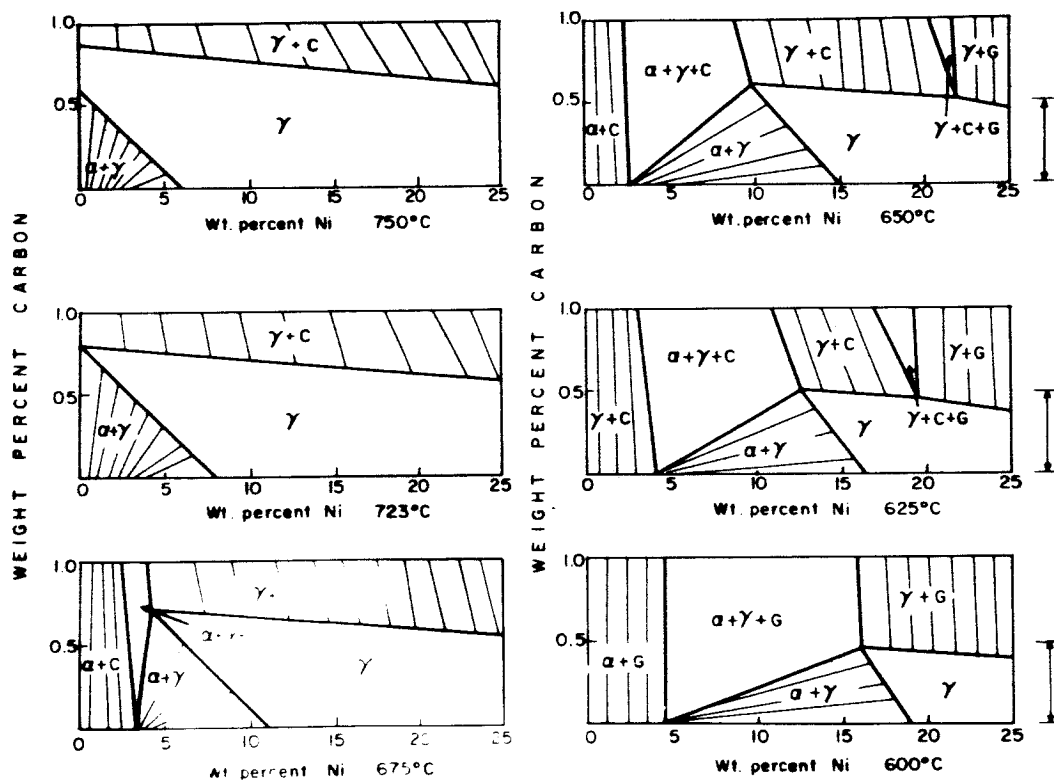
following the thermodynamic reasoning of Meljering (1959) for ferrite-austenite type equilibria.

3. The maximum carbon content of taenite at any given temperature was determined from the binary data by interpolating between the solubilities in the binary systems Fe-C and Ni-C.

Using the experimental data of Mehl and Wells (1937) and Hansen and Anderko (1958), the logarithm of the atomic fraction of carbon in taenite coexisting with Fe_3C was plotted versus the reciprocal of absolute temperature. The plot was linear, suggesting that the solution of Fe_3C in taenite behaves ideally. This plot was used for extrapolation to determine the matastable extension of the taenite-Fe_3C boundary below the eutectoid.

4. The composition of taenite in equilibrium with cohenite + kamacite at any given isotherm was obtained from the intersection of the taenite - taenite + cohenite boundary (see above), with the taenite - taenite + kamacite boundary. The latter was obtained by interpolating the experimental data of Goldstein and Ogilvie (1965a) for the composition of taenite in equilibrium with kamacite at fixed temperature for the Fe-Ni system with the calculated data on taenite compositions of Andrews (1956) for the Fe-C system.

5. The composition of kamacite coexisting with taenite and cohenite was assumed to be very close to the composition of kamacite in equilibrium with taenite at any given temperature.

6. Both cobalt and phosphorous have been ignored in the construction and discussion of the diagrams. Iron meteorites usually contain about 0.5 wt. percent cobalt, which tends to follow iron; whereas phosphorus is only present to about 0.2 wt. percent (Buddhue, 1946). Both elements are present in insufficient quantities in meteorites to affect the present conclusions.

7. The 600° C isotherm in figure 6 represents a change in assemblages according to the reaction taenite + cohenite = kamacite + graphite. This is not strictly a change in tie lines, but represents a postulated change in cohenite from a metastable to an unstable state at 600° C. The evidence for the change is that both increase in total nickel content and decrease in temperature and are known to increase

the free energy of formation of cohenite (Ringwood, 1960). Kamacite +
graphite is thus favored by falling temperature and the concomitant in-
crease of the nickel content of taenite. If the change occurs at 600° C
then cohenite does not form in alloys of meteoritic composition contain-
ing more than approximately 8 wt. percent nickel. This is consistent
with natural occurrence, so 600° C was accordingly chosen as the tempera-
ture of the change.

An examination of the isothermal sections reveals the following
details:

(1) Taenite is stabilized by carbon so that the nickel con-
tent of the carbon-saturated phase in equilibrium with kamacite is
appreciably less than that of carbon-free taenite. At 723° C, where
experimental data are abundant, the difference in nickel content is
8 wt. percent.

(b) The temperature at which cohenite appears in alloys of
meteoritic compositions is very sensitive to both nickel and carbon
contents of the bulk composition and varies from 723° to about 600° C
(the temperature at which cohenite no longer forms metastably).

The system Fe-Ni-C at high pressures

The phase equilibria for the system at 50 kb and 600° C are as
shown in figure 7, which was drawn using the data available on Fe-Ni
(Ringwood and Kaufman, 1962) and Fe-C (Kaufman, 1965). Cohenite is a
stable phase with respect to metal + graphite at this pressure (Ringwood,
1960), hence figure 7 is a true equilibrium diagram.

Kinetics of cohenite decomposition

Mechanism of decomposition

Cementite decomposition consists of cementite solution and graphite
nucleation within the surrounding matrix, or at cementite-metal interfaces
(Hickley and Quarrel, 1954; Higgins and Jeminson, 1965). Hickley and
Quarrell published photographs of the graphitization phenomenon and point
out that graphite spherules coalesce in time, the larger ones growing at
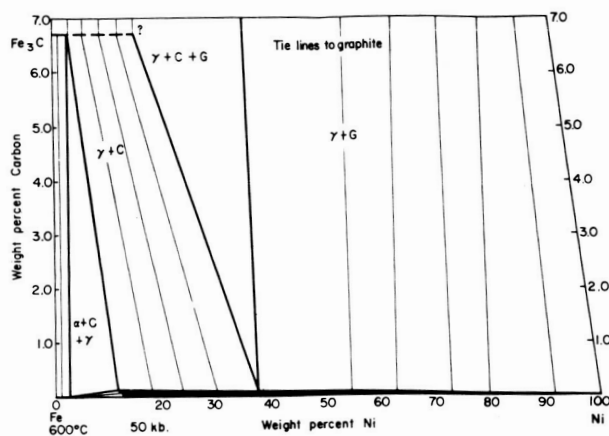the expense of the smaller.

Fig. 7.--Isothermal section of portion of the system Fe-Ni-C at 600° C and 50 kb. All phases including cohenite are stable. Symbols as in figure 5.
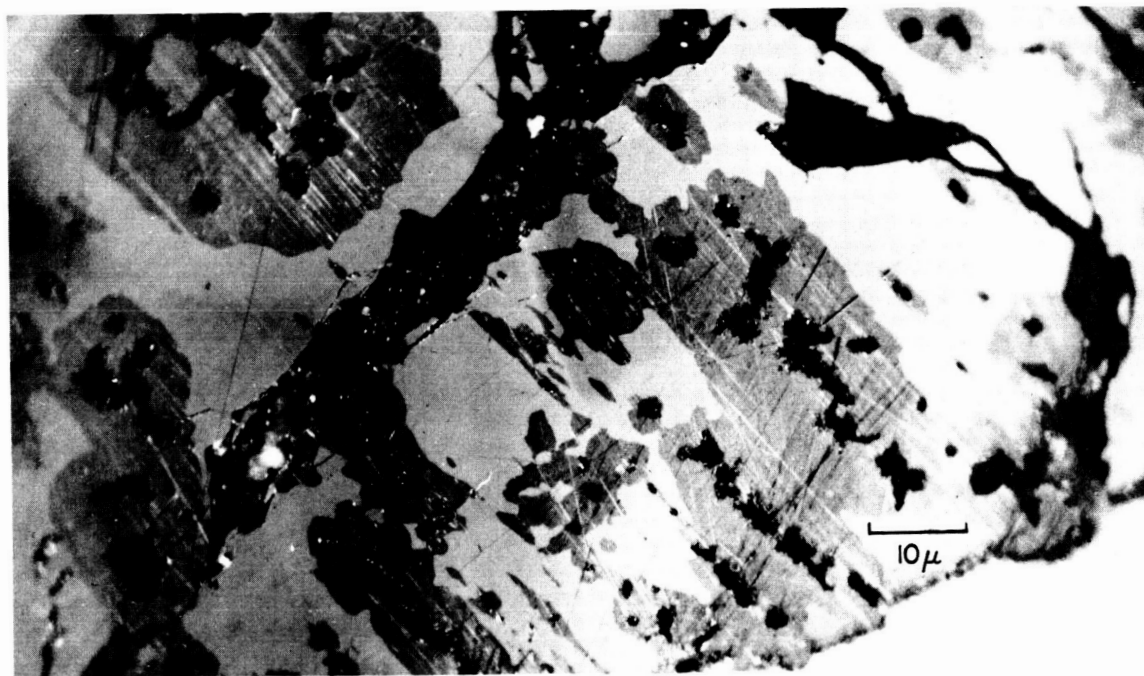

Fig. 8.--Cohenite from Coolac octahedrite (light gray) decomposed to graphite (black) and metal (dark gray). Black masses not surrounded by dark gray are fractures. Note graphite orientation. Cohenite held at 650° C for 80 days. Crossed nicols. (Photo by P. Ramdohr.)

Both Lipschutz and Anders (1964) and Ringwood (1965) appear to have assumed incorrectly that the graphitization of meteoritic cohenite takes place within the cohenite grains themselves.

If cohenite or cementite grains are fractured, as is generally the case in meteorites which have suffered impact, graphite nucleation is preferential along cracks, as shown by the studies of Lipschutz and Anders (1964) and Ringwood (1965). If cohenite grains are removed from metal, decomposition takes place along crystallographically oriented planes after nuclei have formed along any fractures that may be present (fig. 6). Once decomposition begins, the decomposition process is that described by Higgins and Jeminson (1965), namely, solution of cohenite, diffusion of carbon to the graphite mass, and precipitation of carbon with concomitant diffusion of metal away from the growing graphite.

Rate of decomposition

There has been little work on the kinetics of decomposition of cementite or cohenite that is strictly comparable to the decomposition of cohenite in nature. Many studies on synthetic alloys of considerable impurity have been performed in the presence of graphite nuclei. Higgins and Jeminson (1965), among others, have demonstrated the increased rate of graphitization in the presence of nickel. Approximately 1 wt. percent nickel decreased decomposition times by an order of magnitude.

Present decomposition studies

Method.--The present decomposition studies are similar in method to those of Ringwood and Seabrook (1962). Pieces of meteorite which contained cohenite were initially used as starting materials; however, as nucleation occurred along cracks in cohenite in these specimens, as in separated cohenite grains, pure meteoritic cohenite was used for most runs. It was not possible to find unfractured grains.

Small polished pieces of the Coolac octahedrite that contained grains of cohenite and separated grains of cohenite from the Cosby's Creek octahedrite were placed in separate silica glass tubes, which were evacuated and sealed. The tubes were then heated at 650°, 750°, and 850° C. The tubes were quenched at given times.

Results.--Microscopic examination shows that after a period of in-
duction decomposition occurs initially along fractures, then within the
body of the crystals as shown in figure 8. Note the apparent crystallo-
graphic control of the graphite particles along pinacoidal planes (P.
Ramdohr, oral communication, 1964). It is noteworthy that El Goresey and
Ramdohr (A. El Goresey, written communication, 1965) have observed ex-
tremely fine twinning parallel to a pinacoidal plane in cohenite from
Canyon Diablo. Coalescence of the rounded graphite particles occurs with
time. No pseudomorphs of graphite after cohenite were observed.

In any given run, the decomposition of some cohenite grains was
considerably advanced, whereas in other less fractured grains no trace
of graphite was evident. Microscopic point-counts were made of cohenite,
metal, and graphite abundances in all runs made at 650° C. When the
metal and graphite decomposition products were calculated in terms of
mole percent, good agreement (within 5 percent) was obtained with the
formula $(Fe,Ni)_3C$. When percent decomposition was plotted against time,
considerable scatter was obtained. The results are similar in nature to
those of Brett (1964), who, in studying the kinetics of decomposition
of certain sulfide solid solutions, concluded that each determined point
lies along one of a family of similar rate curves, each curve having a
given but unknown nucleation period. Nucleation of graphite appears to
be the rate-controlling step in cohenite decomposition (Lipschutz and
Anders, 1964).

The duration of runs in which total decomposition of cohenite had
occurred was noted, and the results are plotted in figure 9, together
with those of Ringwood and Seabrook. In view of the scattering observed
at 650° C, the time of decomposition at any given isotherm can be con-
sidered correct only within a factor of 2 or 3. The agreement is ex-
cellent between the present results and those of Ringwood and Seabrook
(1962).

The Fe_3C decomposition curve for 50 percent decomposition as given
by Lipschutz and Anders (1964) from Klein's (1934) data on a synthetic
alloy is also plotted in figure 9. Note that it differs from the present
results over the experimental range by over 3 orders of magnitude. Such

data can be similar only qualitatively to the data for natural cohenite decomposition, as pointed out by Ringwood (1965).

The present results represent a minimum for the time of total decomposition of cohenite in nature in that nucleation occurred within fractures in a shocked crystal. In cooling meteorites in nature, grains are unfractured, so that nucleation must take place at interfaces in metal at distances up to centimeters from the given cohenite grain, causing distances for diffusion to be greater and hence decomposition times to be slower.

Decomposition of cohenite in meteorites

The only iron meteorites, so far as the writer is aware, which show possible evidence of thermal decomposition of cohenite similar to that caused by laboratory annealing of cohenite (fig. 8) are Dungannon (Perry, 1944, Plate 62) and Canyon Diablo (Heymann and others, 1965). Dungannon, which is a metamorphosed medium-to-coarse octahedrite, has a (Ni + Co) content of 7.4 wt. percent and is highly oxidized (Merrill, 1923). P. Ramdohr (written communication, 1965) states that cohenite may decompose on oxidation to graphite + metal. Heymann and others ascribe the rare graphitization in Canyon Diablo cohenite to shock-induced heating caused by impact.

The scalloped textures of cohenite are evidence for decomposition, by analogy with synthetic decomposition. Both Hickley and Quarrell (1954, figs. 4 and 6) and Burke and Owen (1954, fig. 8) show photographs of partially graphitized cementite very similar in texture to meteoritic and terrestrial cohenite, which suggests that meteoritic cohenite has partially decomposed.

Conditions of formation of cohenite

Temperature of formation

It is now possible to speculate on the conditions of formation of cohenite in nature using the data reviewed and presented above on the phase equilibria of its formation (figs. 5-7) and kinetic data on its decomposition (fig. 9).

It is clear from figure 6 that the lower the nickel content, the higher the temperature of the reaction taenite → kamacite + cohenite for any given carbon content. Figure 6 shows that the field boundaries kamacite + cohenite - kamacite + taenite + cohenite and kamacite + taenite - kamacite + taenite + cohenite move toward increasing nickel contents with falling temperature. Meteorites containing up to 6 wt. percent nickel had precipitated all their cohenite from solid solution, regardless of the carbon content, when the temperature had fallen to about 640° C. As cooling continued below this temperature, at 1 to 10° C per million years in iron meteorites (Wood, 1964; Short and Anderson, 1965; Goldstein and Ogilvie, 1965), meteorites containing more than 6 wt. percent nickel began to deposit cohenite, the higher the carbon content the higher the temperature at which cohenite first appeared. Cohenite precipitation continued until the phase became unstable at about 600° C.

The instability of cohenite below 600° C prevented the formation of cohenite in meteorites containing more than about 8 wt. percent nickel. Carbon contents in iron meteorites average only about 0.2 wt. percent (Buddhue, 1946) and 0.4 wt. percent is an exceptionally high carbon content (Perry, 1944). Therefore, at 600° C such meteoritic alloys of more than 8 wt. percent nickel lie in the two phase region taenite + kamacite of figure 5, and no cohenite formed.

Hexahedrites, whose compositions lie in the range 4 to 6 wt. percent nickel, doubtless precipitated cohenite on cooling, but since the cohenite formed at a temperature some 30° C or so higher than cohenite in coarse octahedrites, it had an additional 3 to 30 million years annealing time at temperatures around 650° C in which to decompose, and did so.

It is postulated that cohenite in coarse octahedrites, formed at lower temperatures, did not totally decompose in the cooling time available. For total decomposition to have taken place in hexahedrites and not in octahedrites requires a decomposition rate curve in which the decomposition time at 650° C is a little over 4 orders of magnitude greater than that determined experimentally. The position of this curve is shown in figure 9. It has already been pointed out that the experimentally determined cohenite decomposition times are probably much less than
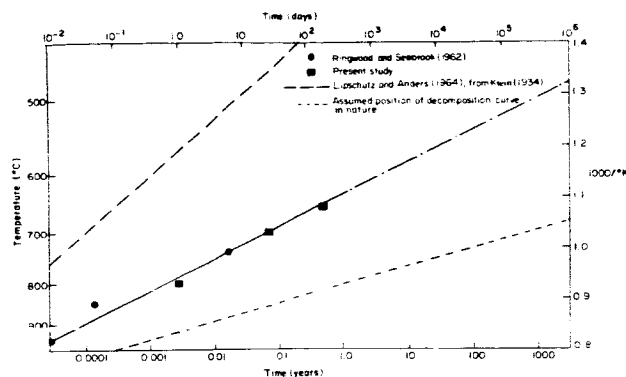
Fig. 9.--Plot of temperature vs. time for total decomposition of Coolac cohenite, using present data and those of Ringwood and Seabrook (1962). The curve of Lipschutz and Anders (1964) from the data of Klein (1934) represents 50 percent decomposition. Bottom curve shows the decomposition curve which is compatible with natural occurrence of cohenite.
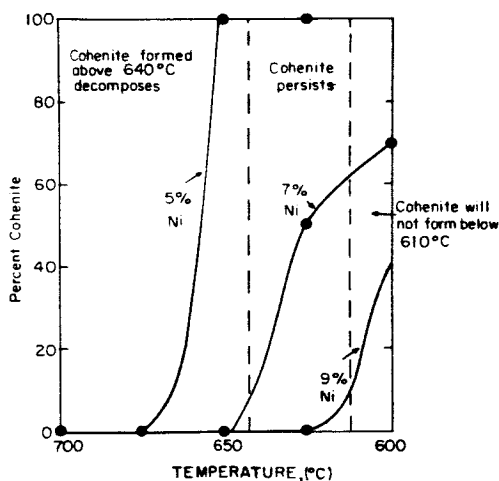

Fig. 10.--Plot of cumulative percentage of cohenite formed vs. temperature for 3 meteorite compositions, each containing 0.3 wt. percent carbon.

decomposition times in nature. Four orders of magnitude difference
does not appear unreasonable. If nucleation of kamacite in meteorites
is delayed by supercooling effects of up to 100° C (Wood, 1964; Short
and Anderson, 1965; Goldstein and Ogilvie, 1965), then temperatures of
cohenite formation would also be depressed by amounts up to 100° C.
Hence the situation shown in the 650° C isotherm would actually occur
at 550° C and the decomposition time would then be required to be a
little over 2 orders of magnitude slower than that measured experimentally
to be compatible with the present hypothesis.

Figure 10 shows the cumulative percentage of cohenite formed with
decreasing temperature compared to the total that can possibly form
(assuming that all carbon reacted to form cohenite) for alloys of
different nickel content, assuming a total carbon content in each alloy
of 0.3 wt. percent. Results are approximately the same for slightly
higher and slightly lower carbon contents. Percentages were obtained by
applying the well-known Lever Law to the isotherms in figure 6. It is
apparent from figure 10 that if all cohenite formed at temperatures
above 640° C decomposed during meteoritic cooling and that if cohenite
does not form below 600° C, then the only cohenite which persists in
meteorites is in those containing from 6 to 8 wt. percent nickel.

Cohenite occurrences in meteorites that do not lie in the 6 to 8 wt.
percent range can now be discussed.

Breece and Tambo Quemada are the only medium octahedrites that con-
tain cohenite. Henderson and Perry (1958) state that there is considerable
free carbon in Breece. The mineral has not been so painstakingly searched
for in other medium octahedrites; it possibly occurs in similar fine-
grained form in others which contain more than about 0.5 wt. percent car-
bon. For compositions high in nickel and carbon, figure 6 indicates that
cohenite forms from about 630° C to 600° C, at which temperature graphite
precipitates instead of cohenite. The rarity of cohenite in medium octa-
hedrites is explained by the rarity of meteorites with such high carbon
contents.

In the nickel-poor ataxites Locust Grove and Chesterville, cohenite
should form in the same temperature range as the hexahedrites and should

therefore have decomposed during slow meteoritic cooling. However, the
dendritic and eutectoid textures involving cohenite in these two meteor-
ites (Perry, 1944) indicate extremely rapid cooling or shock (Heymann
and others, 1965), which explains the presence of the cohenite.

Perry (1942-53) states that in the nickel-poor ataxite Navajo, the
cohenite is extremely fine grained. To explain the presence of cohenite
in this meteorite it must either (1) have locally high nickel contents
or (2) have cooled faster than $1°$ to $10°$ C per million years. Fast cool-
ing is not surprising, since the meteorite is classed as a nickel-poor
ataxite, all of which appear to have been thermally metamorphosed (Mason,
1962) and hence had a different cooling history than unmetamorphosed iron
meteorites.

The preservation of cohenite in the enstatite chondrites Abee and
St. Mark's may be explained by rapid cooling. Pearlitic cohenite textures
would support this (Ramdohr, 1963).

The nickel content of metal in Indarch is in the range of coarse
octahedrites (6 to 8 wt. percent nickel), so the presence of cohenite in
this meteorite is not incompatible with very slow cooling; however, like
the other enstatite chondrites, the meteorite probably cooled rapidly.

Cohenite in Disko Island basalt may also be explained by rapid
cooling.

Cohenite both from meteorites and Disko Island should be partially
decomposed if the present hypothesis is correct. The rounded scalloped
borders of many cohenite grains would suggest that this is so, the graph-
ite migrating either to preexisting graphite inclusions or forming the
numerous small graphite particles found in iron meteorites.

Pressure of formation of cohenite

Meteorites containing cohenite could have cooled at any pressure,
at least so far as the presence of cohenite is concerned. If the cooling
of metallic meteorites took place at 50 kb (fig. 7), then cohenite once
formed would remain stable for all compositions of metallic meteorites
over the entire cooling range (Ringwood, 1960). However, the fact that
cohenite is limited to a narrow meteoritic composition range argues for
cooling at pressures compatible with a parent body of asteroidal rather

than lunar dimensions if a common origin is assumed for the iron meteorites.

Conclusions

A consistent explanation has been suggested for the natural occurrence of cohenite. The explanation might be criticized because it is involved and requires the coincidence that cohenite formed at or near temperatures below which its rate of decomposition became negligible. It is not unreasonable to require such a coincidence considering the extremely narrow range of occurrence of cohenite. An indication of this narrow range is the irregular occurrence of cohenite within a single meteorite. This certainly reflects slight local variations in carbon and nickel content [see Perry, 1944, Pl. 64 (2)].

If the hypothesis on cohenite formation is correct, it follows that:

1. The presence of a few tenths of 1 percent of carbon in a nickel-iron alloy may reduce the temperature at which the kamacite separates by more than 50° C, assuming equilibrium conditions. The "supercooling" effect in which nucleation of the α phase may be inhibited in iron meteorites by over 100° C according to Wood (1964), Short and Anderson (1965), and Goldstein and Ogilvie (1965b) may therefore be partly due to carbon solubility in metal.

2. Cohenite formed between about 650 and 600° C in meteorites that contain it. It formed in meteorites with lower nickel content than 6 wt. percent at higher temperatures, but readily decomposed during cooling.

3. The narrow range of composition of meteorites containing cohenite is explained by the restricted temperature range of formation in which decomposition is not effective, and by the fact that cohenite does not form below 600° C.

4. The greater the nickel or the carbon content of an alloy in the range of meteorite compositions, the lower the temperature of cohenite formation.

5. The time for decomposition of unfractured cohenite crystals within a meteorite during cooling may be as great as several million years.

6. On the basis of cohenite occurrence only, cohenite could have formed in meteorites in any pressure environment.

7. The presence or absence of cohenite in meteorites may be explained in terms of phase equilibria and decomposition kinetics at 1 atm. The lack of cohenite in meteorites of composition such that cohenite could precipitate indicates low pressures during cooling.

Acknowledgments

References

Anders, E., 1964, Origin, age, and composition of meteorites: Space Sci. Rev., v. 3, p. 583-714.

Andrews, K. W., 1956, The calculation of transformation temperatures and austenite-ferrite equilibria in steels: Iron and Steel Inst. Jour., v. 184, p. 414-427.

Brett, R., 1964, Kinetics of exsolution in two sulfide systems [abs.]: Geol. Soc. America Program, 1964 Ann. Meeting, Miami Beach, Fla.

Brown, J. D., and Lipschutz, M. E., 1965, Electron-probe microanalysis of the Odessa iron meteorite: Icarus, v. 4, p. 436-441.

Buddhue, J. D., 1946, The average composition of meteoritic iron: Pop. Astronomy, v. 54, p. 149-152.

Burke, J., and Owen, W. S., 1954, Kinetics of first stage graphitization in iron-carbon-silicon alloys: Iron and Steel Inst. Jour., v. 176, p. 147-155.

Dawson, K. R., Maxwell, J. A., and Parsons, D. E., 1960, A description of the meteorite which fell near Abee, Alberta, Canada: Geochim. et Cosmochim. Acta, v. 21, p. 127-144.

Goldstein, J. I., and Ogilvie, R. E., 1965a, Fe-Ni phase diagram: Am. Inst. Mining Metall. Petroleum Engineers Trans. (in press).

_____ 1965b, The growth of the Widmanstaetten pattern in metallic meteorites: Geochim. et Cosmochim. Acta, v. 29, p. 893-920.

El Goresey, A., 1965, Mineralbestand und strukturen der Graphit - und Sulfideinschlüsse in Eisenmeteoriten: Geochim. et Cosmochim. Acta, v. 29, p. 1131-1151.

Hansen, M., and Anderko, K., 1958, Constitution of binary alloys 2d ed.: New York, McGraw-Hill, 1305 p.

Heide, F., Herschkowitsch, E., and Preuss, E., 1932, Ein neuer Hexaedrit von Cerros del Buen Huerto, Chile: Chem. der Erde, v. 7, p. 483-502.

Heller, W., and Branner, J., 1964, Untersuchungen uber die Diffusion und Auscheidung von Kohlenstaff in ferritischen Eisen-Nickel-Legierungen durch Dampfungsmessungen: Archiv. Eisenhuttenw., v. 35, p. 1105-1110.

Henderson, E. P., and Perry, S. H., 1958, Studies of seven siderites. U.S. Natl. Museum Proc., v. 107, p. 339-403.

Herbstein, F. H., and Snyman, 1964, Identification of the Eckstron-Adcock iron carbide as Fe_7C_3: Inorganic Chem., v. 3, p. 894-896.

Heymann, D., Lipschutz, M. E., Nielsen, B., and Anders, E., 1965, Canyon Diablo meteorite: metallographic and mass spectrometric study of 56 fragments: Jour. Geophys. Research (in press).

Hickley, R. H., and Quarrell, A. G., 1954, The graphitization of steel at subcritical temperatures: Iron and Steel Inst. Jour., v. 178, p. 337-346.

Higgins, A. T., and Jeminson, G. V., 1965, Observations on the role of aluminum, silicon, and nickel in the graphitization of high purity 0.15 percent carbon steels: Iron and Steel Inst. Jour., v. 203, p. 146-152.

Hofer, L. J. E., Cohn, E. M., and Peebles, W. C., 1949, The modifications of the carbide, Fe$_2$C; their properties and identification: Am. Chem. Soc. Jour., v. 71, p. 189-195.

_____ 1950, Isothermal decomposition of nickel carbide: Jour. Phys. Colloid Chemistry, v. 54, p. 1161-1169.

Kaufman, L., 1965, Condensed state reactions at high pressure (in preparation), Cambridge, Mass., Manlabs Inc.

Kaufman, L., and Ringwood, A. E., 1961, High pressure equilibria in the iron-nickel system, and the structure of metallic meteorites: Acta Metallurgica, v. 9, p. 941-944.

Kihlgren, T. E., and Eash, J. R., 1948, Carbon-nickel in Lyman, T. (ed.), Metals Handbook, Cleveland, Ohio, Amer. Soc. Metals, p. 1183.

Klein, E. H., 1934, Der zeitliche Verlauf des Zementitzerfalls im Gusseisen: Stahl u. Eisen, v. 54, p. 827-830.

Lander, J. J., Kern, H. E., and Beach, A. L., 1952, Solubility and diffusion coefficient of carbon in nickel: reaction rates of nickel-carbon alloys with barium oxide: Jour. Appl. Physics, v. 23, p. 1305-1309.

Lipschutz, M. E., and Anders, E., 1961, The record in the meteorites--IV. Origin of diamonds in iron meteorites: Geochim. et Cosmochim. Acta, v. 24, p. 83-105.

_____ 1964, Cohenite as a pressure indicator in iron meteorites?: Geochim. et Cosmochim. Acta, v. 28, p. 699-711.

Löfquist, H., and Benedicks, C., 1941, Det store Nordenskjöldska Jarnblocket fran Ovifak; Mikvostruktur och Bildningssät: K. Svenska Vetensk. Akad. Handl., v. 19, no. 3, 96 p.

Lovering, J. F., 1964, Electron microprobe analysis of terrestrial and meteoritic cohenite: Geochim. et Cosmochim. Acta, v. 28, p. 1745-1756.

Lovering, J. F., Hichiporuk, W., Chodos, A., and Brown, H., 1957, The distribution of gallium, germanium, cobalt, chromium, and copper in iron and stony-iron meteorites in relation to nickel content and structure: Geochim. et Cosmochim. Acta, v. 11, p. 263-278.

References--Continued

Mason, B., 1962, Meteorites: New York, John Wiley, 274 p.

Mehl, R. F., and Wells, C., 1937, Constitution of high-purity iron-carbon alloys: Am. Inst. Mining Metall. Petroleum Engineers Trans., v. 125, p. 429-469.

Meljering, J. L., 1959, Thermodynamical calculation of phase diagrams: Symposium No. 9, Phys. and Chem. of Metallic Solutions and Inter-metallic Compounds Proc., June 1959, v. 2, p. 1-20.

Merrill, G. P., 1923, A meteoric metabolite from Dungannon, Virginia: U.S. Natl. Museum Proc., v. 42, art. 18, 2 p.

Nininger, H. H., 1952, Out of the sky: Denver, Univ. Denver Press, 336 p.

Olsen, E., 1964, Some calculations concerning the effect of nickel on the stability of cohenite in meteorites: Geochim. et Cosmochim. Acta, v. 28, p. 609-617.

Palache, C., Berman, H., and Frondel, C., 1944, The system of mineralogy, v. 1: New York, John Wiley, 834 p.

Perry, S. H., 1944, The metallography of meteoritic iron: U.S. Natl. Museum Bull., v. 184, 206 p.

_____ 1942-53, Photomicrographs of meteoric irons, 9 vols.: Circulated privately by the author.

Pinsker, Z. G., and Kaverin, S. V., 1956, Electronographic determination of the structure of the iron carbide, Fe_4C: Kristallografiia, v. 1, p. 66-72 (in Russian).

Prior, G. T., 1953, Catalogue of meteorites, 2d ed. revised by M. H. Hey: London, Trustees of Brit. Mus. 472 p.

Ramdohr, P., 1953, Neue Beobachtungen am Bühl-Eisen. Sitzungber. der Deutsche Akad. Wiss., Berlin Abh., Kl. Math. u. allg. Naturw., Jahrg. 1952, no. 5, p. 9-24.

_____ 1963, The opaque minerals in stony meteorites: Jour. Geophys. Research, v. 68, p. 2011-2036.

_____ 1964, Einges uber die Opakerze in Achondriten und Enstatitchon-driten: Sitzungber. Deutsche Akad. Wiss. Kl. Chem., Geol., u. Biol., 1964, no. 5, 40 p.

<u>References--Continued</u>

Ringwood, A. E., 1960, Cohenite as a pressure indicator in iron
    meteorites: Geochim. et Cosmochim. Acta, v. 20, p. 155-158.

_____ 1965, Cohenite as a pressure indicator in iron meteorites - III:
    Geochim. et Cosmochim. Acta, v. 29, p. 573-579.

Ringwood, A. E., and Kaufman, L., 1962, The influence of high pressure
    on transformation equilibria in iron meteorites: Geochim. et
    Cosmochim. Acta, v. 26, p. 999-1009.

Ringwood, A. E., and Seabrook, M., 1962, Cohenite as a pressure in-
    dicator in iron meteorites - II: Geochim. et. Cosmochim. Acta,
    v. 26, p. 507-509.

Samuel, P., Finch, L. G., and Rait, J. R., 1955, A phase diagram for
    one percent carbon-iron alloys containing up to 16 percent nickel:
    Nature, v. 175, p. 37-38.

Senateur, J. P., Fruchart, R., and Michel, A., 1962, Formule et struc-
    ture crystalline du carbure de Ragg: Acad. Sci. (Paris) Comptes
    rendus, v. 255, p. 1615-1616.

Short, J. M., and Anderson, C. A., 1965, Electron microprobe analyses
    of the Widmanstaetten structure of nine iron meteorites: Jour.
    Geophys. Research, v. 70, p. 3745 - 3759.

Wiik, H. B., 1956, The chemical composition of some stony meteorites:
    Geochim. et Cosmochim. Acta, v. 9, p. 279-289.

Wood, J. A., 1964, The cooling rates and parent planets of several
    iron meteorites: Icarus, v. 3, p. 429-459.

Yavnel, A. A., 1958, Classification of meteorites according to their
    chemical composition: Meteoritika, v. 15, p. 115-135; Internat.
    Geol. Rev., v. 2, p. 298-310.

COSMIC DUST INVESTIGATIONS

by M. B. Duke and M. H. Carr

Knowledge of the origin and history of cosmic dust is basic to our understanding of the present nature and past history of the solar system. Cosmic dust may originate from several sources, both within and beyond the solar system; these sources include the Moon, asteroids, and comets. Ultimately, information regarding these sources can be gained from a study of cosmic dust. Identification of cosmic constituents in sediments of the Earth and other planets may give evidence of past cosmic events and may facilitate interplanetary geologic correlation.

The means of collecting, recognizing, concentrating and analyzing cosmic dust pushes on the frontiers of many aspects of engineering and science and are in a stage of only preliminary development. Some of the problems encountered in collecting above the atmosphere stem from the low flux rates and high speeds of the particles and from the predominance of very small particles (less than 1 μ diameter). For any reasonable sampling time the extremely low flux rates prevent collection of anything but small particles (less than 20 μ diameter). As a result, development of new techniques for analyzing and handling small particles has been necessary. The small particle size also makes it necessary that all work be done in carefully controlled dust-free atmospheres. During fiscal year 1964, ultra-clean laboratories were therefore established in both Washington, D.C., and Menlo Park, California.

We have been invited by other agencies to participate in experiments to collect material above the atmosphere. In fiscal year 1964 we prepared prototypes of the sampling surfaces to be flown as part of the Gemini collection experiment. Sampling surfaces were also flown on the first engineering flight of the Luster program. We do not have as yet, however, any material that was collected above the atmosphere. During fiscal year 1965 we anticipate obtaining samples from both the Luster and Gemini experiments.

Meanwhile, work has been continuing on dust collected within the atmosphere. Here the principal problem is in recognizing the extra-terrestrial component of the dust sampled from the terrestrial component. The extent of terrestrial contamination depends on the size of the particle, on the altitude of collection, and on various meteorologic conditions. As a first step in the process of discriminating between extra-terrestrial and terrestrial particles, we have been systematically cataloguing the different types of particles found in the atmosphere at elevations above 30,000 feet. This material has also been used in the development of techniques of particle manipulation and transfer, and of particle analysis. The existing analytical facilities pertinent to analysis of small particles are being added to and improved upon. During fiscal year 1965 the electron microprobe and electron microscope facilities in Washington, D.C., were upgraded and during fiscal year 1966 electron microprobe and electron microscope laboratories will be established in Menlo Park.

The ultimate aim of the cosmic dust program is to completely characterize cosmic dust morphologically, mineralogically, and chemically. Attainment is presently hampered by the lack of samples in which cosmic dust concentrations are large enough to work with conveniently. Further exploration of methods of sampling, especially by high altitude airplane or balloon, are needed.